The Local-Scale Origin of Ferroic Properties in $BiVO_4$

Bryce G. Mullens,[1,2] Frederick P. Marlton,[3,*] Helen E.A. Brand,[4] Helen E. Maynard-Casely,[5] Michelle Everett,[6] Matthew G. Tucker,[6] Emily R. Van Auken,[6] Alicia M. Manjon-Sanz,[6] Gianguido Baldinozzi,[7] Simon M. Vornholt,[2] Karena W. Chapman,[2] and Brendan J. Kennedy[1,*]

[1] School of Chemistry, the University of Sydney, Sydney, NSW 2006, Australia.

[2] Department of Chemistry, Stony Brook University, 100 Nicolls Road, Stony Brook, NY 11790, USA.

[3] Centre for Clean Energy Technology, School of Mathematical and Physical Sciences, Faculty of Science, University of Technology Sydney, Sydney, NSW 2007, Australia.

[4] Australian Synchrotron, Australian Nuclear Science and Technology Organisation, Clayton, VIC 3168, Australia.

[5] Australian Centre for Neutron Scattering, Australian Nuclear Science and Technology Organisation, Lucas Heights, NSW 2234, Australia.

[6] Neutron Scattering Division, Oak Ridge National Laboratory, Oak Ridge, TN 37831, USA.

[7] Université Paris-Saclay, Centralesupélec, Centre National de la Recherche Scientifique, Structures Property and Modeling of Solids Laboratory, Gif-sur-Yvette 91190, France.

* Corresponding Authors: Frederick P. Marlton (frederick.marlton@uts.edu.au) and Brendan J. Kennedy (brendan.kennedy@sydney.edu.au)

Table of Contents

Crystallographic Structures

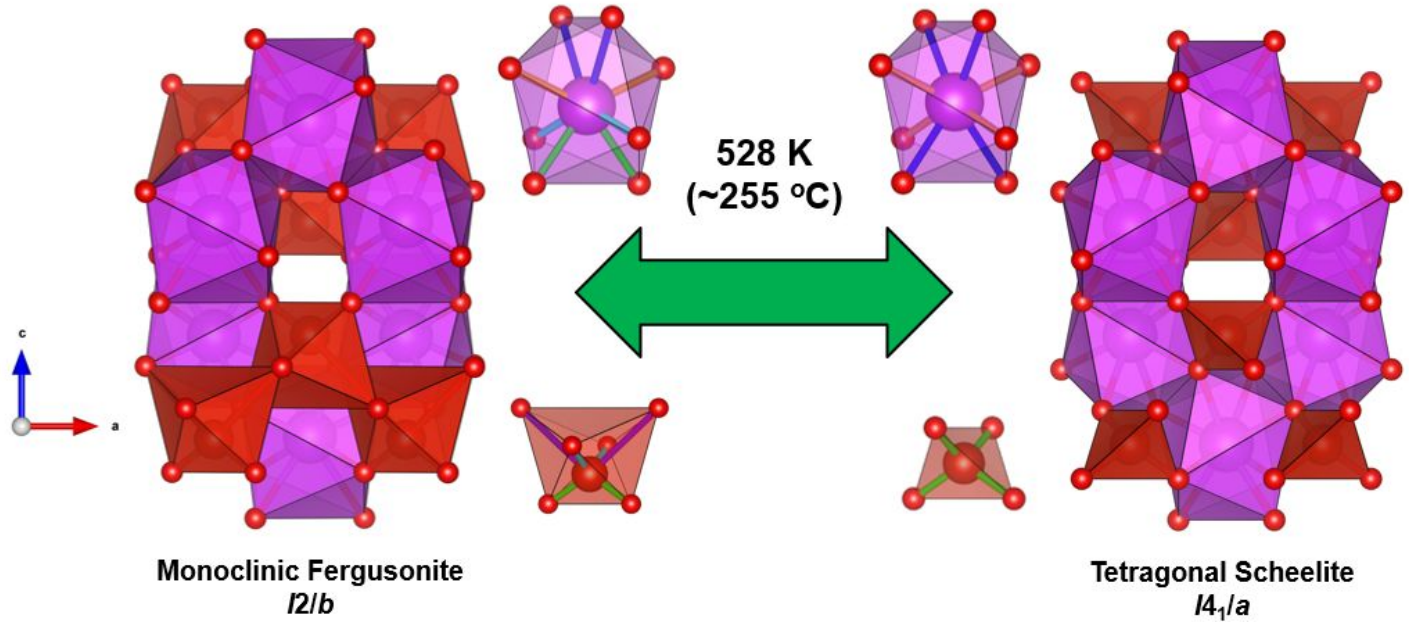

Figure S1: Phase transition in bismuth vanadate ($BiVO_4$). At room temperature, the structure is monoclinic fergusonite before undergoing an increase in symmetry to tetragonal scheelite at ~525 K (~250 °C). In the monoclinic fergusonite phase, the BiO_8 polyhedra have four different Bi–O bond lengths (as indicated with four different colors), and the VO_4 tetrahedra have two different V–O bond lengths (drawn here as VO_6 polyhedra to emphasize the difference between the two phases). In the tetragonal fergusonite phase, the BiO_8 polyhedra have two different Bi–O bond lengths (as indicated with two different colors), and the VO_4 tetrahedra have a unique V–O bond length. In this figure, the pink spheres/polyhedra represent the bismuth cations, the orange spheres/polyhedra represent the vanadium cations, and the red spheres/polyhedra represent the oxygen anions.

Synchrotron X-Ray Diffraction Data – Australian Synchrotron

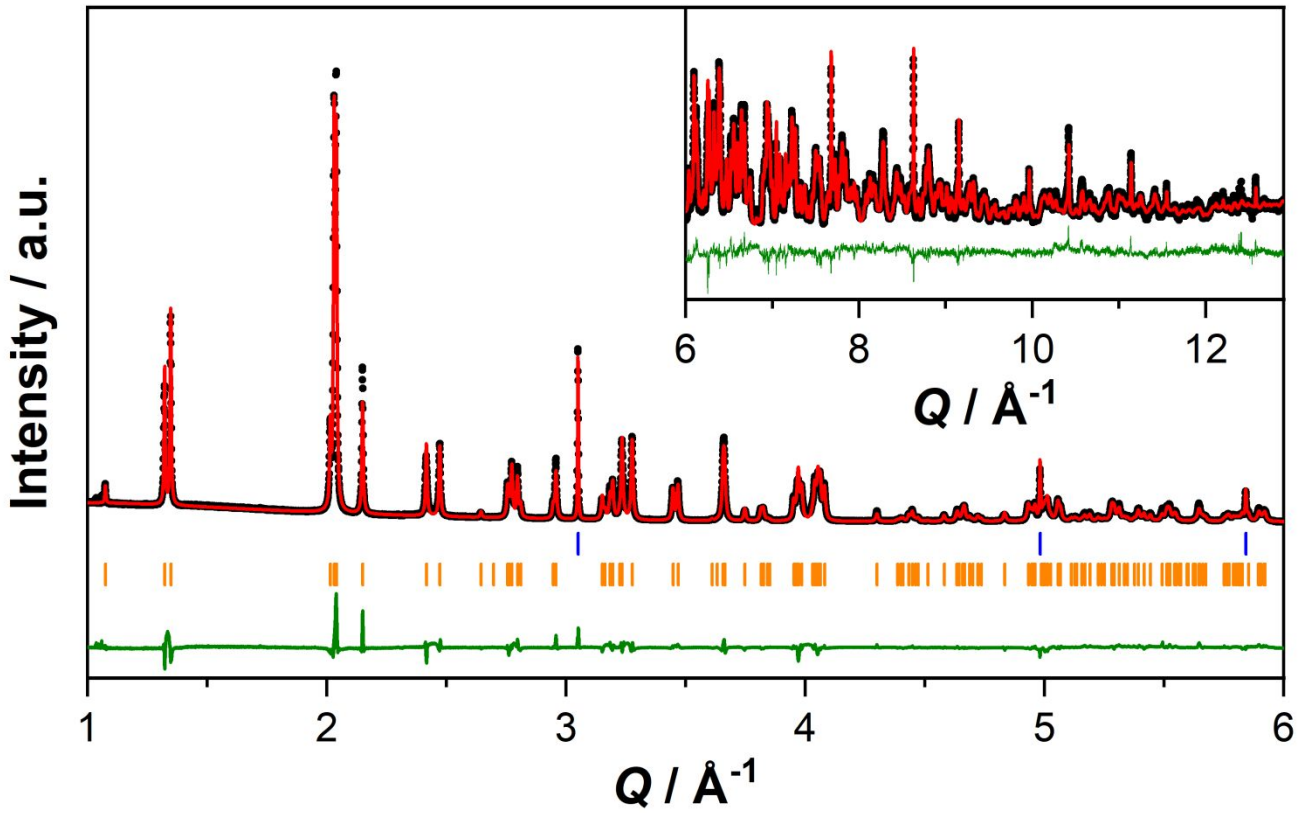

Figure S2: Synchrotron X-ray diffraction data for $BiVO_4$ at 90 K, collected on the Powder Diffraction beamline at the Australian Synchrotron (λ = 0.59007 Å, 21.0 keV). The sample was diluted with diamond powder in a 50:50 by weight ratio. The black circles represent the collected data, the red line represents the Rietveld refinement to the monoclinic fergusonite model, the green line represents the difference between the fit and the data, and the blue and orange ticks represent the *hkl* space group-allowed reflections of the diamond ($Fm\bar{3}m$) and $BiVO_4$ ($I2/b$) respectively.

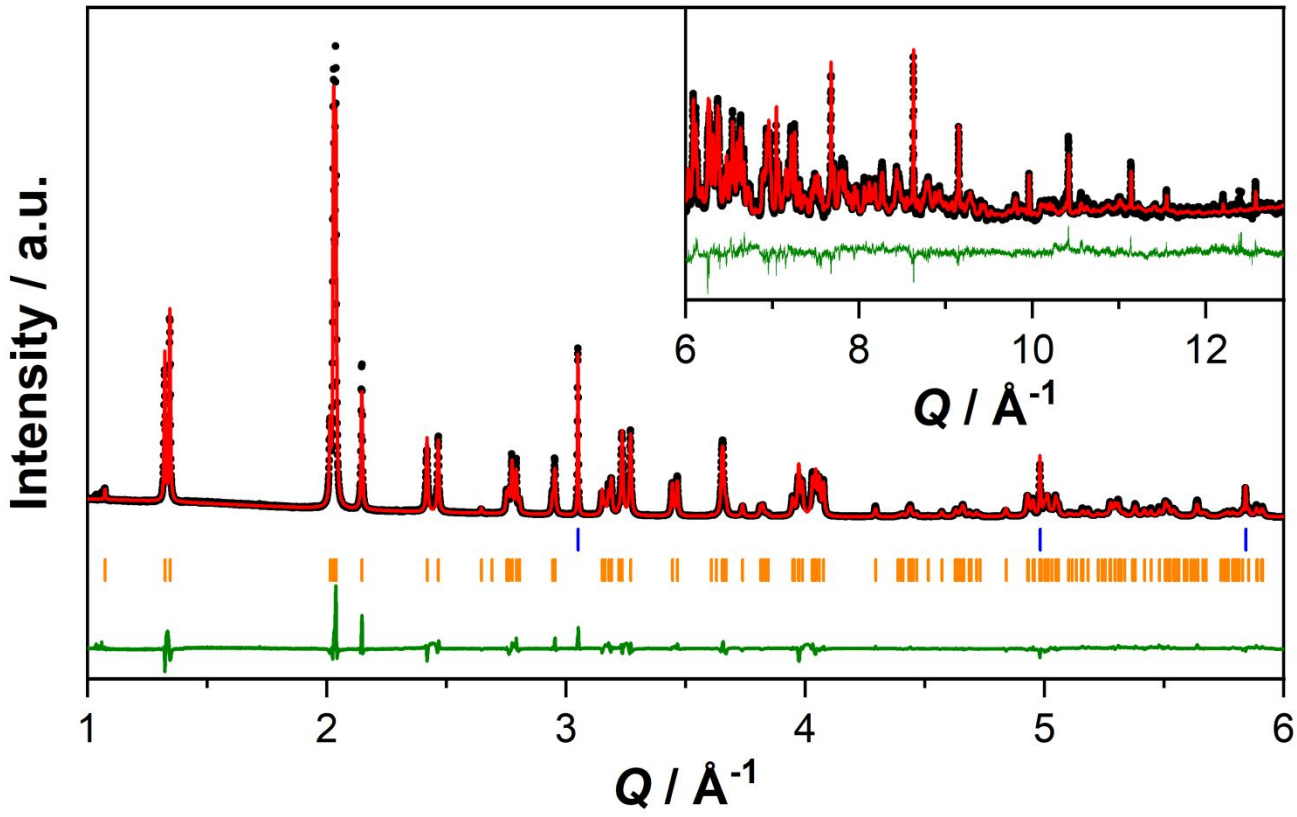

Figure S3: Synchrotron X-ray diffraction data for $BiVO_4$ at 300 K, collected on the Powder Diffraction beamline at the Australian Synchrotron (λ = 0.59007 Å, 21.0 keV). The sample was diluted with diamond powder in a 50:50 by weight ratio. The black circles represent the collected data, the red line represents the Rietveld refinement to the monoclinic fergusonite model, the green line represents the difference between the fit and the data, and the blue and orange ticks represent the *hkl* space group-allowed reflections of the diamond ($Fm\bar{3}m$) and $BiVO_4$ ($I2/b$) respectively.

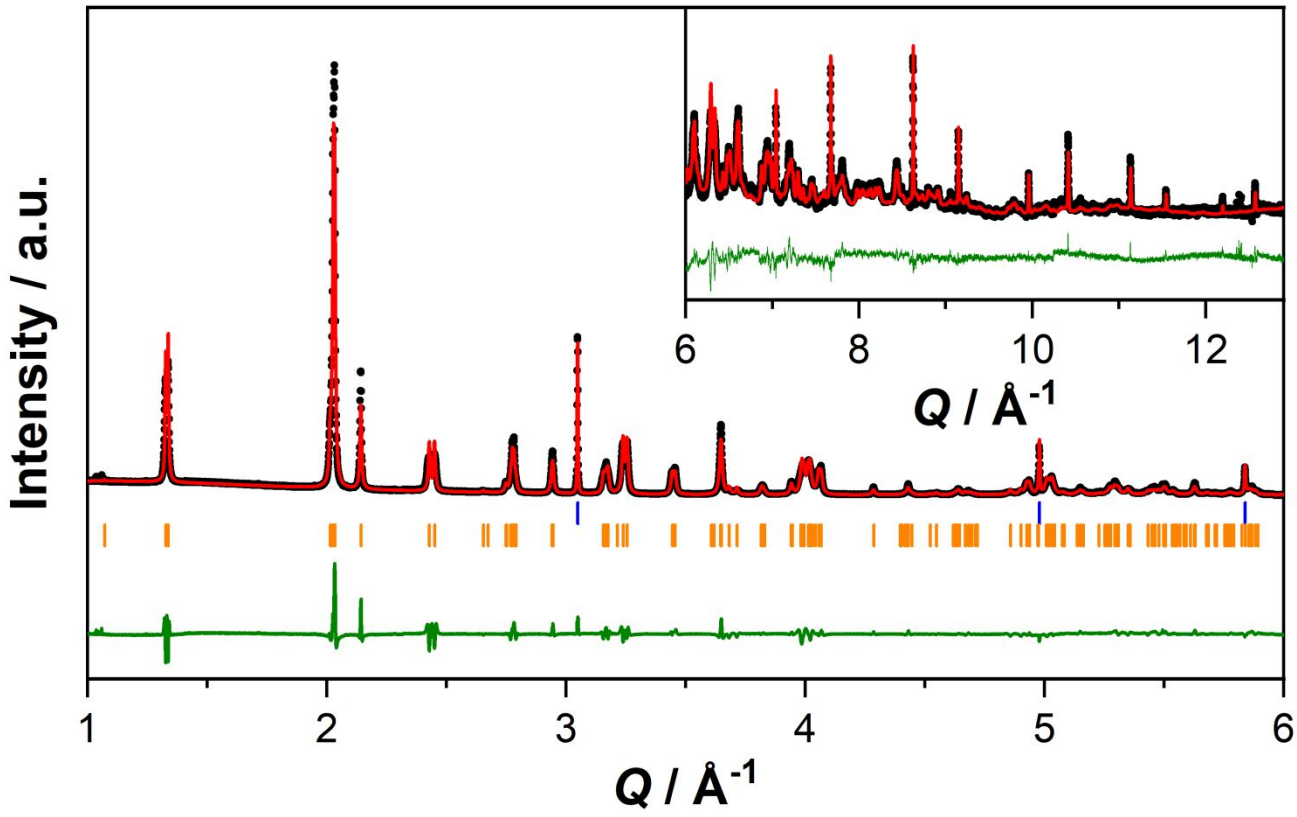

Figure S4: Synchrotron X-ray diffraction data for $BiVO_4$ at 502 K, collected on the Powder Diffraction beamline at the Australian Synchrotron (λ = 0.59007 Å, 21.0 keV). The sample was diluted with diamond powder in a 50:50 by weight ratio. The black circles represent the collected data, the red line represents the Rietveld refinement to the monoclinic fergusonite model, the green line represents the difference between the fit and the data, and the blue and orange ticks represent the *hkl* space group-allowed reflections of the diamond ($Fm\bar{3}m$) and $BiVO_4$ ($I2/b$) respectively.

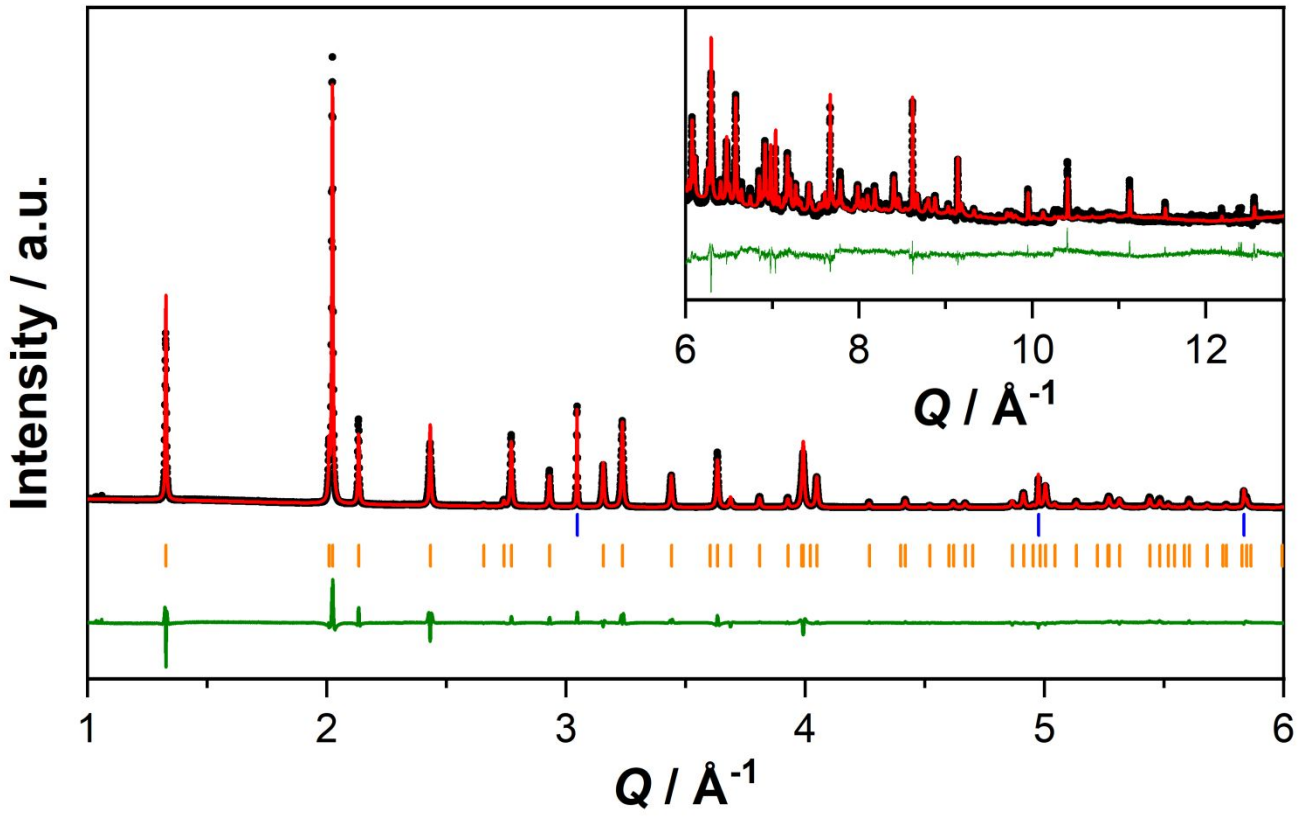

Figure S5: Synchrotron X-ray diffraction data for $BiVO_4$ at 743 K, collected on the Powder Diffraction beamline at the Australian Synchrotron (λ = 0.59007 Å, 21.0 keV). The sample was diluted with diamond powder in a 50:50 by weight ratio. The black circles represent the collected data, the red line represents the Rietveld refinement to the tetragonal scheelite model, the green line represents the difference between the fit and the data, and the blue and orange ticks represent the *hkl* space group-allowed reflections of the diamond ($Fm\bar{3}m$) and $BiVO_4$ ($I4_1/a$) respectively.

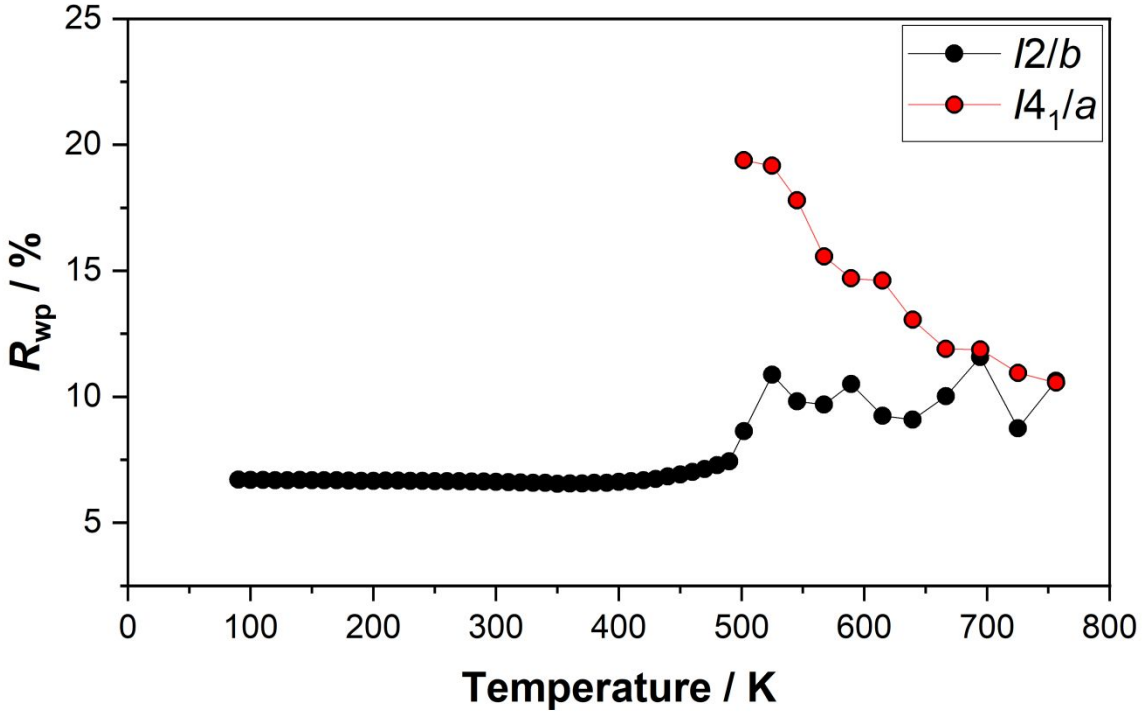

Figure S6: Weighted profile (R_{wp}) exported from the Rietveld refinements of $BiVO_4$ using synchrotron X-ray diffraction data for $BiVO_4$ collected on the Powder Diffraction beamline at the Australian Synchrotron. The black circles represent fits to the monoclinic fergusonite *I*2/*b* model, whereas the red circles represent fits to the tetragonal scheelite *I*4_1/*a* model.

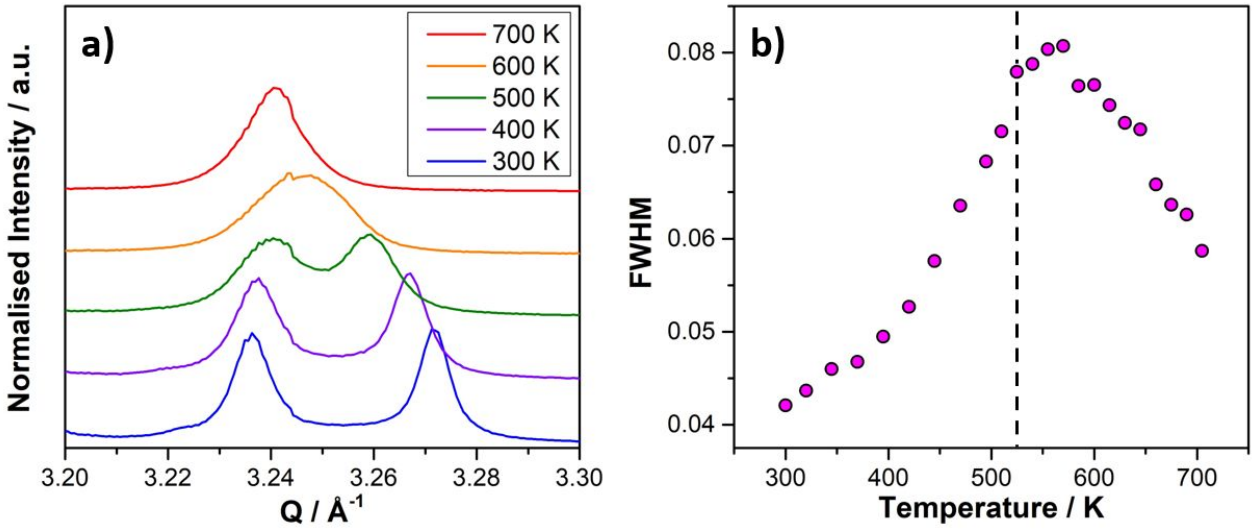

Figure S7: (a) Synchrotron X-ray diffraction data for $BiVO_4$ heating from 300-700 K, highlighting the (200) and (020) reflections in the low-temperature data and the (004) reflection in the high-temperature data. (b) The plotted

full width at half maximum of the reflections across the temperature range, fitted using two Gaussians of equal width. The dotted line indicates the monoclinic fergusonite *I*2/*b* to tetragonal scheelite $I4_1/a$ phase transition.

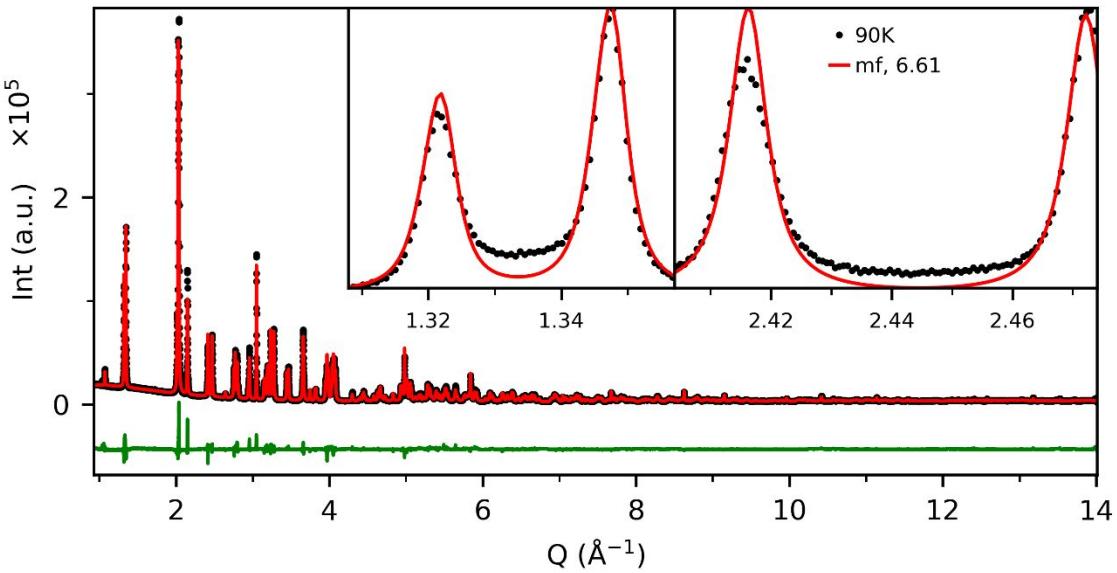

Figure S8: Synchrotron X-ray diffraction data for $BiVO_4$ at 90 K, collected on the Powder Diffraction beamline at the Australian Synchrotron (λ = 0.59007 Å, 21.0 keV). The sample was diluted with diamond powder in a 50:50 by weight ratio. The black circles represent the collected data, the red line represents the Rietveld refinement to the monoclinic fergusonite model, the green line represents the difference between the fit and the data. The insets show the $(101)_{mf}$ and $(011)_{mf}$ reflections, and the $(200)_{mf}$ and $(020)_{mf}$ reflections.

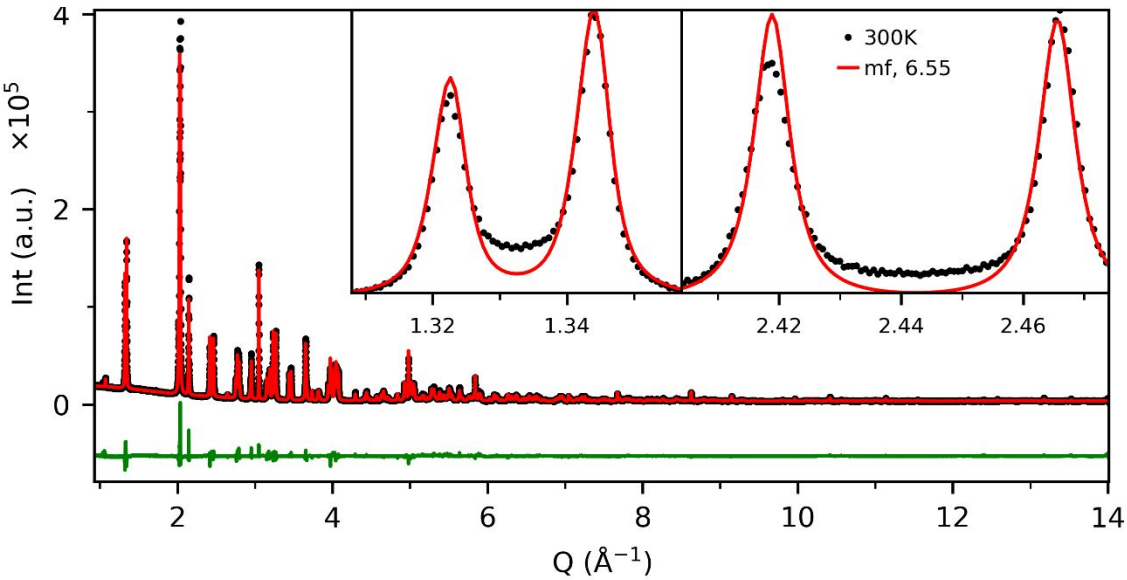

Figure S9: Synchrotron X-ray diffraction data for $BiVO_4$ at 300 K, collected on the Powder Diffraction beamline at the Australian Synchrotron (λ = 0.59007 Å, 21.0 keV). The sample was diluted with diamond powder in a 50:50 by weight ratio. The black circles represent the collected data, the red line represents the Rietveld refinement to the monoclinic fergusonite model, the green line represents the difference between the fit and the data. The insets show the $(101)_{mf}$ and $(011)_{mf}$ reflections, and the $(200)_{mf}$ and $(020)_{mf}$ reflections.

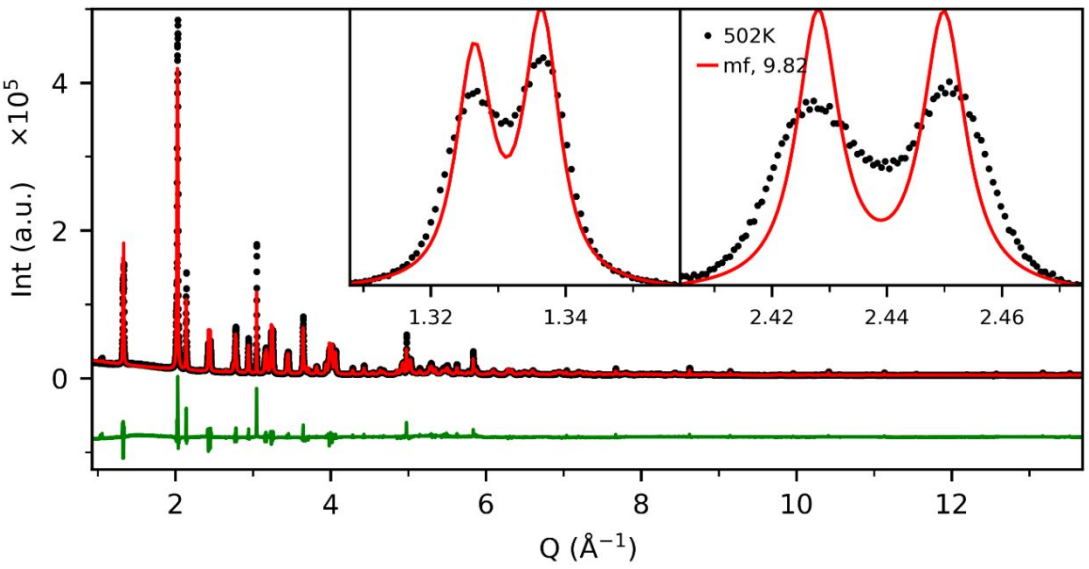

Figure S10: Synchrotron X-ray diffraction data for $BiVO_4$ at 502 K, collected on the Powder Diffraction beamline at the Australian Synchrotron (λ = 0.59007 Å, 21.0 keV). The sample was diluted with diamond powder in a 50:50 by weight ratio. The black circles represent the collected data, the red line represents the Rietveld refinement to the monoclinic fergusonite model, the green line represents the difference between the fit and the data. The insets show the $(101)_{mf}$ and $(011)_{mf}$ reflections, and the $(200)_{mf}$ and $(020)_{mf}$ reflections.

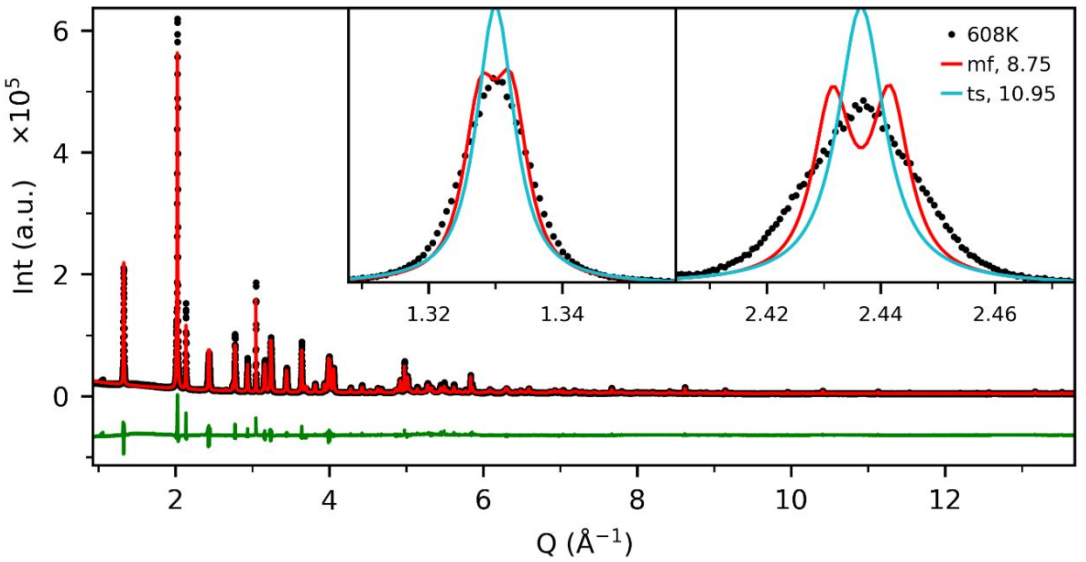

Figure S11: Synchrotron X-ray diffraction data for $BiVO_4$ at 608 K, collected on the Powder Diffraction beamline at the Australian Synchrotron (λ = 0.59007 Å, 21.0 keV). The sample was diluted with diamond powder in a 50:50 by weight ratio. The black circles represent the collected data, the red line represents the Rietveld refinement to the monoclinic fergusonite model, the blue line represents the Rietveld refinement to the tetragonal scheelite model, the green line represents the difference between the monoclinic fergusonite fit and the data. The insets

show the $(101)_{mf}$ and $(011)_{mf}$ reflections along with the $(101)_{ts}$ reflection, and the $(200)_{mf}$ and $(020)_{mf}$ reflections along with the $(200)_{ts}$ reflection.

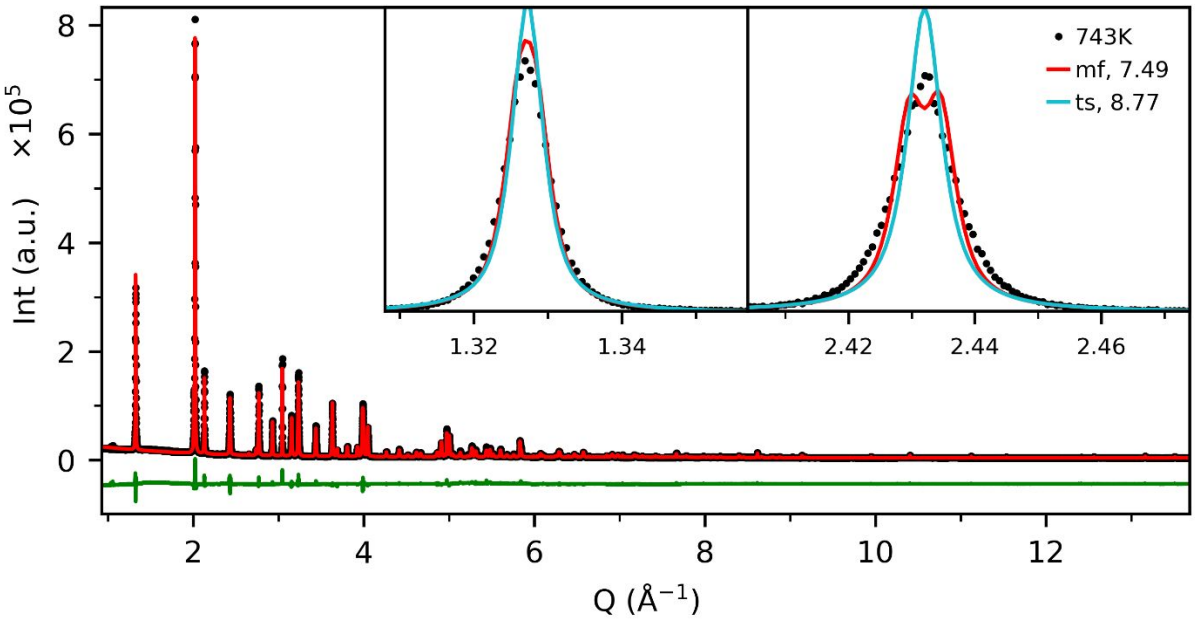

Figure S12: Synchrotron X-ray diffraction data for $BiVO_4$ at 743 K, collected on the Powder Diffraction beamline at the Australian Synchrotron (λ = 0.59007 Å, 21.0 keV). The sample was diluted with diamond powder in a 50:50 by weight ratio. The black circles represent the collected data, the red line represents the Rietveld refinement to the monoclinic fergusonite model, the blue line represents the Rietveld refinement to the tetragonal scheelite model, the green line represents the difference between the monoclinic fergusonite fit and the data. The insets show the $(101)_{mf}$ and $(011)_{mf}$ reflections along with the $(101)_{ts}$ reflection, and the $(200)_{mf}$ and $(020)_{mf}$ reflections along with the $(200)_{ts}$ reflection.

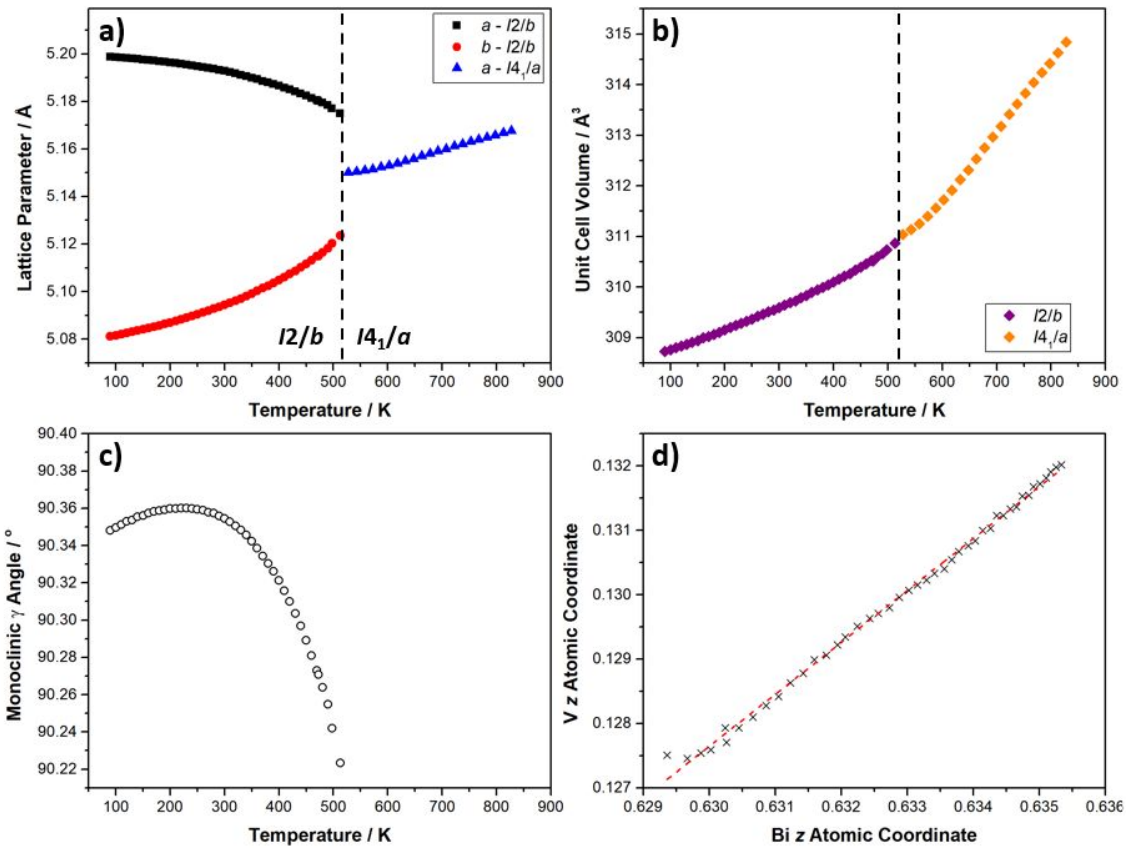

Figure S13: Rietveld refinements for the synchrotron X-ray diffraction variable temperature dataset of $BiVO_4$, with (a) the *a* and *c* lattice parameters, (b) the unit cell volume, (c) the monoclinic *γ* angle, and (d) the *z* atomic coordinates of Bi^{3+} and V^{5+} plotted against each other. The black dashed line represents the temperature of the monoclinic fergusonite *I*2/*b* to tetragonal scheelite *I*4_1/*a* phase transition, and the red dashed line is a linear fit (zPosV = 0.824*zPosBi – 0.3915).

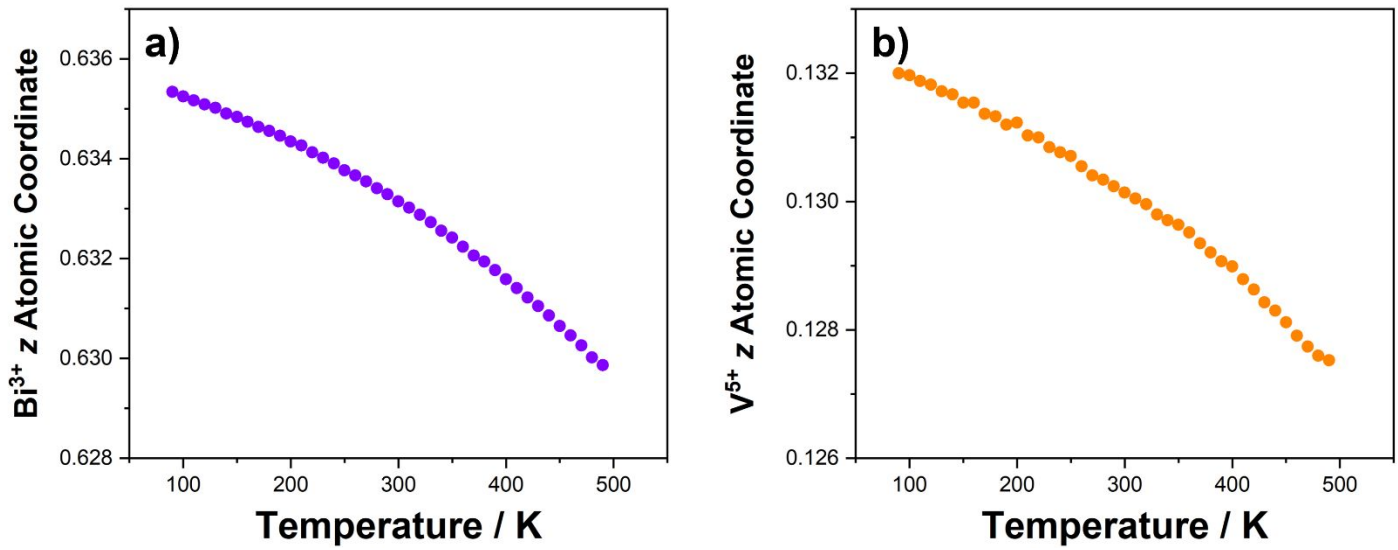

Figure S14: The atomic coordinates of (a) Bi^{3+} and (b) V^{5+} calculated from Rietveld refinements of the synchrotron X-ray diffraction variable temperature dataset of $BiVO_4$.

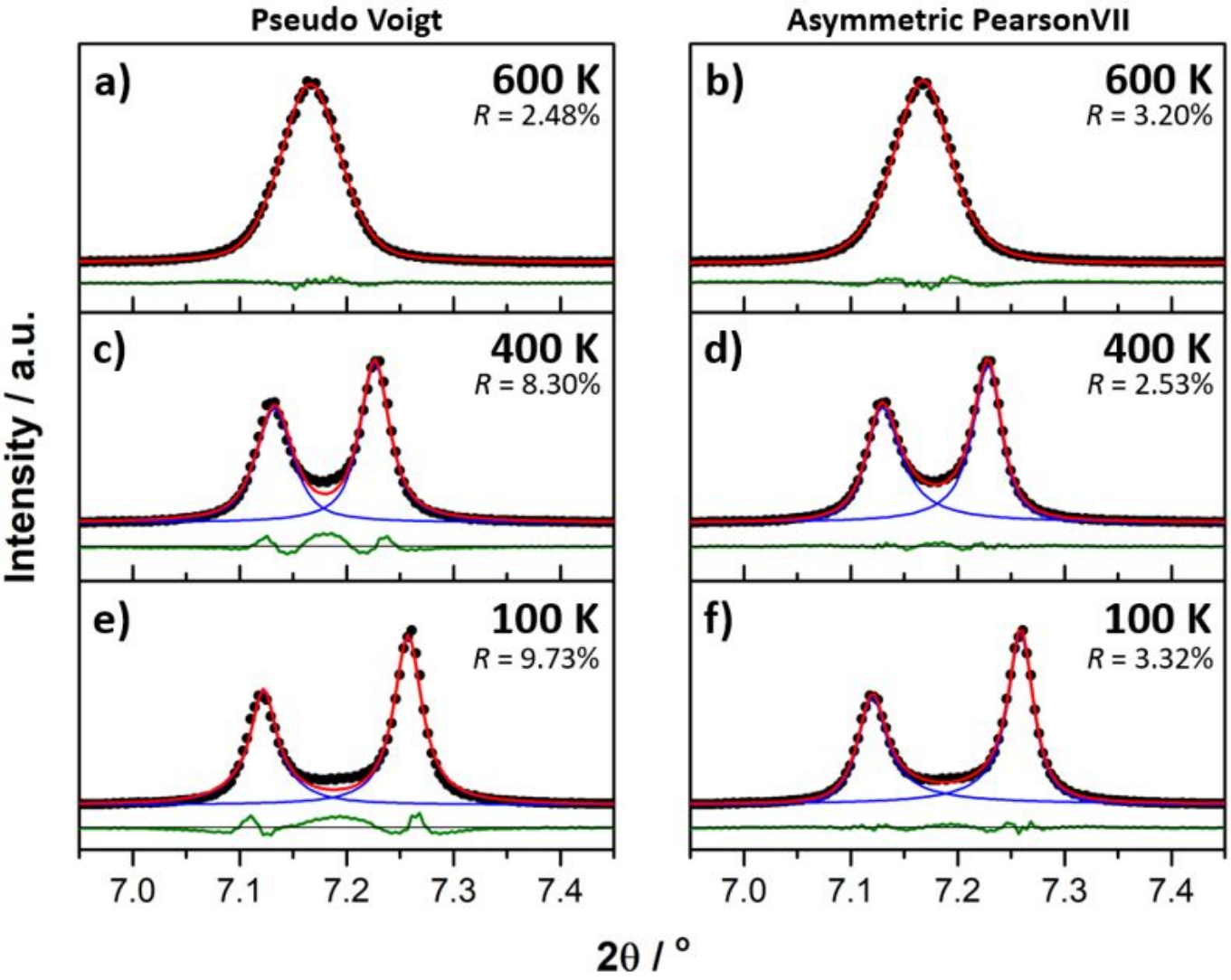

Figure S15: Individual peak shape fitting of the synchrotron X-ray powder diffraction peaks of $BiVO_4$. (a,c,e) Performed using the standard pseudo Voigt function and (b,d,f) the same temperature using the asymmetric PearsonVII model used to model domain wall contributions.

The *R* factor is calculated using

$$R = \sqrt{\frac{\sum |y_{\text{obs.}} - y_{\text{calc.}}|^2}{\sum |y_{\text{obs.}}|^2}}\ \%. \qquad \text{(S1)}$$

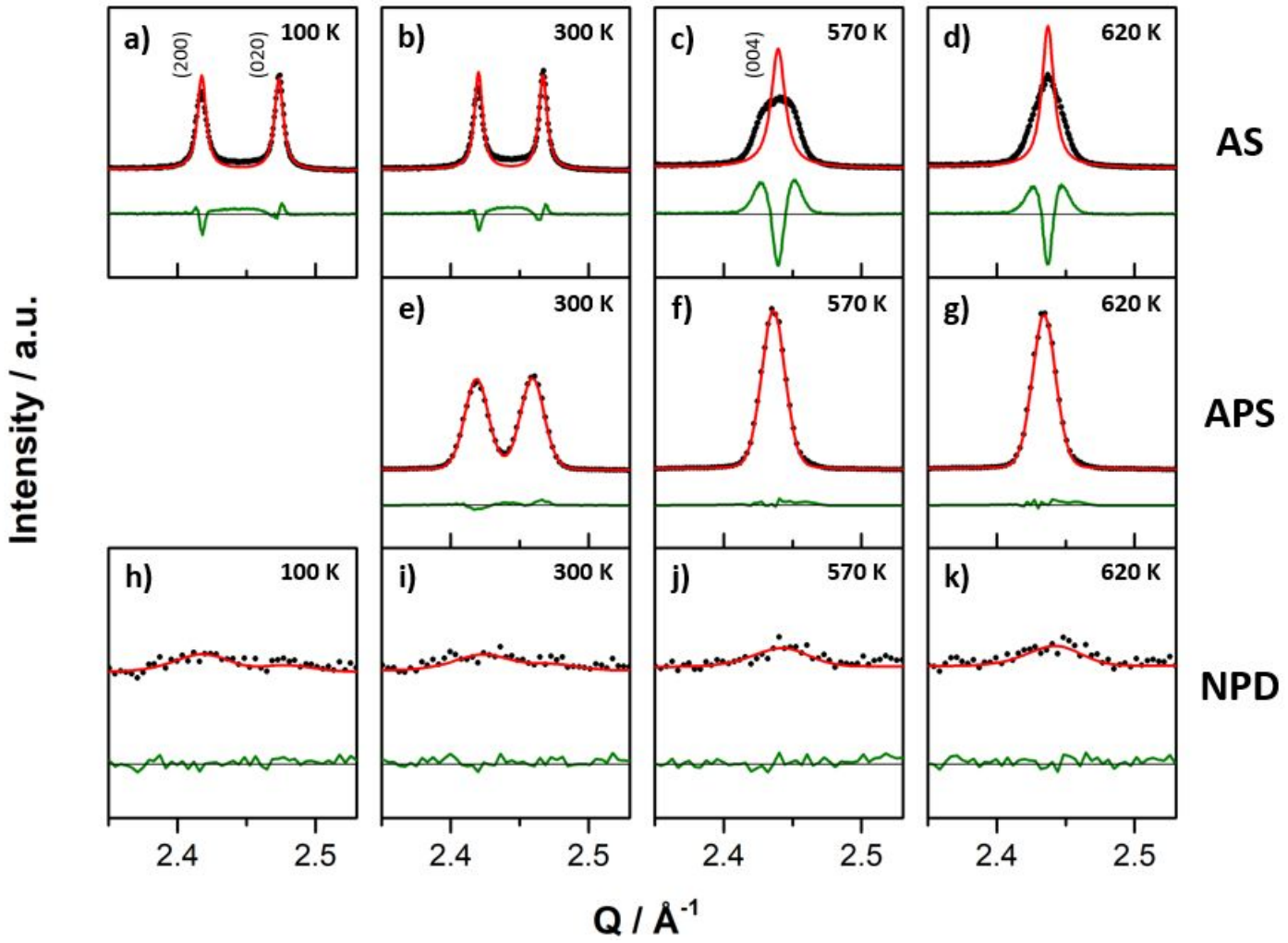

Figure S16: Rietveld refinements to the variable temperature datasets of $BiVO_4$ collected using (a-d) the Powder Diffraction beamline at the Australian Synchrotron, (e-g) the 11-ID-B beamline at the Advanced Photon Source, and (h-k) the Wombat instrument at the Australian Centre for Neutron Scattering. The black circles represent the data, the red lines represent the calculated profile, and the green line represents the difference between the data and the calculated profile.

Synchrotron X-Ray Diffraction Data – Advanced Photon Source

X-ray total scattering measurements for $BiVO_4$ were performed on beamline 11-ID-B of the Advanced Photon Source at Argonne National Laboratory (λ = 0.2115 Å, 58.62 keV). A small amount of finely ground sample was loaded into a borosilicate glass capillary (inner diameter 0.7 mm) to a height of 3 cm. Data were collected under ambient conditions for the sample, an empty capillary, and the empty sample environment. The sample was loaded into a flow-cell furnace and heated from 400–630 K before being cooled.[1] During heating, the 2D area detected was placed far from the sample (1000 mm), yielding data suitable for Rietveld refinement, whereas, during cooling, the detector was placed close to the sample (180 mm) for XPDF data collection. The 2D image data were corrected for polarization, detector transmission, and flat field, with poorly performing pixels masked before integration to 1D using the GSAS-II program.[2] The XPDF $G(r)$ were calculated using the PDFgetX3 software from the xPDFsuite.[3, 4] Calculations were performed using a Q_{max} of 14.2 $Å^{-1}$.

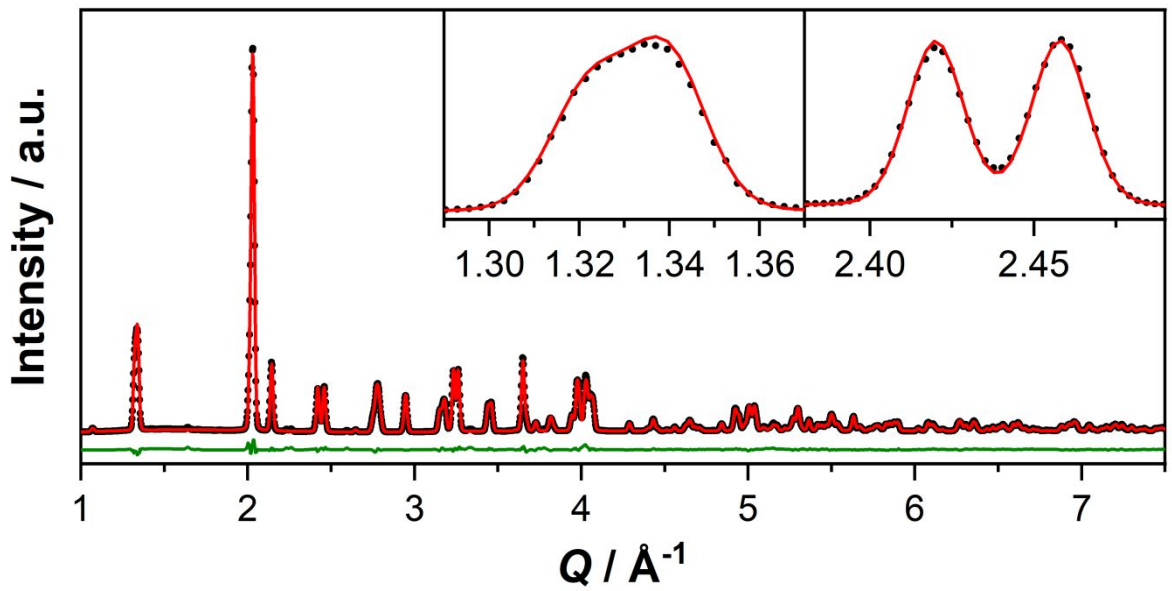

Figure S17: Synchrotron X-ray diffraction data for $BiVO_4$ at 400 K, collected on the 11-ID-B beamline at the Advanced Photon Source at Argonne National Laboratory (λ = 0.2116 Å, 58.6 keV). The black circles represent the collected data, the red line represents the Rietveld refinement to the monoclinic fergusonite model, the green line represents the difference between the fit and the data. The insets show the $(101)_{mf}$ and $(011)_{mf}$ reflections, and the $(200)_{mf}$ and $(020)_{mf}$ reflections.

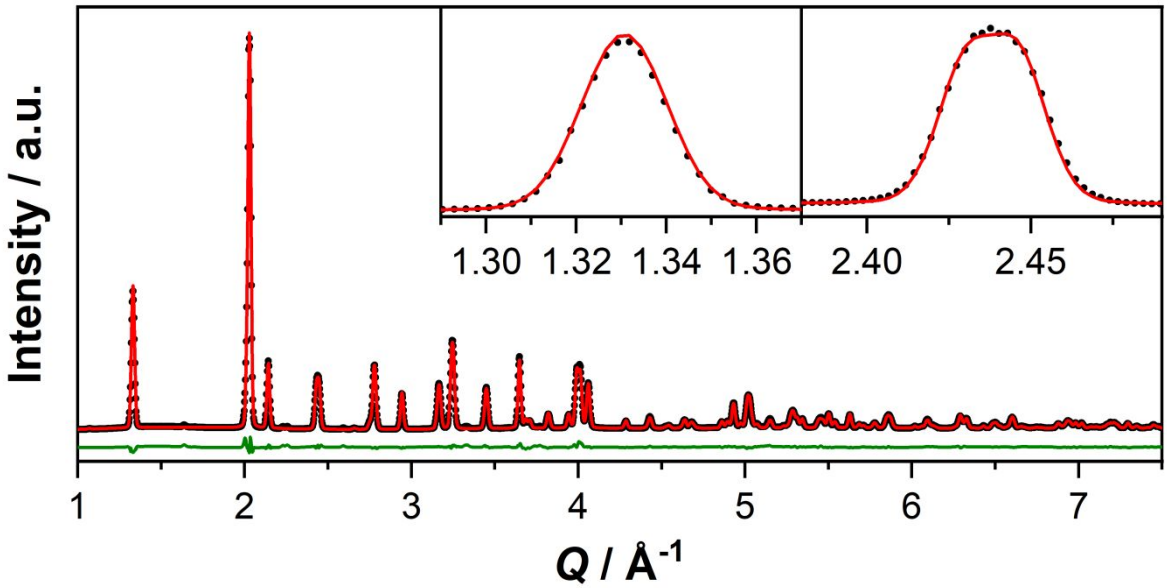

Figure S18: Synchrotron X-ray diffraction data for $BiVO_4$ at 500 K, collected on the 11-ID-B beamline at the Advanced Photon Source at Argonne National Laboratory (λ = 0.2116 Å, 58.6 keV). The black circles represent the collected data, the red line represents the Rietveld refinement to the monoclinic fergusonite model, the green line represents the difference between the fit and the data. The insets show the $(101)_{mf}$ and $(011)_{mf}$ reflections, and the $(200)_{mf}$ and $(020)_{mf}$ reflections.

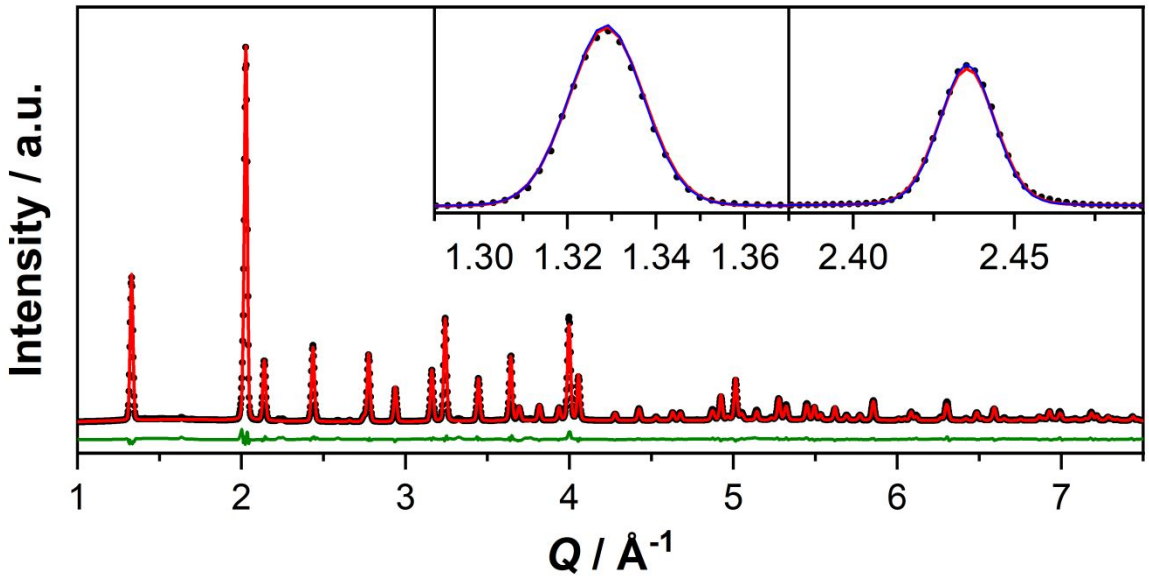

Figure S19: Synchrotron X-ray diffraction data for $BiVO_4$ at 600 K, collected on the 11-ID-B beamline at the Advanced Photon Source at Argonne National Laboratory (λ = 0.2116 Å, 58.6 keV). The black circles represent the collected data, the red line represents the Rietveld refinement to the monoclinic fergusonite model, the blue line represents the Rietveld refinement to the tetragonal scheelite model, the green line represents the difference

between the fit and the data. The insets show the $(101)_{mf}$ and $(011)_{mf}$ reflections along with the $(101)_{ts}$ reflection, and the $(200)_{mf}$ and $(020)_{mf}$ reflections along with the $(200)_{ts}$ reflection.

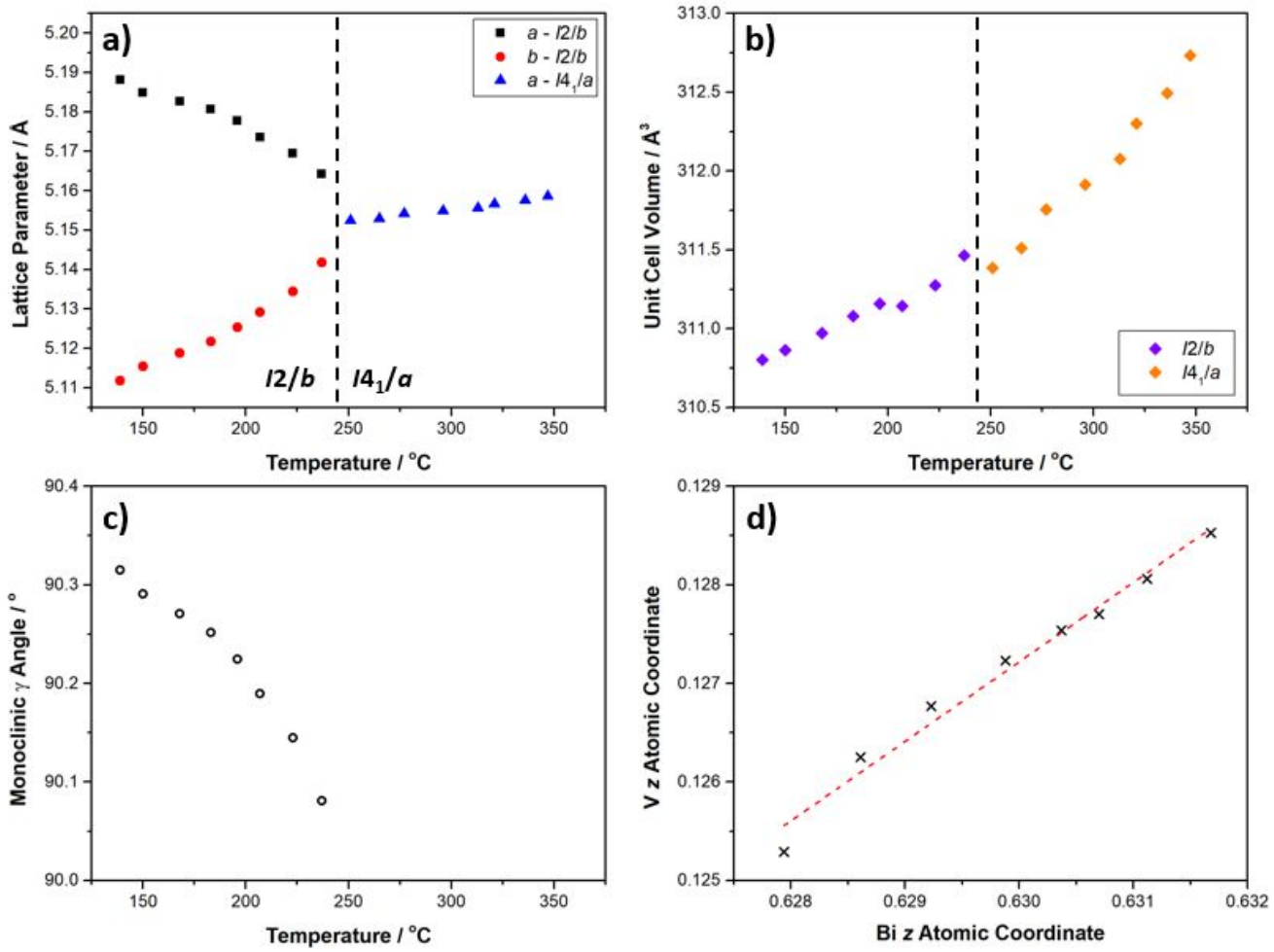

Figure S20: Rietveld refinements for the synchrotron X-ray diffraction variable temperature dataset of $BiVO_4$, with (a) the *a* and *c* lattice parameters, (b) the unit cell volume, (c) the monoclinic *γ* angle, and (d) the *z* atomic coordinates of Bi^{3+} and V^{5+} plotted against each other. The black dashed line represents the temperature of the monoclinic fergusonite *I*2/*b* to tetragonal scheelite $I4_1/a$ phase transition, and the red dashed line is a linear fit.

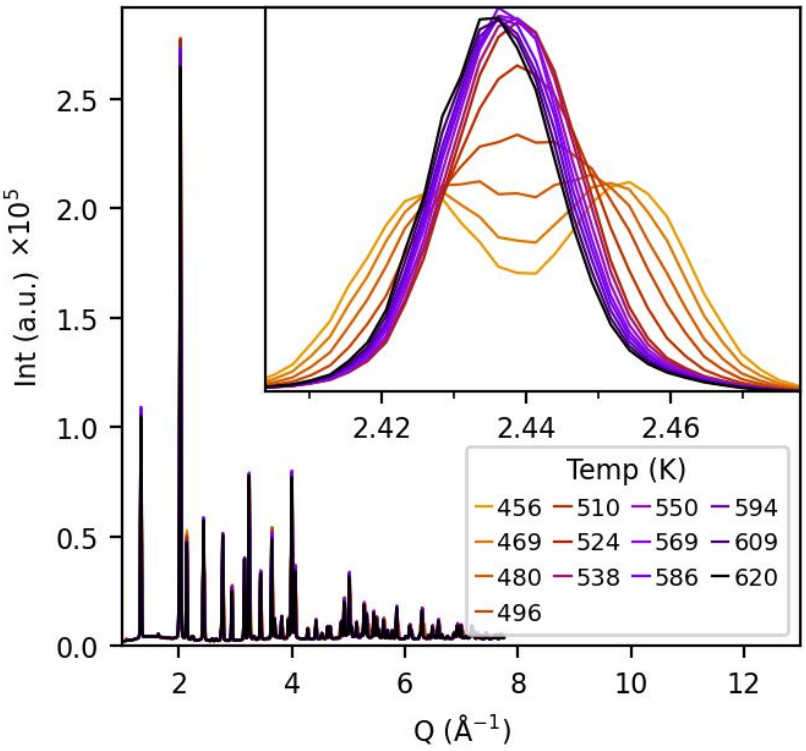

Figure S21: Variable temperature synchrotron X-ray diffraction pattern of $BiVO_4$ collected at 11-ID-B at the Advanced Light Source. The inset shows the $(200)_{mf}$ and $(020)_{mf}$ reflections merging to form the $(004)_{ts}$ reflection across the monoclinic fergusonite *I*2/*b* to tetragonal scheelite *I*4$_1$/*a* structure.

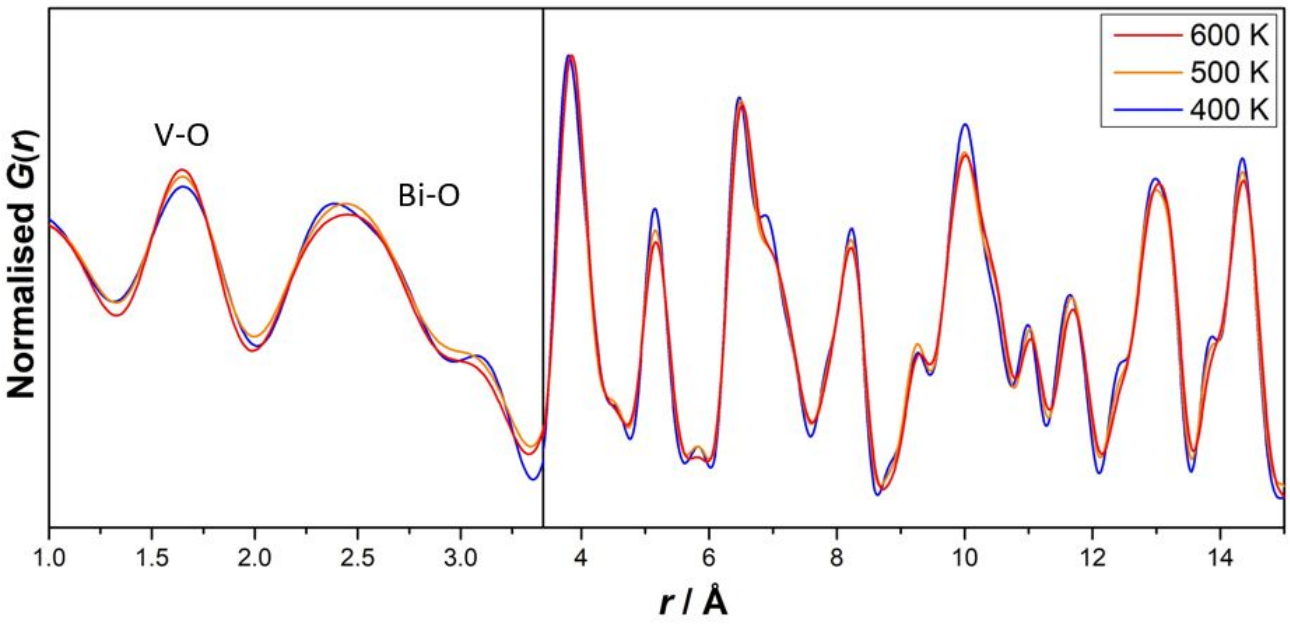

Figure S22: X-ray pair distribution function data for $BiVO_4$. The data were taken at 400 K (blue), 500 K (orange), and 600 K (red).

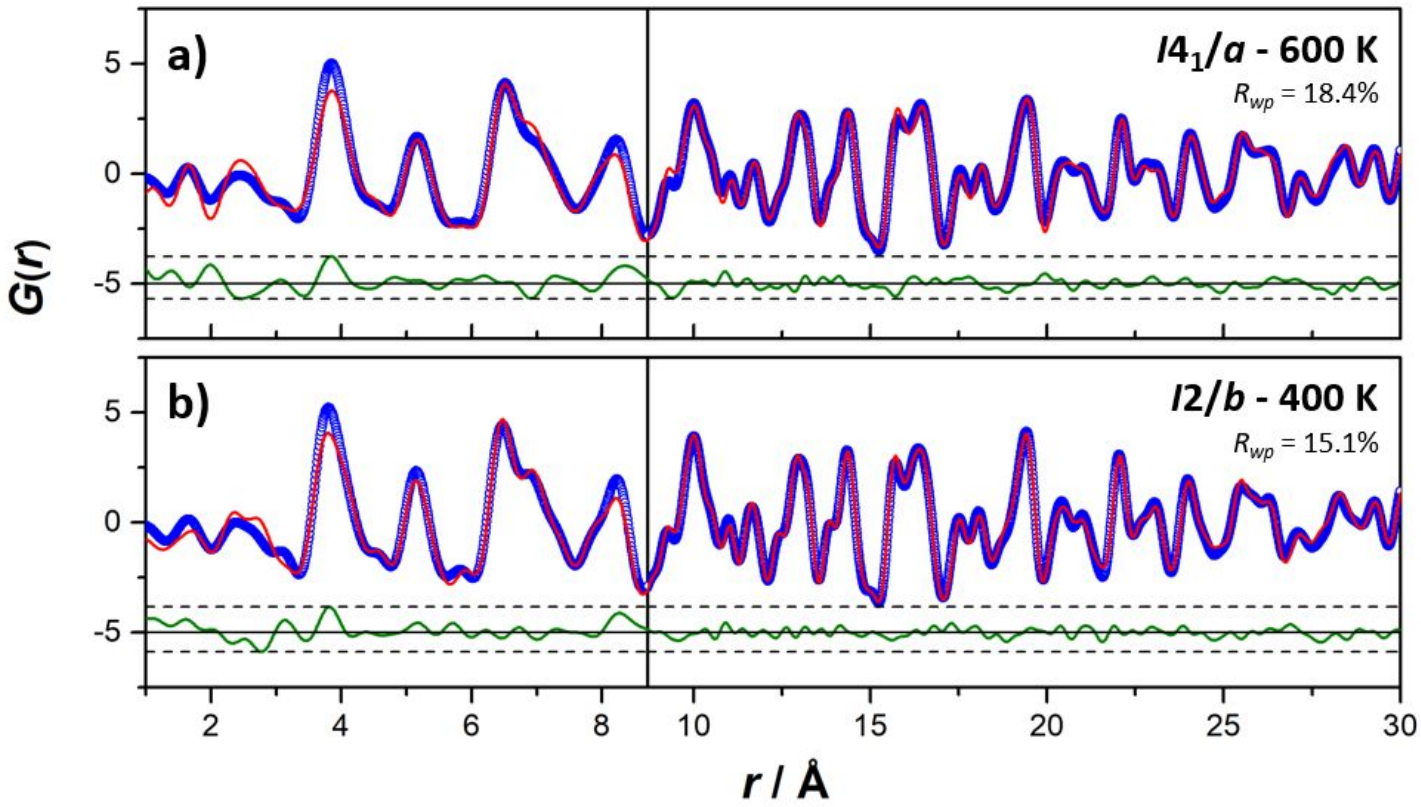

Figure S23: X-ray pair distribution function fits for the variable temperature dataset of $BiVO_4$ over a range of 1.0-30 Å. Data taken at (a) 600 K and fit to the tetragonal scheelite $I4_1/a$ model, and (b) 400 K fit to the monoclinic fergusonite $I2/b$ model. The blue circles represent the measured data, the solid red line represents the calculated profile, the green line represents the difference between the observed and calculated profiles.

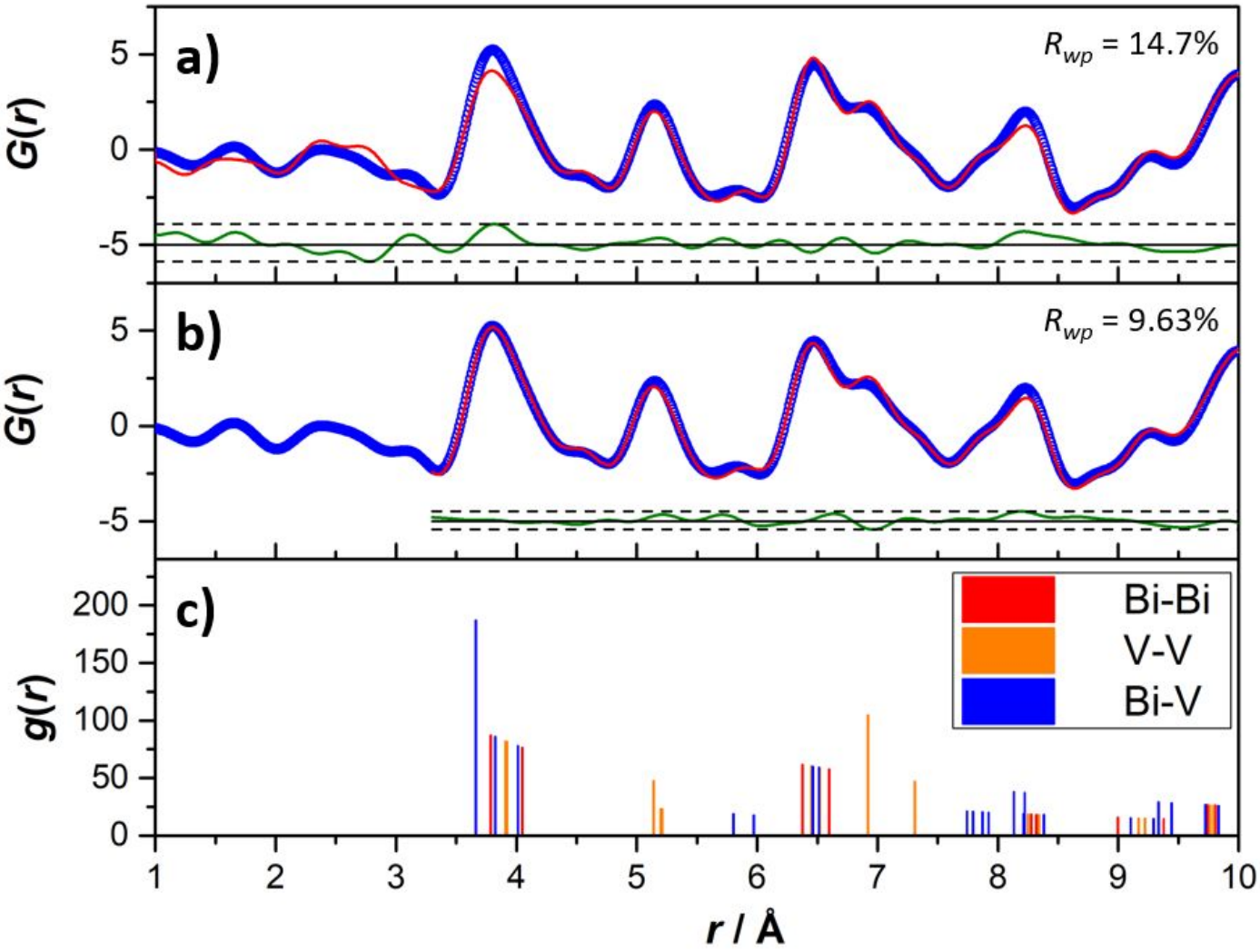

Figure S24: X-ray pair distribution function data for $BiVO_4$ at 400 K fitted over a range of (a) 1.0-30 Å and (b) 3.3-30 Å . (c) The calculated partial fits, with focus placed on the cation-cation distances. The blue circles represent the measured data, the solid red line represents the calculated profile, the green line represents the difference between the observed and calculated profiles.

Neutron Powder Diffraction Data - Wombat

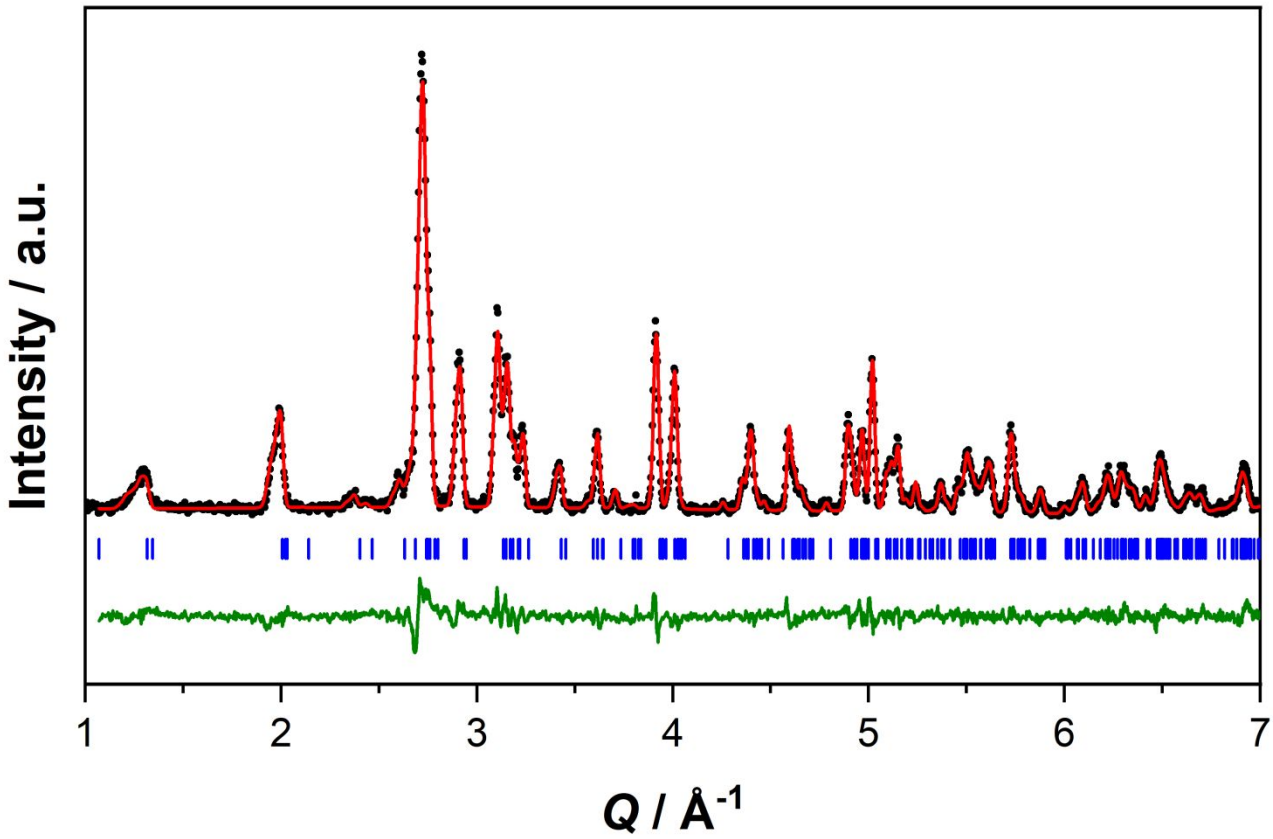

Figure S25: Neutron powder diffraction data for $BiVO_4$ at 50 K, collected on the Wombat instrument at the Australian Centre for Neutron Scattering (λ = 1.6 Å). The black circles represent the collected data, the red line represents the Rietveld refinement to the monoclinic fergusonite model, the green line represents the difference between the fit and the data, and the blue ticks represent the *hkl* space group-allowed reflections.

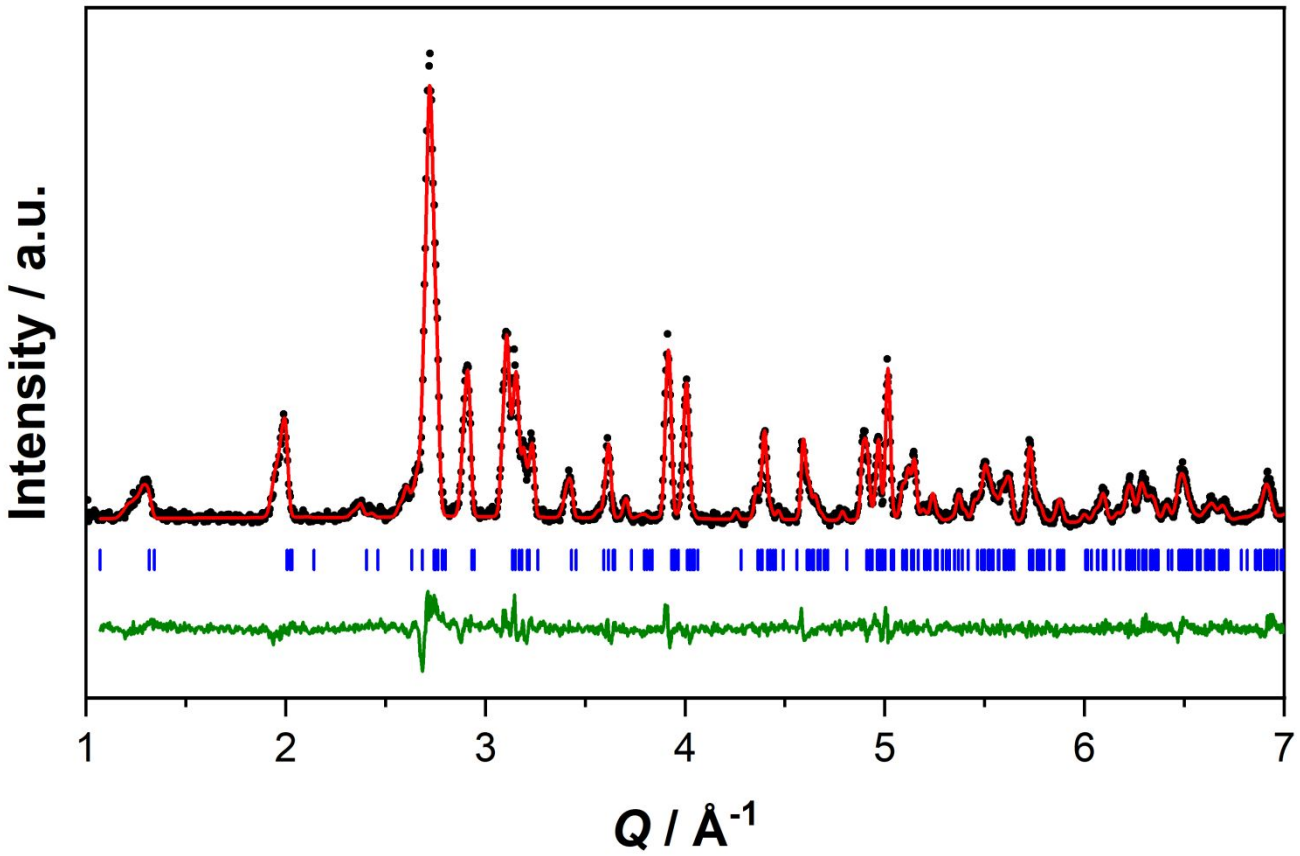

Figure S26: Neutron powder diffraction data for $BiVO_4$ at 150 K, collected on the Wombat instrument at the Australian Centre for Neutron Scattering (λ = 1.6 Å). The black circles represent the collected data, the red line represents the Rietveld refinement to the monoclinic fergusonite model, the green line represents the difference between the fit and the data, and the blue ticks represent the *hkl* space group-allowed reflections.

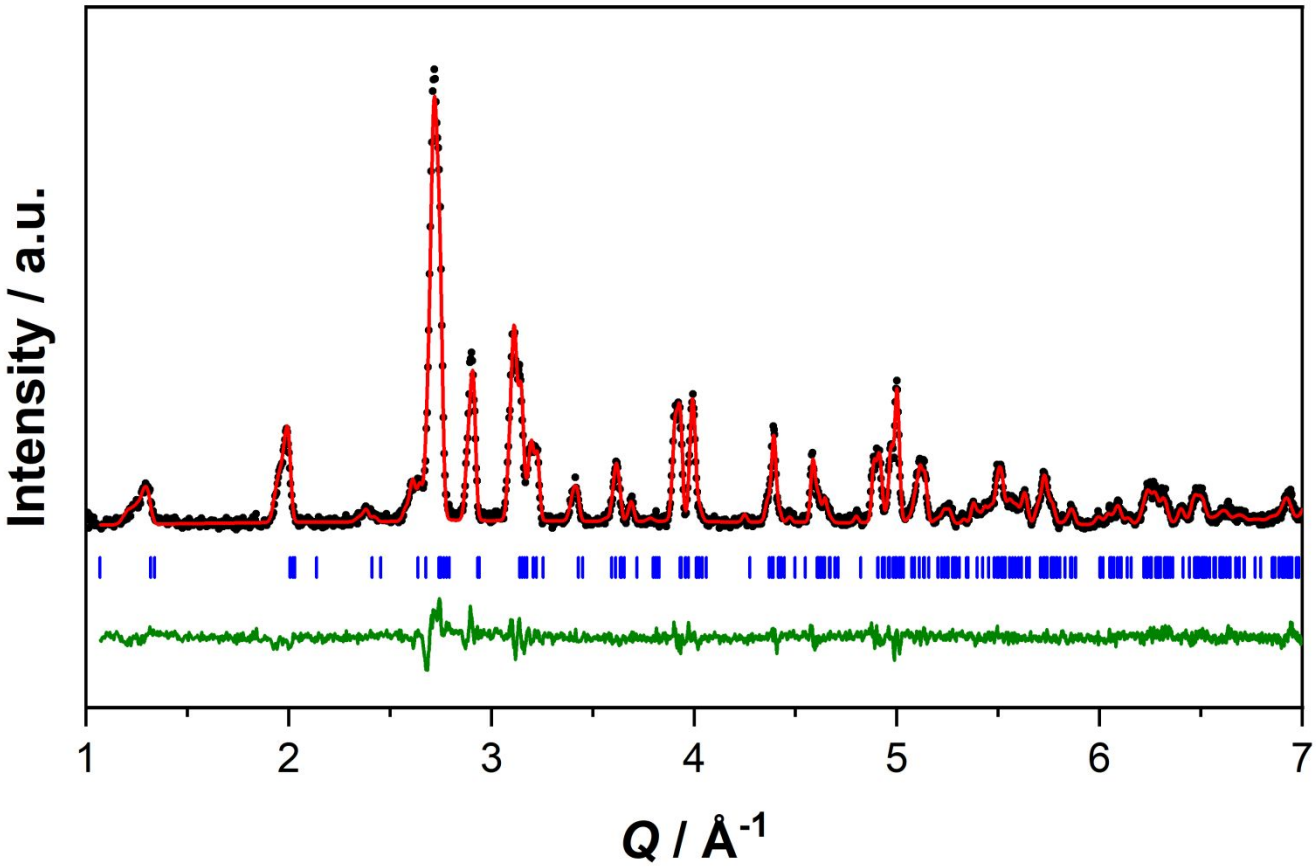

Figure S27: Neutron powder diffraction data for $BiVO_4$ at 350 K, collected on the Wombat instrument at the Australian Centre for Neutron Scattering (λ = 1.6 Å). The black circles represent the collected data, the red line represents the Rietveld refinement to the monoclinic fergusonite model, the green line represents the difference between the fit and the data, and the blue ticks represent the *hkl* space group-allowed reflections.

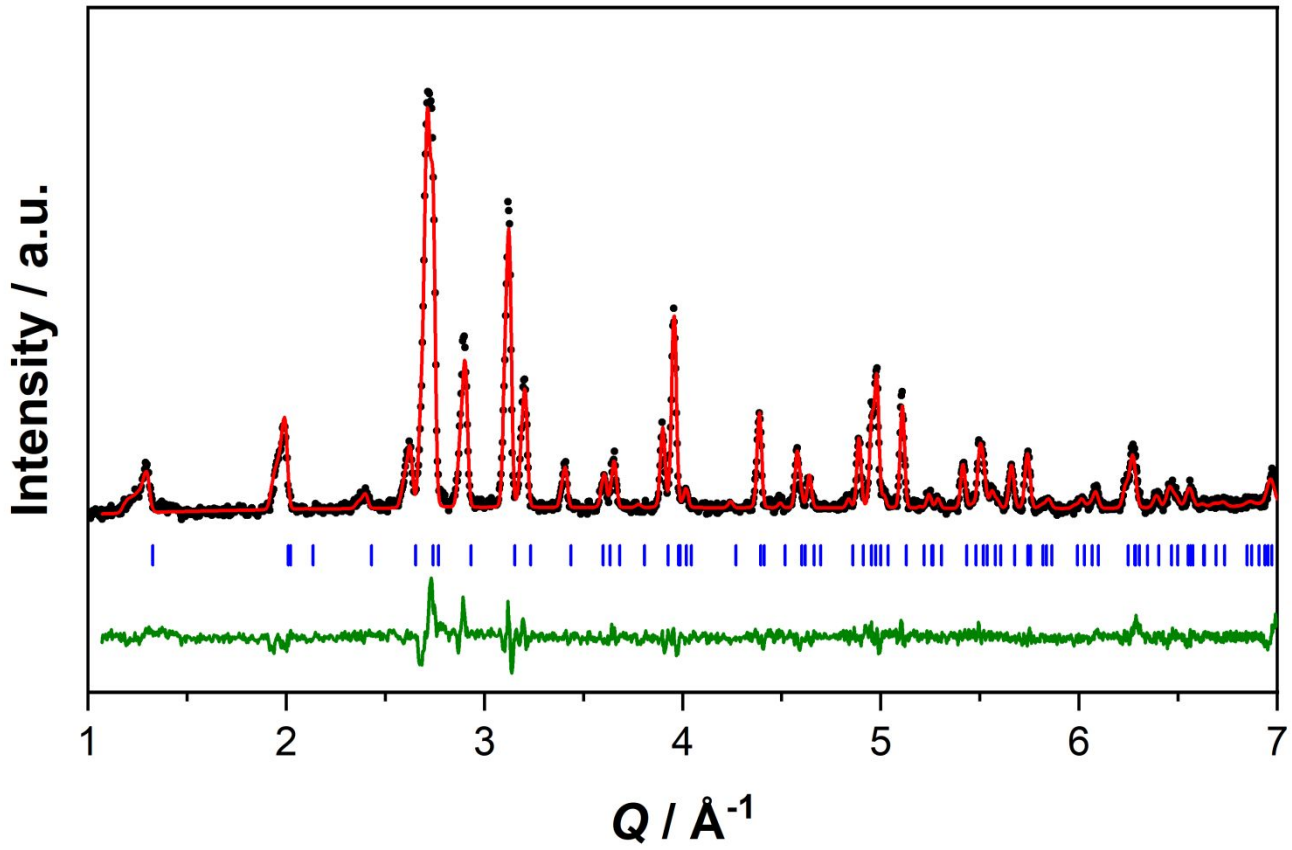

Figure S28: Neutron powder diffraction data for $BiVO_4$ at 550 K, collected on the Wombat instrument at the Australian Centre for Neutron Scattering (λ = 1.6 Å). The black circles represent the collected data, the red line represents the Rietveld refinement to the tetragonal scheelite model, the green line represents the difference between the fit and the data, and the blue ticks represent the *hkl* space group-allowed reflections.

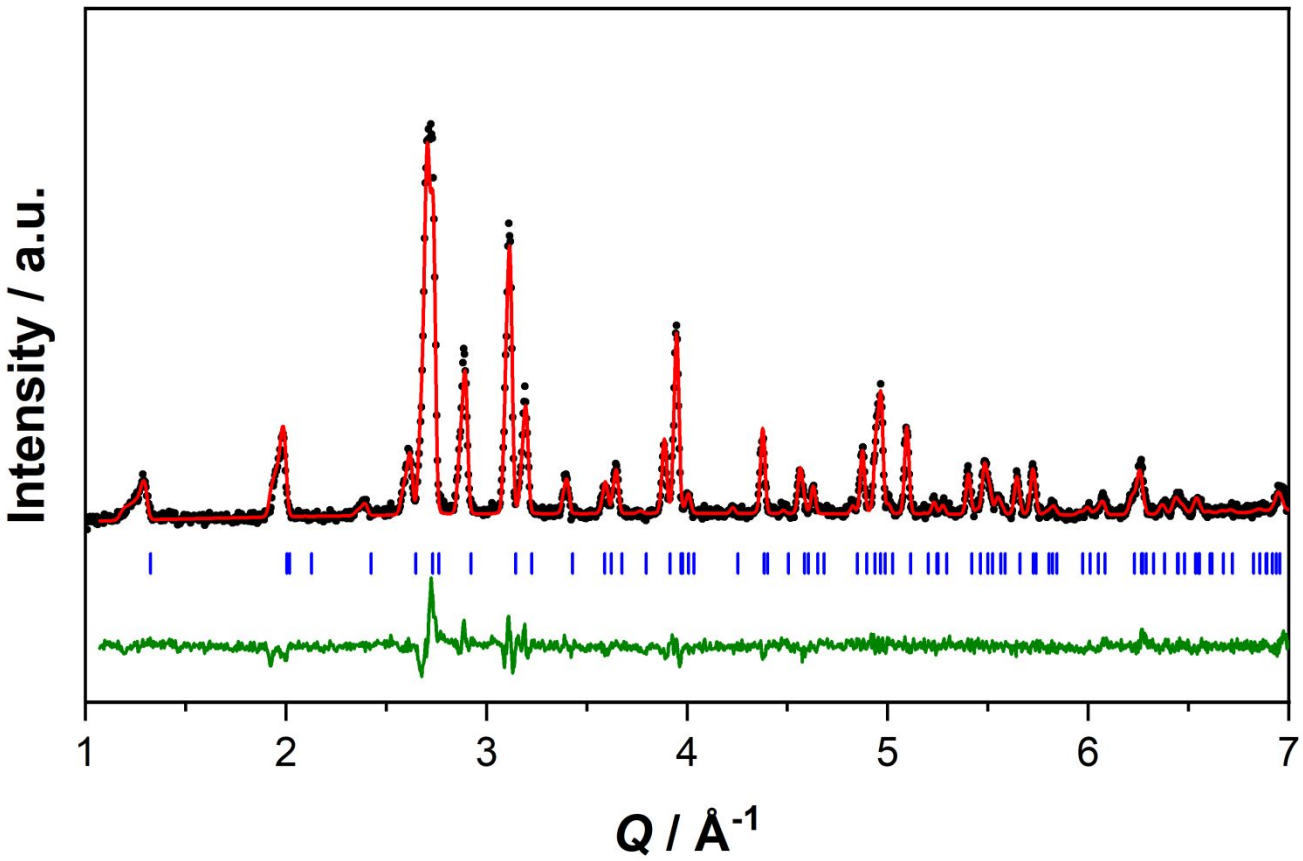

Figure S29: Neutron powder diffraction data for $BiVO_4$ at 750 K, collected on the Wombat instrument at the Australian Centre for Neutron Scattering (λ = 1.6 Å). The black circles represent the collected data, the red line represents the Rietveld refinement to the tetragonal scheelite model, the green line represents the difference between the fit and the data, and the blue ticks represent the *hkl* space group-allowed reflections.

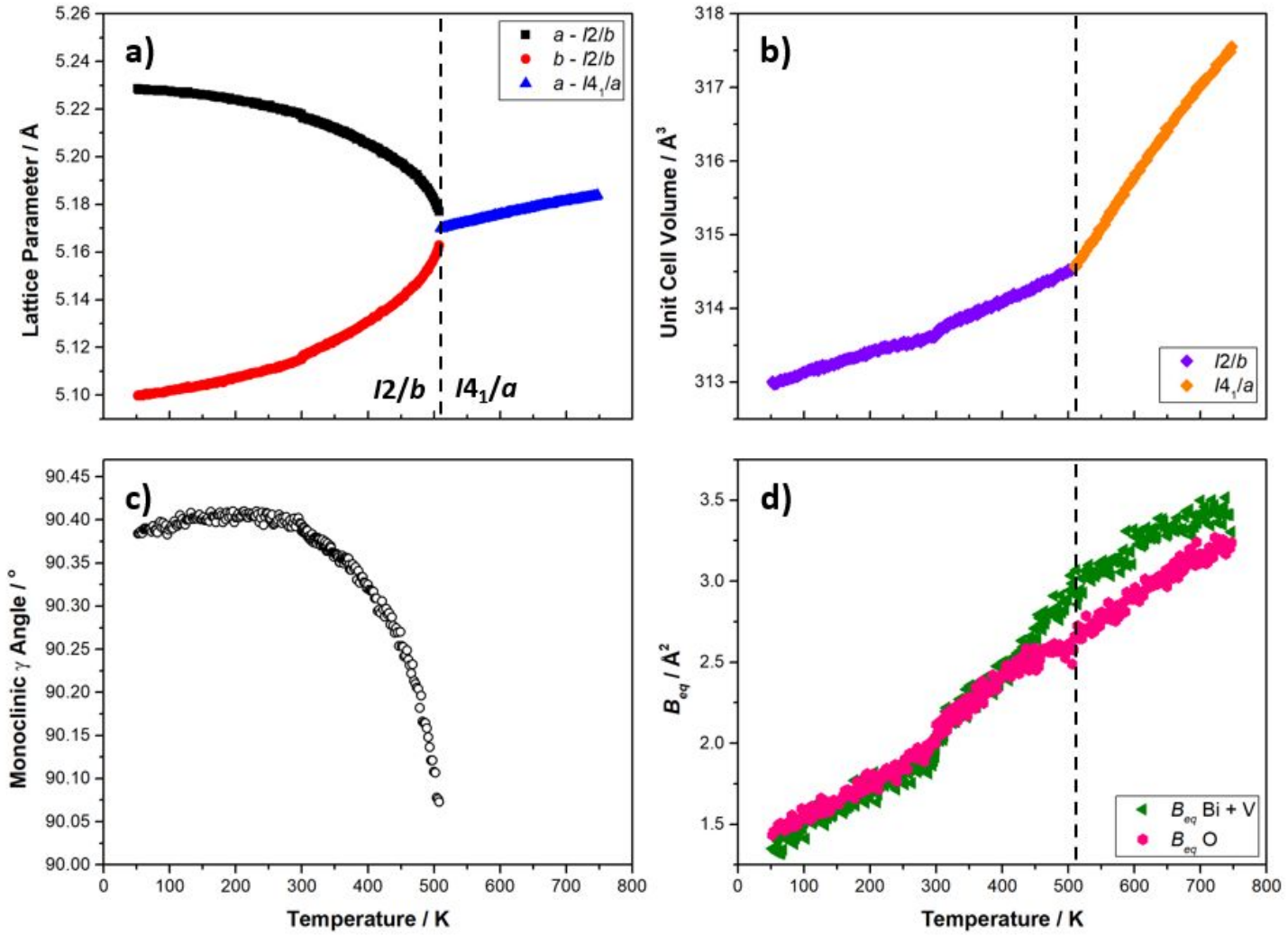

Figure S30: Rietveld refinements for the neutron powder diffraction variable temperature dataset of $BiVO_4$, with (a) the *a* and *c* lattice parameters, (b) the unit cell volume, (c) the monoclinic *γ* angle, and (d) the atomic displacement parameters of Bi + V, as well as O. The black dashed line represents the temperature of the monoclinic fergusonite *I*2/*b* to tetragonal scheelite *I*4$_1$/*a* phase transition.

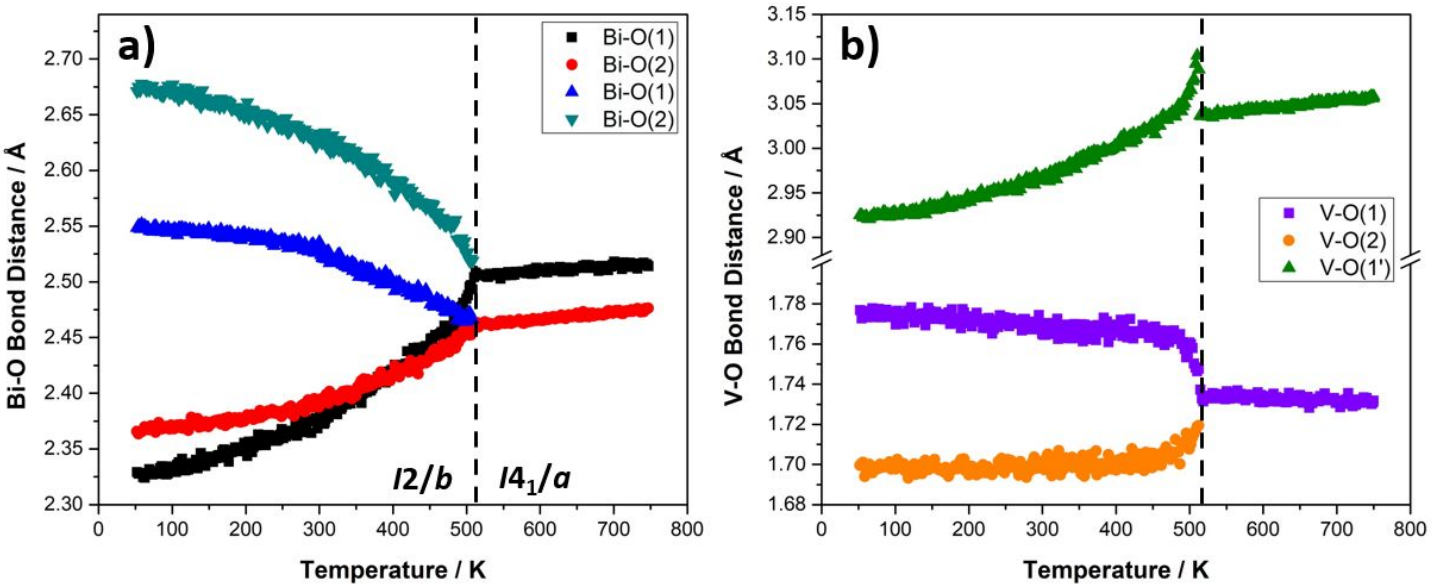

Figure S31: Temperature dependence of the (a) Bi-O bond distances and (b) V-O bond distances upon heating, as taken from Rietveld refinements to the neutron powder diffraction dataset. The dotted lines indicate the monoclinic fergusonite *I*2/*b* to tetragonal scheelite $I4_1/a$ phase transition.

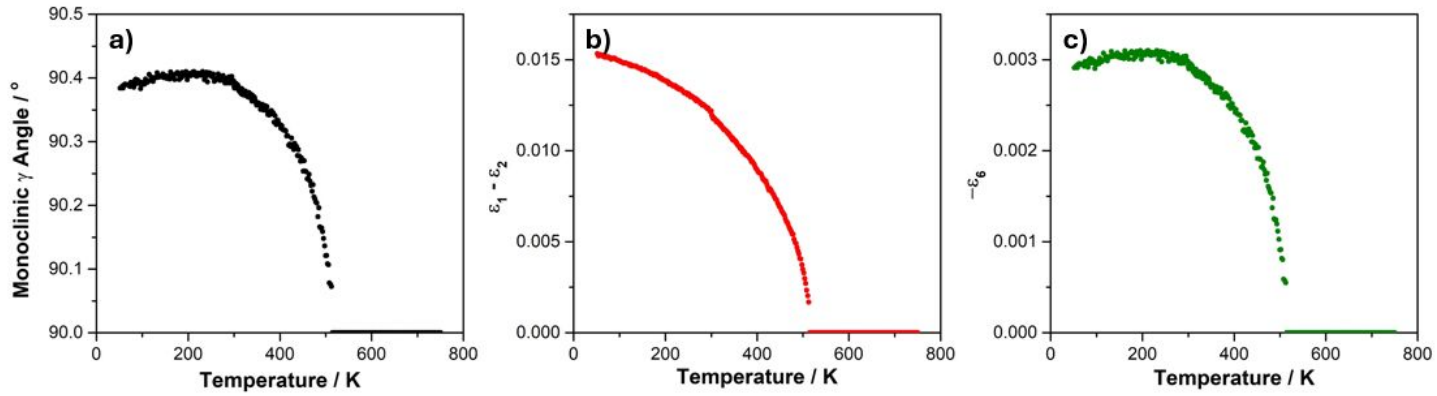

Figure S32: Parameters extrapolated from the Rietveld refinements of the variable temperature neutron powder diffraction dataset. (a) The monoclinic *γ* angle, (b) the $(\epsilon_1 - \epsilon_2)$ strain parameter, and (c) the ϵ_6 strain parameter.

The strain parameters are given as the following:

$$(\epsilon_1 - \epsilon_2) = \frac{2(a_m - b_m)}{a_0 + c_0} \quad \text{(S2)}$$

$$\epsilon_6 = \frac{cos\,\gamma_m(a_m + b_m)}{\sqrt{2}(a_0 + c_0)} \quad \text{(S3)}$$

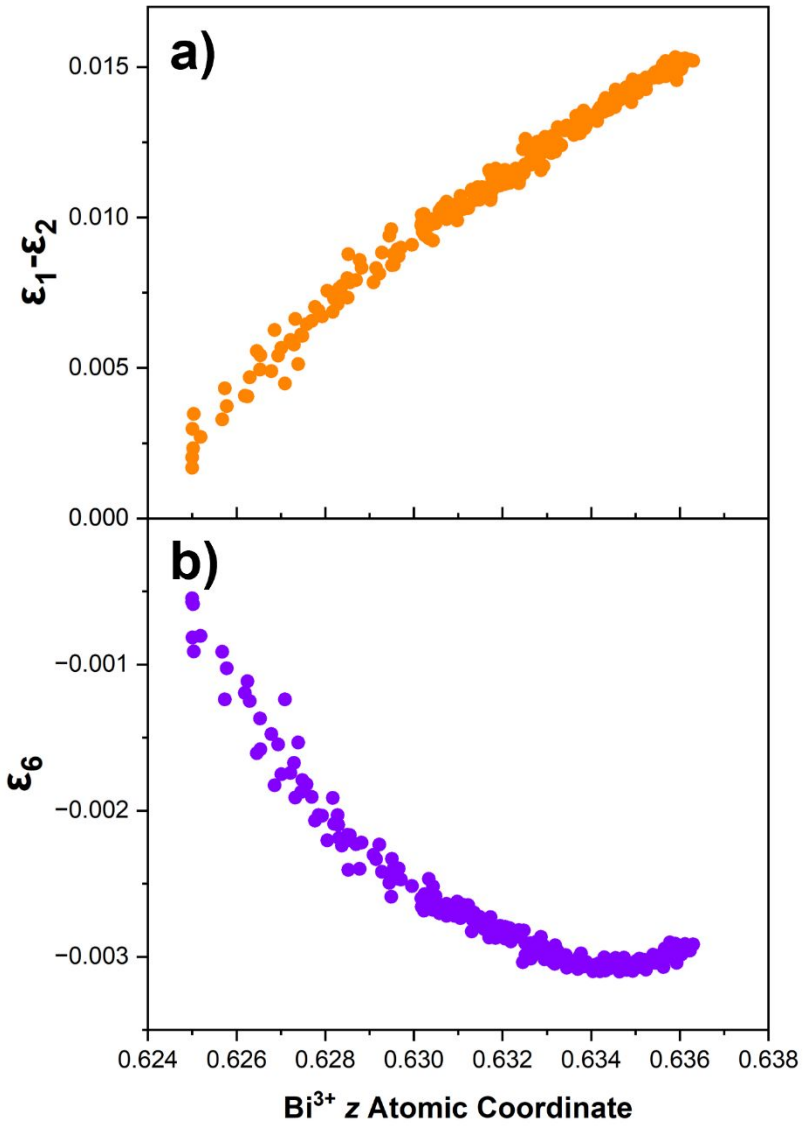

Figure S33: Plotting of the Bi^{3+} *z* atomic coordinate against the two strain order parameters using parameters from the Rietveld refinements of the variable temperature neutron powder diffraction dataset.

Neutron Powder Diffraction Data – NOMAD

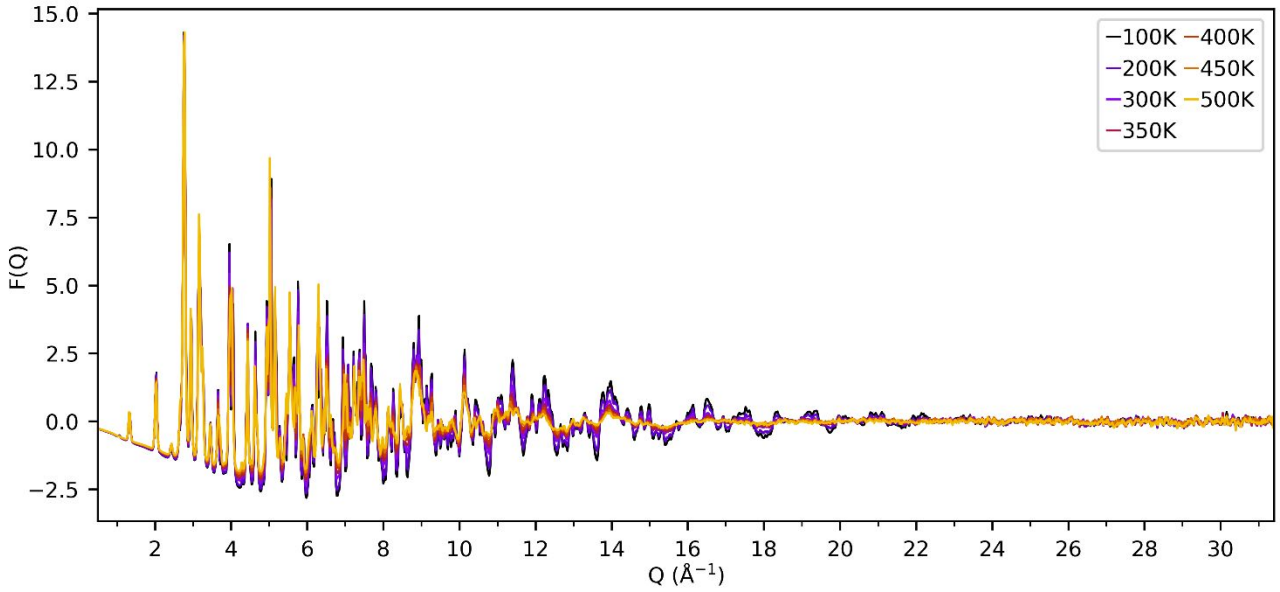

Figure S34: Variable temperature neutron total scattering data, F(Q), in the automated sample changer environment.

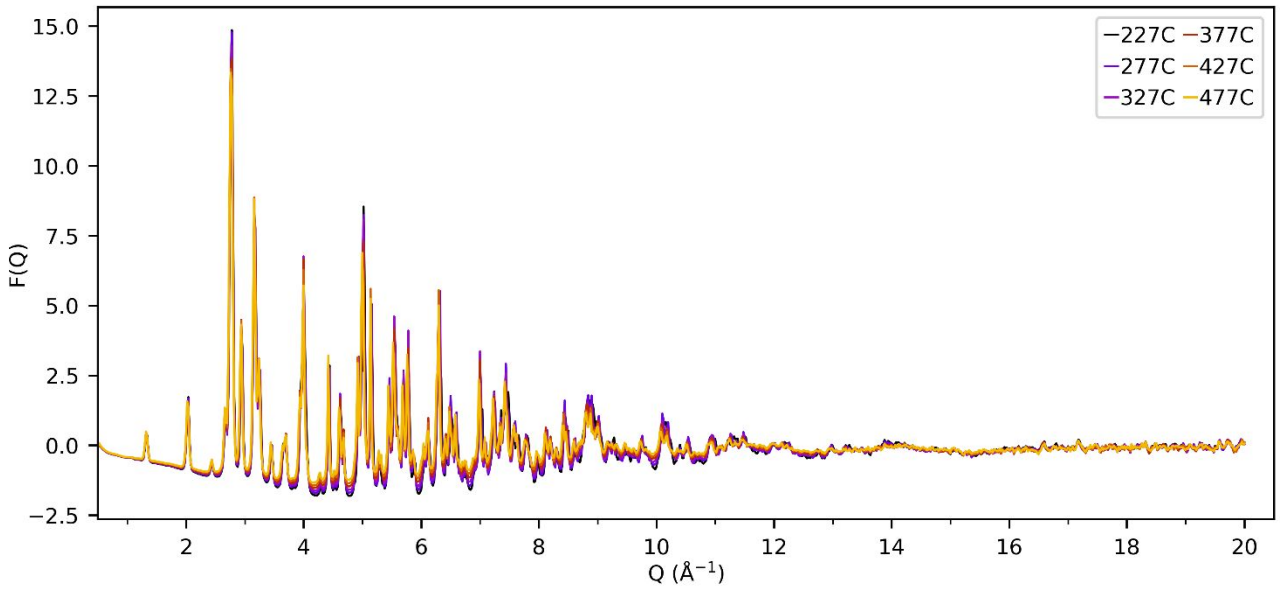

Figure S35: Variable temperature neutron total scattering data, F(Q), in the furnace environment.

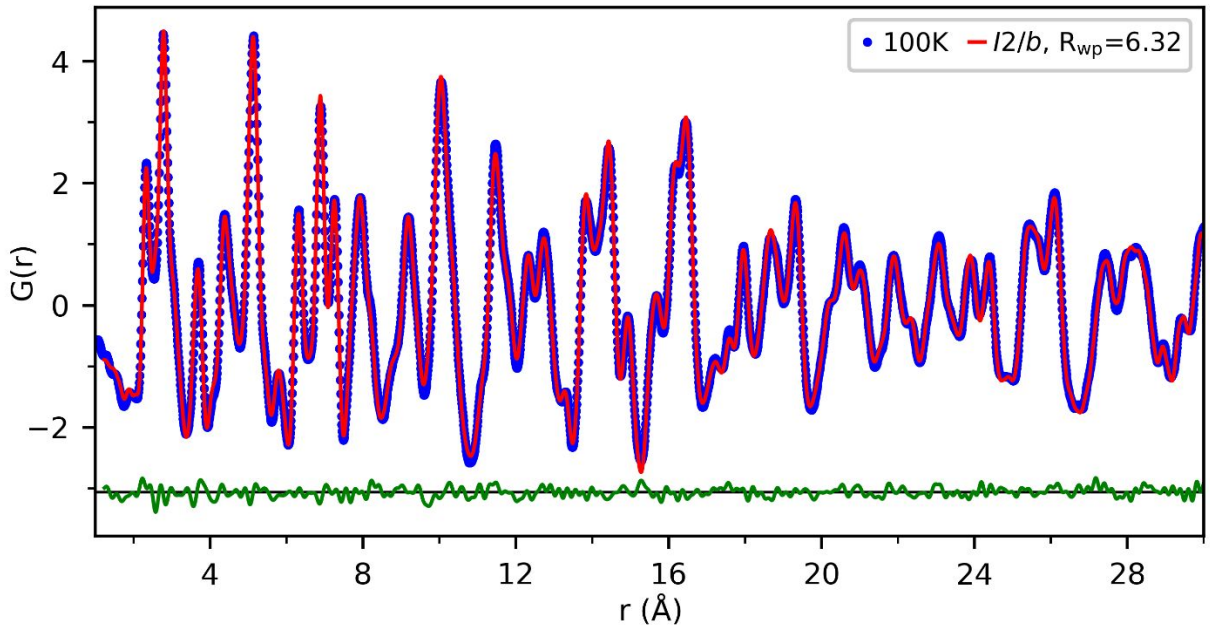

Figure S36: Neutron pair distribution function data collected on $BiVO_4$ at 100 K fitted using a single model. The blue dots represent the data, the red line represents the small box fit to the data in the monoclinic fergusonite *I*2/*b* model, and the green line represents the difference between the two.

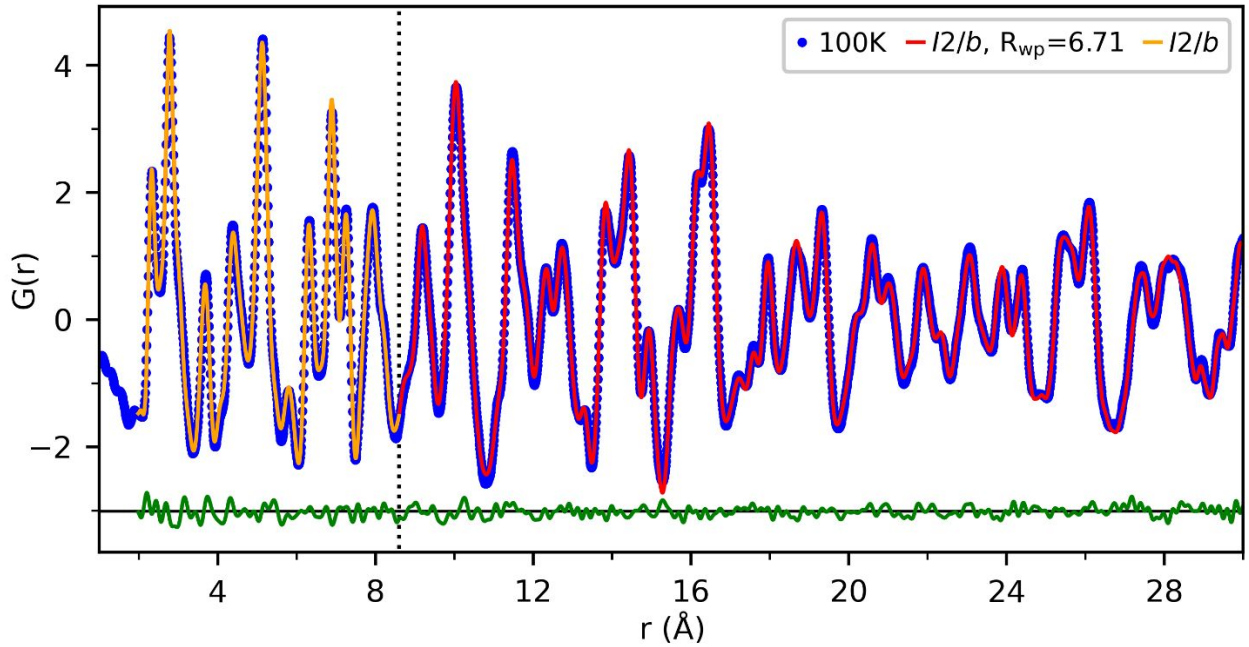

Figure S37: Neutron pair distribution function data collected on $BiVO_4$ at 100 K fitted using a two-phase model. The blue dots represent the data, the red and orange lines represent the small box fit to the data in the monoclinic fergusonite *I*2/*b* model, and the green line represents the difference between the two.

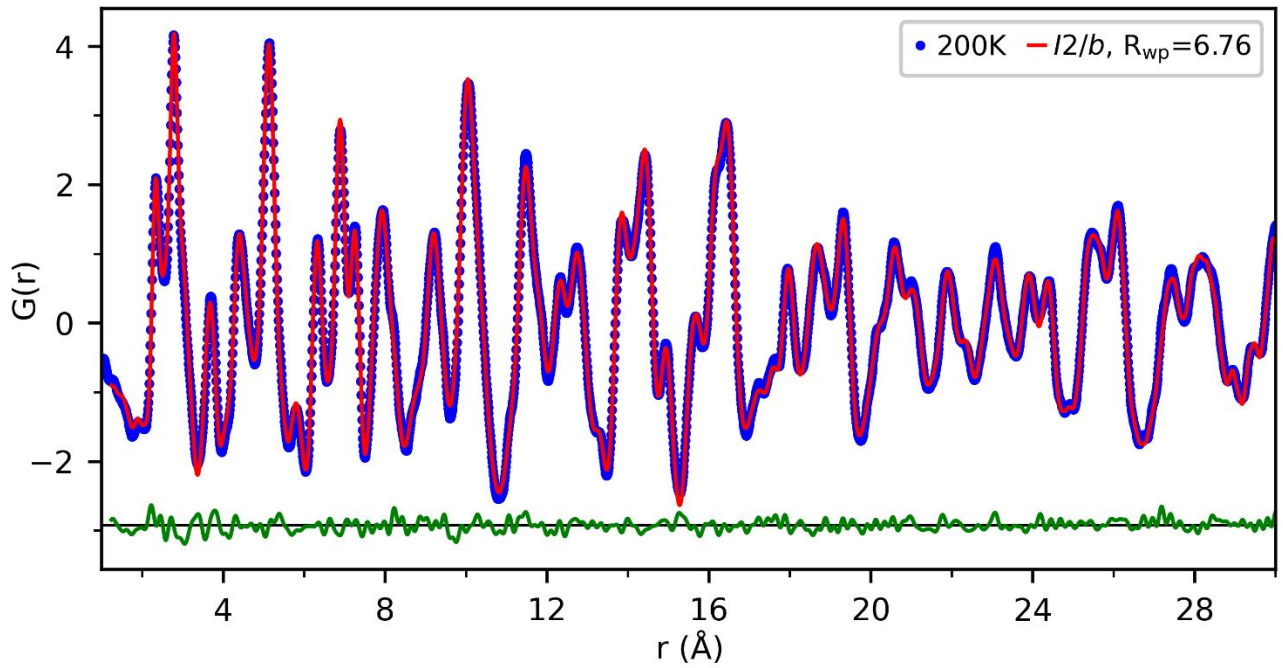

Figure S38: Neutron pair distribution function data collected on $BiVO_4$ at 200 K fitted using a single model. The blue dots represent the data, the red line represents the small box fit to the data in the monoclinic fergusonite *I*2/*b* model, and the green line represents the difference between the two.

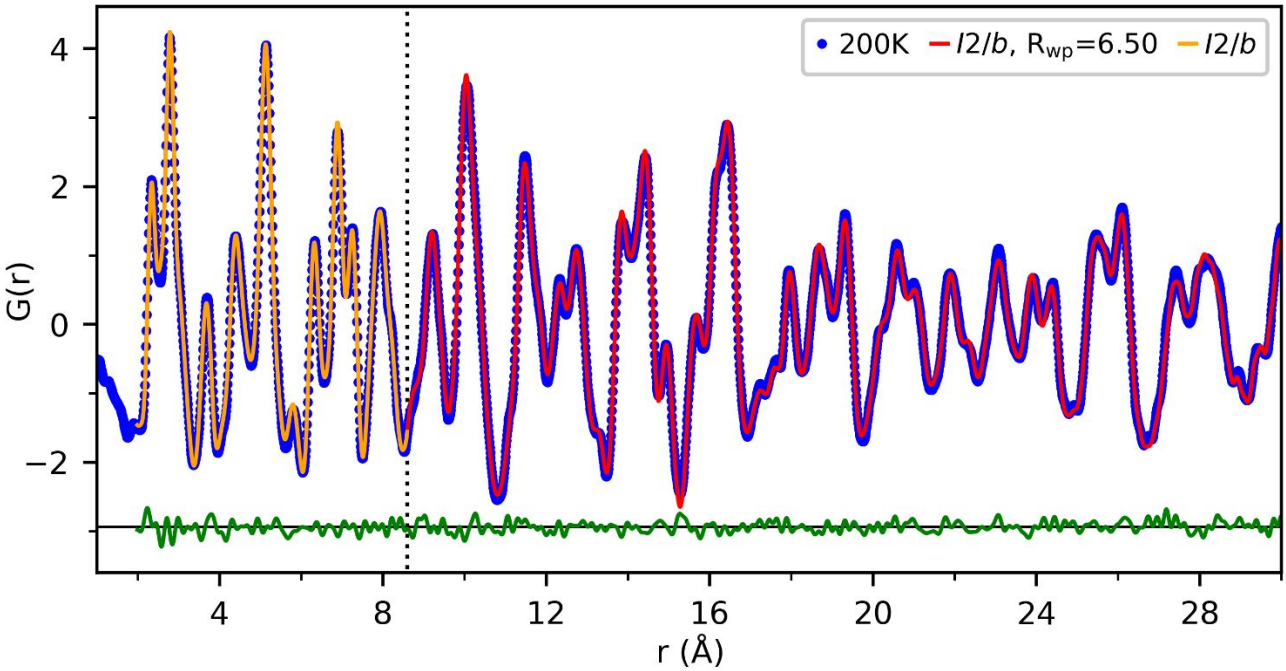

Figure S39: Neutron pair distribution function data collected on $BiVO_4$ at 200 K fitted using a two-phase model. The blue dots represent the data, the red and orange lines represent the small box fit to the data in the monoclinic fergusonite *I*2/*b* model, and the green line represents the difference between the two.

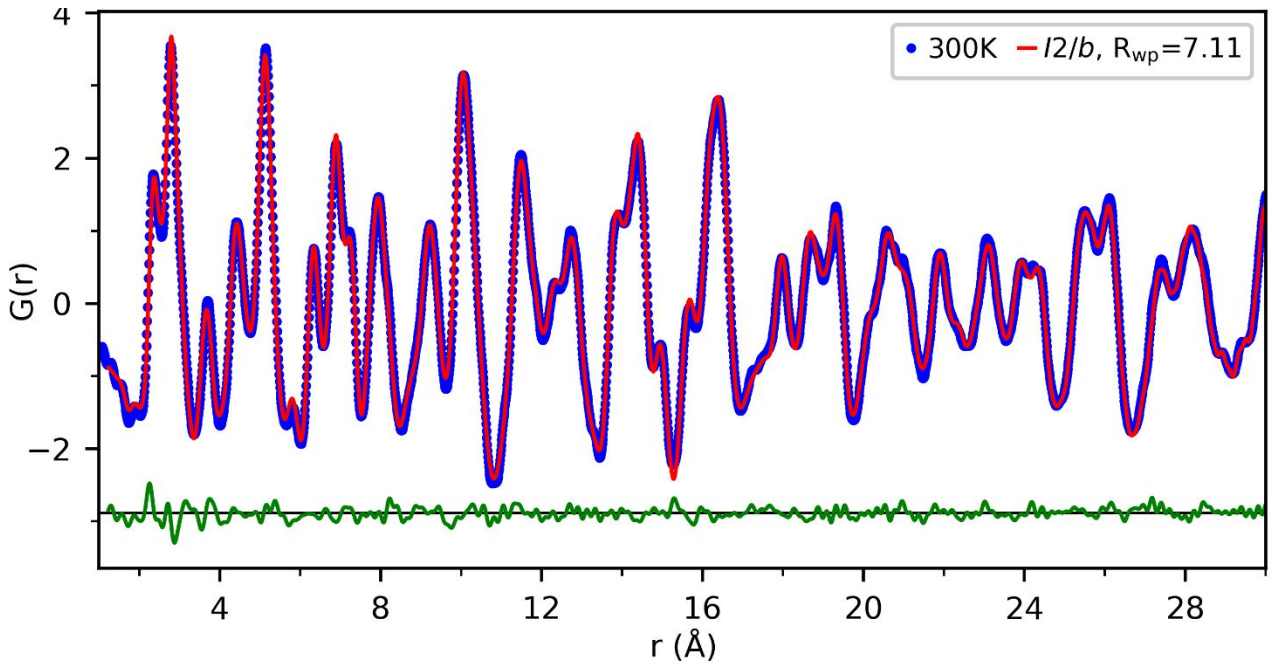

Figure S40: Neutron pair distribution function data collected on $BiVO_4$ at 300 K fitted using a single model. The blue dots represent the data, the red line represents the small box fit to the data in the monoclinic fergusonite *I*2/*b* model, and the green line represents the difference between the two.

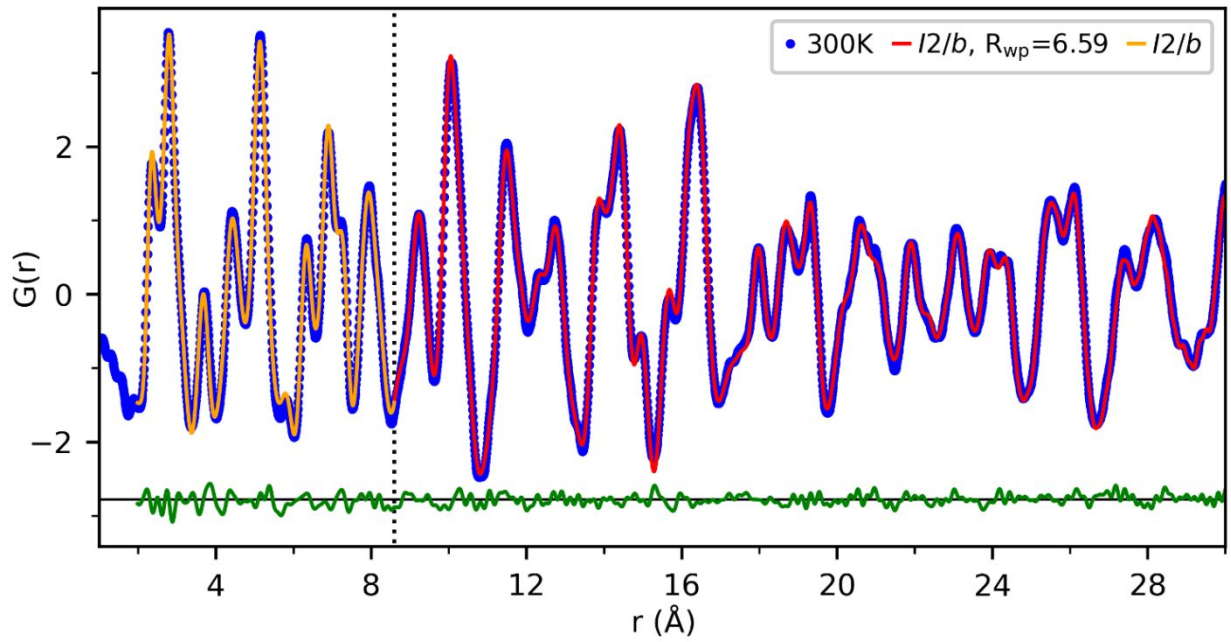

Figure S41: Neutron pair distribution function data collected on $BiVO_4$ at 300 K fitted using a two-phase model. The blue dots represent the data, the red and orange lines represent the small box fit to the data in the monoclinic fergusonite *I*2/*b* model, and the green line represents the difference between the two.

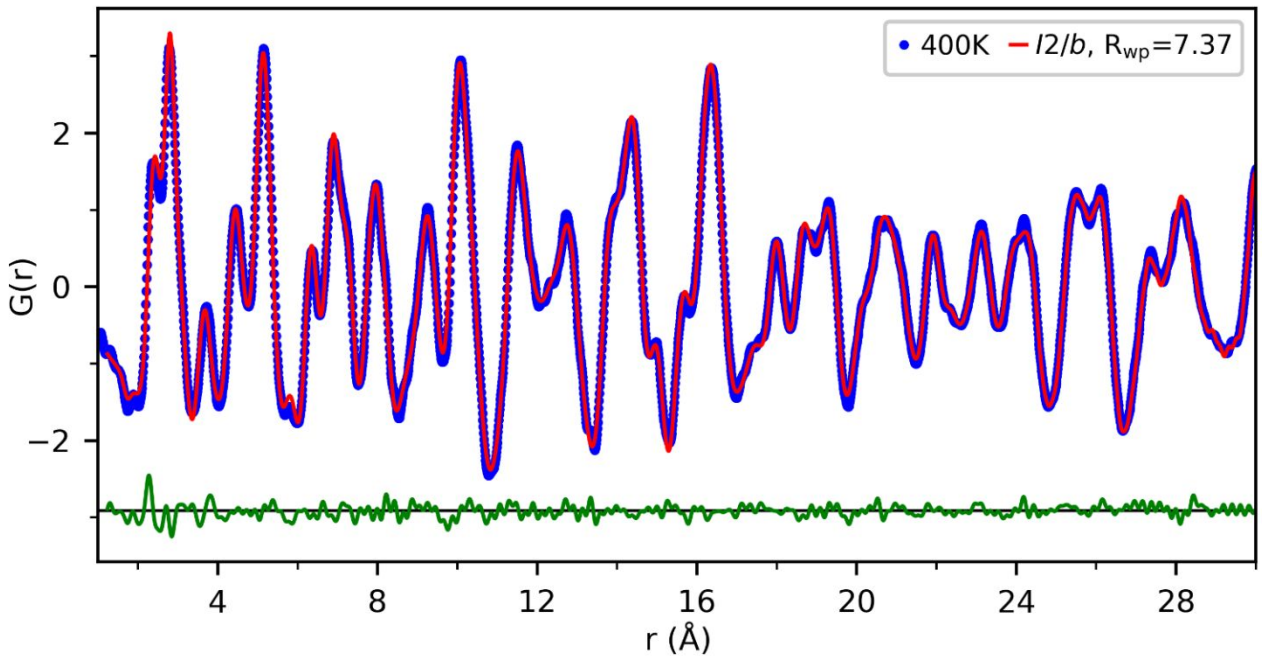

Figure S42: Neutron pair distribution function data collected on $BiVO_4$ at 400 K fitted using a single model. The blue dots represent the data, the red line represents the small box fit to the data in the monoclinic fergusonite *I*2/*b* model, and the green line represents the difference between the two.

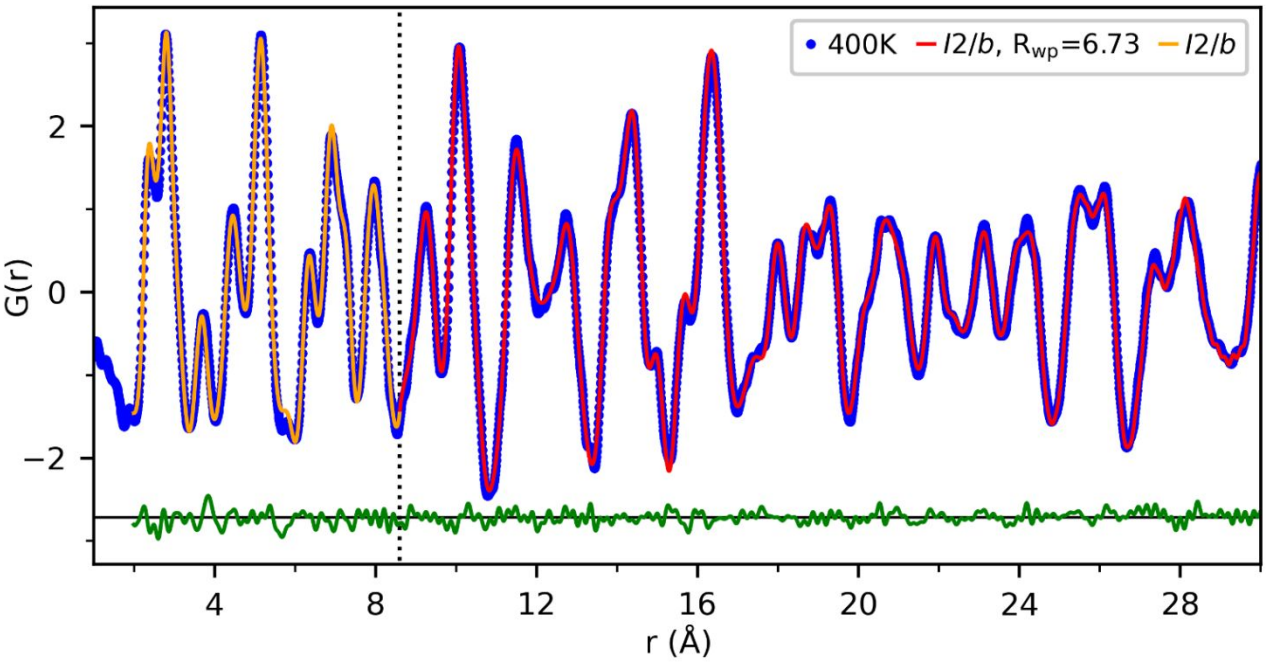

Figure S43: Neutron pair distribution function data collected on $BiVO_4$ at 400 K fitted using a two-phase model. The blue dots represent the data, the red and orange lines represent the small box fit to the data in the monoclinic fergusonite *I*2/*b* model, and the green line represents the difference between the two.

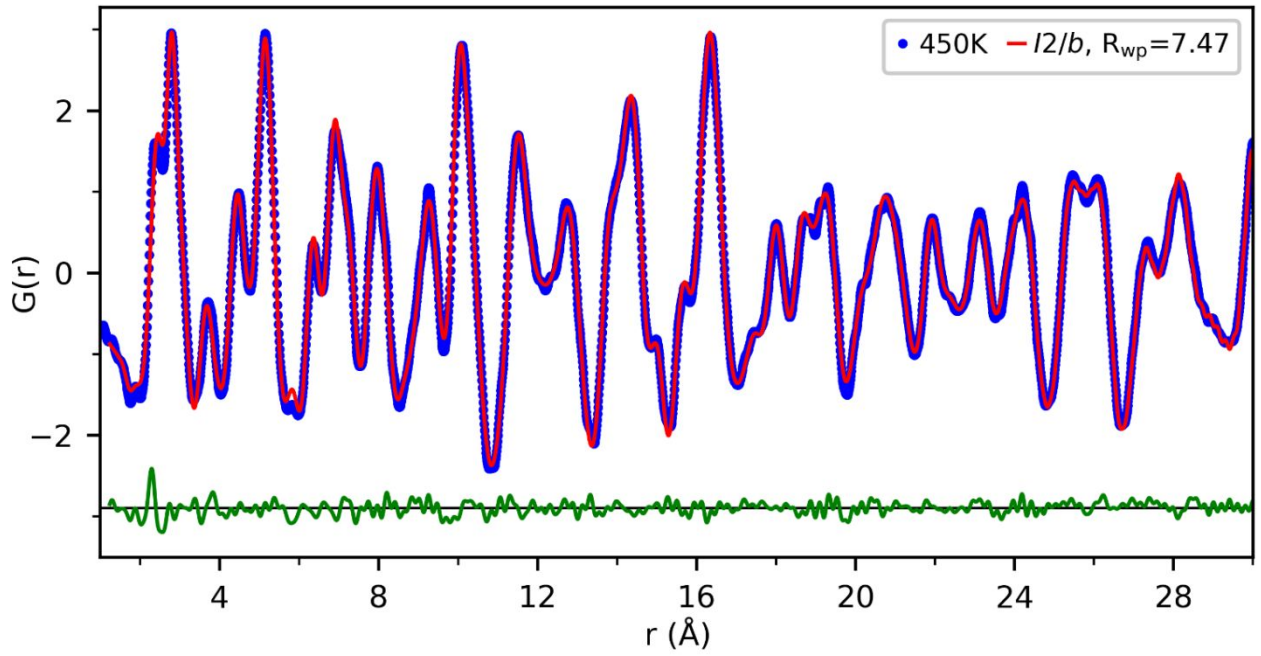

Figure S44: Neutron pair distribution function data collected on $BiVO_4$ at 450 K fitted using a single model. The blue dots represent the data, the red line represents the small box fit to the data in the monoclinic fergusonite *I*2/*b* model, and the green line represents the difference between the two.

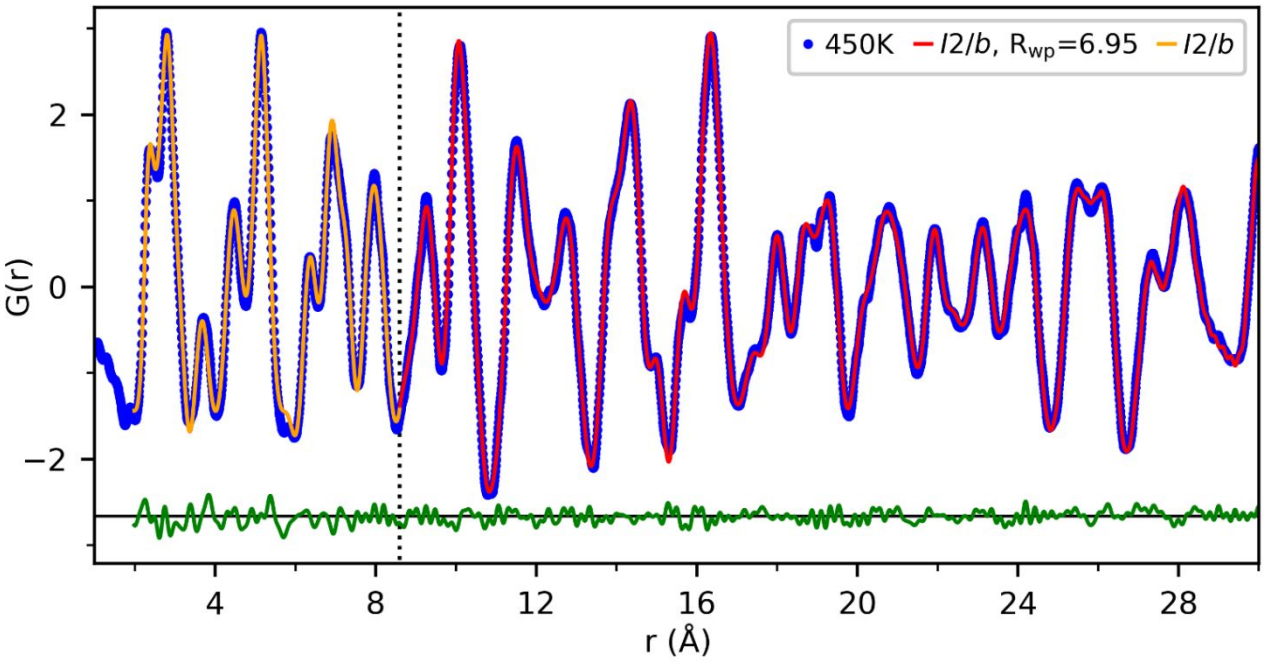

Figure S45: Neutron pair distribution function data collected on $BiVO_4$ at 450 K fitted using a two-phase model. The blue dots represent the data, the red and orange lines represent the small box fit to the data in the monoclinic fergusonite *I*2/*b* model, and the green line represents the difference between the two.

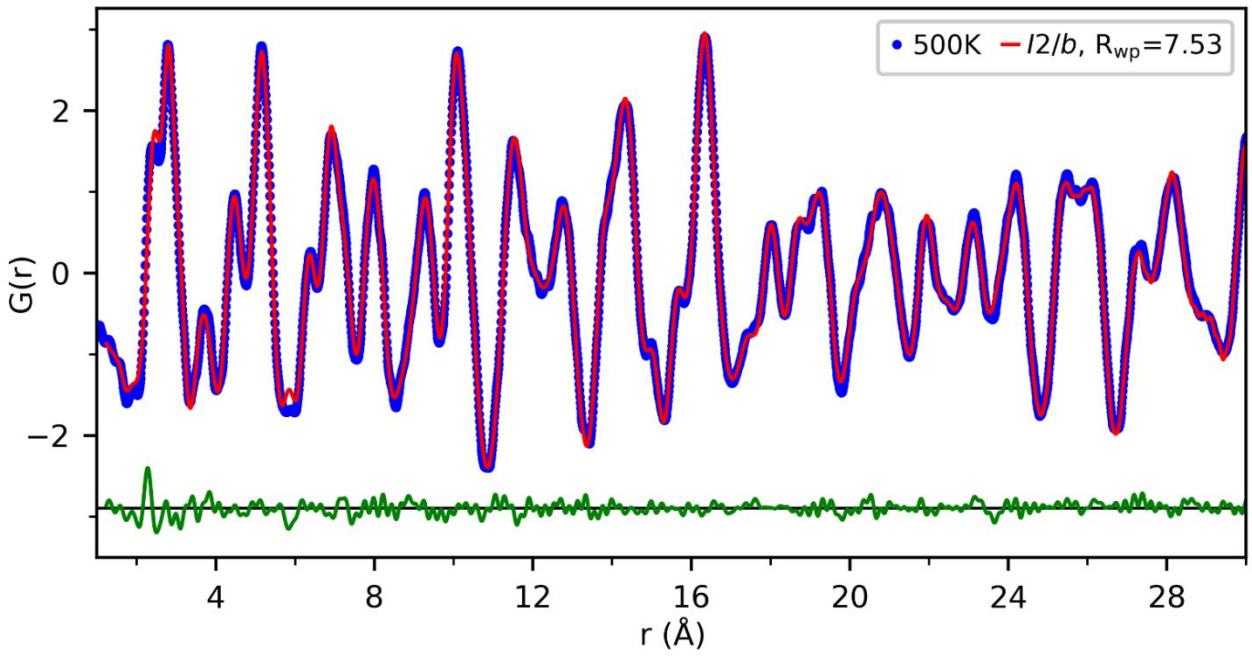

Figure S46: Neutron pair distribution function data collected on $BiVO_4$ at 500 K fitted using a single model. The blue dots represent the data, the red line represents the small box fit to the data in the monoclinic fergusonite *I*2/*b* model, and the green line represents the difference between the two.

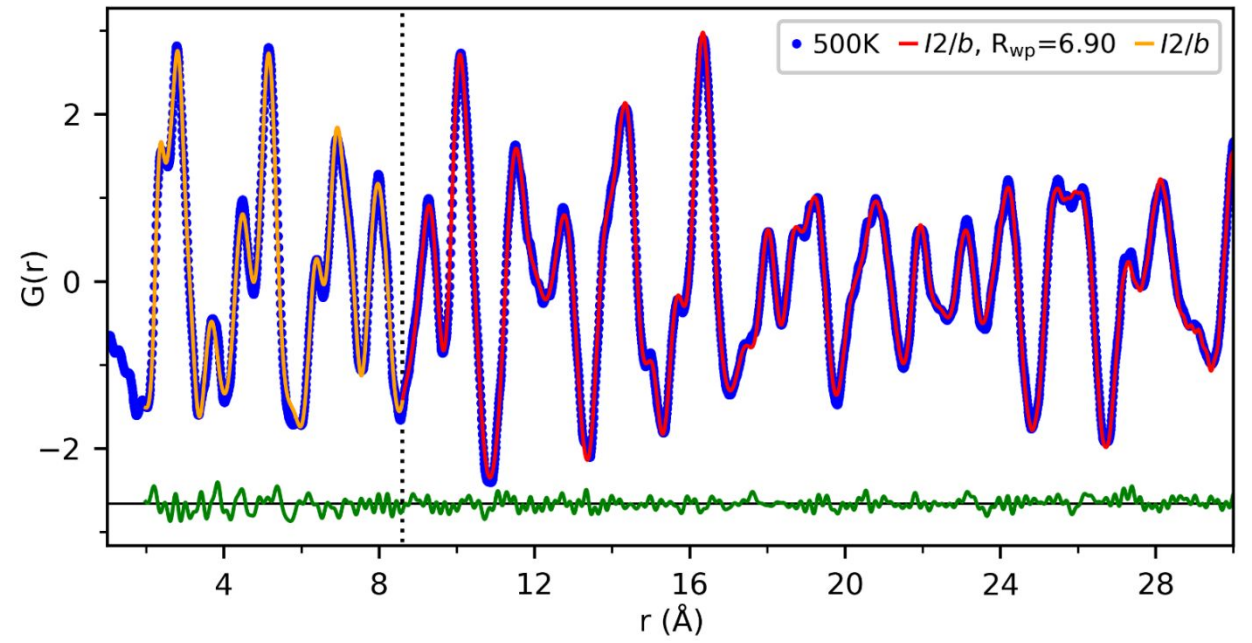

Figure S47: Neutron pair distribution function data collected on $BiVO_4$ at 500 K fitted using a two-phase model. The blue dots represent the data, the red and orange lines represent the small box fit to the data in the monoclinic fergusonite *I*2/*b* model, and the green line represents the difference between the two.

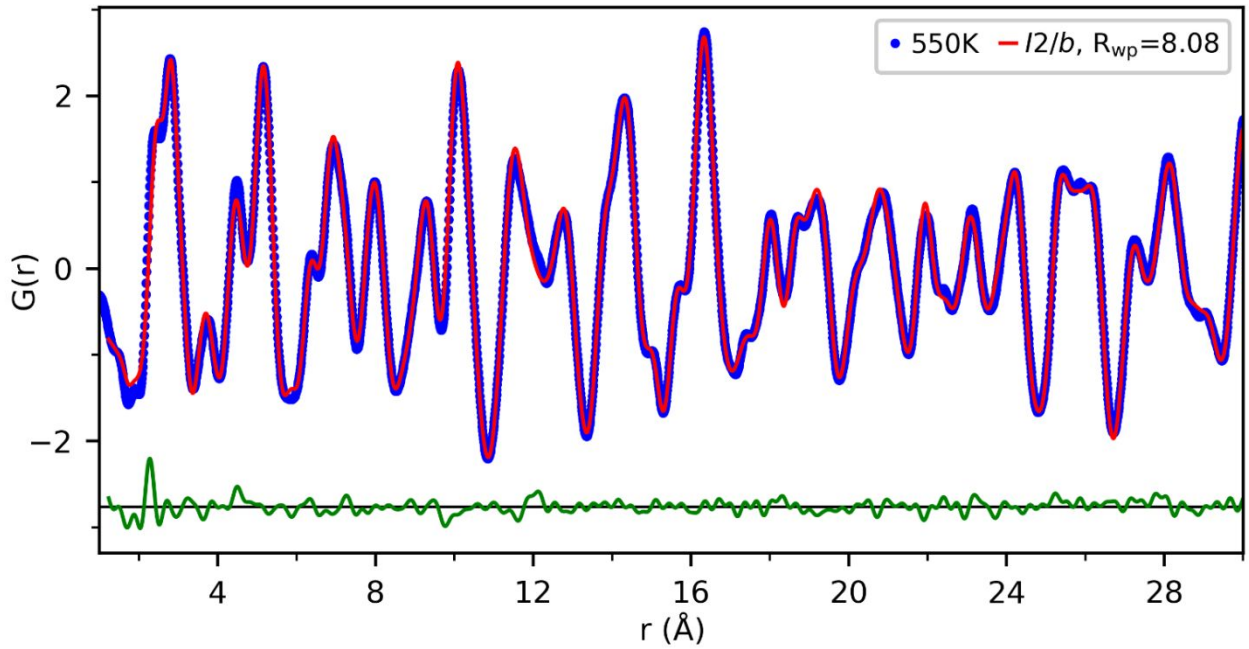

Figure S48: Neutron pair distribution function data collected on $BiVO_4$ at 550 K fitted using a single model. The blue dots represent the data, the red line represents the small box fit to the data in the monoclinic fergusonite *I*2/*b* model, and the green line represents the difference between the two.

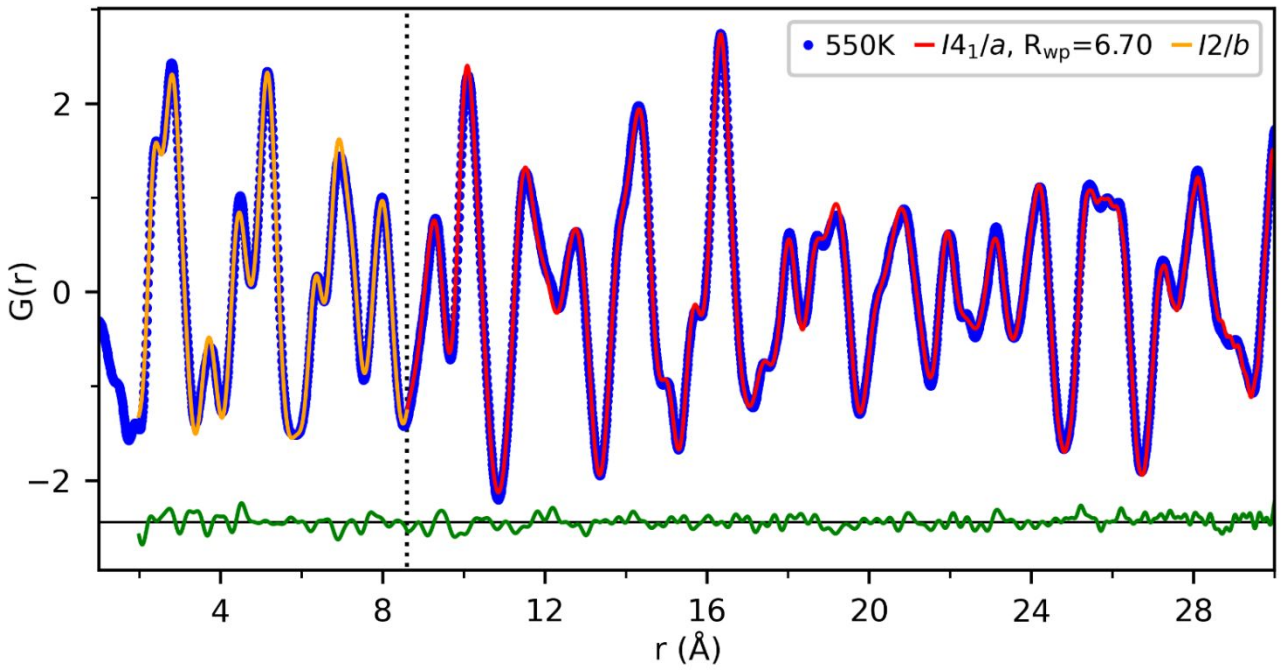

Figure S49: Neutron pair distribution function data collected on $BiVO_4$ at 550 K fitted using a two-phase model. The blue dots represent the data, the red and orange lines represent the small box fit to the data in the monoclinic fergusonite *I*2/*b* model, and the green line represents the difference between the two.

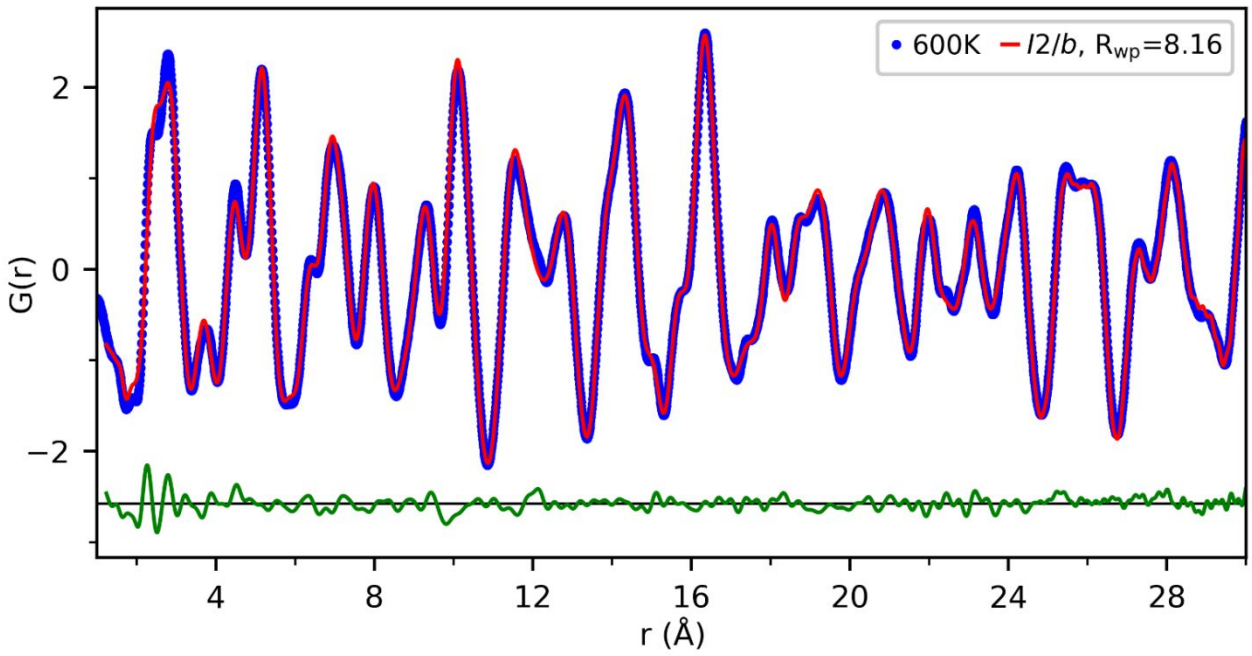

Figure S50: Neutron pair distribution function data collected on $BiVO_4$ at 600 K fitted using a single model. The blue dots represent the data, the red line represents the small box fit to the data in the monoclinic fergusonite *I*2/*b* model, and the green line represents the difference between the two.

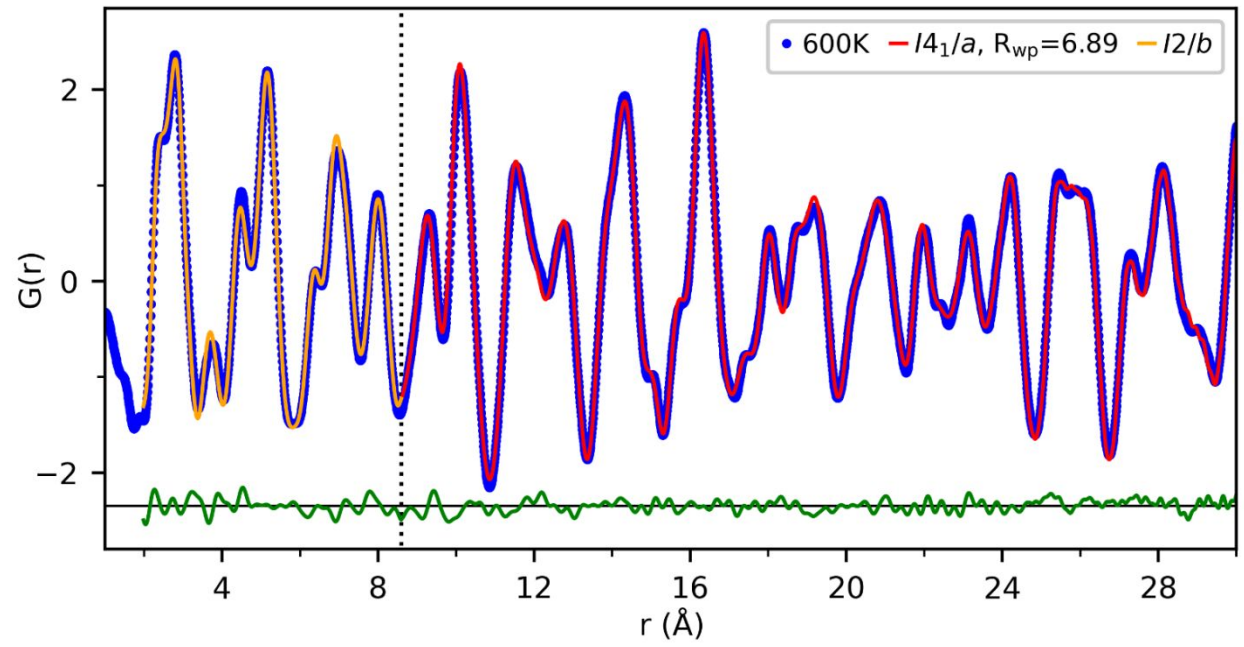

Figure S51: Neutron pair distribution function data collected on $BiVO_4$ at 600 K fitted using a two-phase model. The blue dots represent the data, the red and orange lines represent the small box fit to the data in the monoclinic fergusonite *I*2/*b* model, and the green line represents the difference between the two.

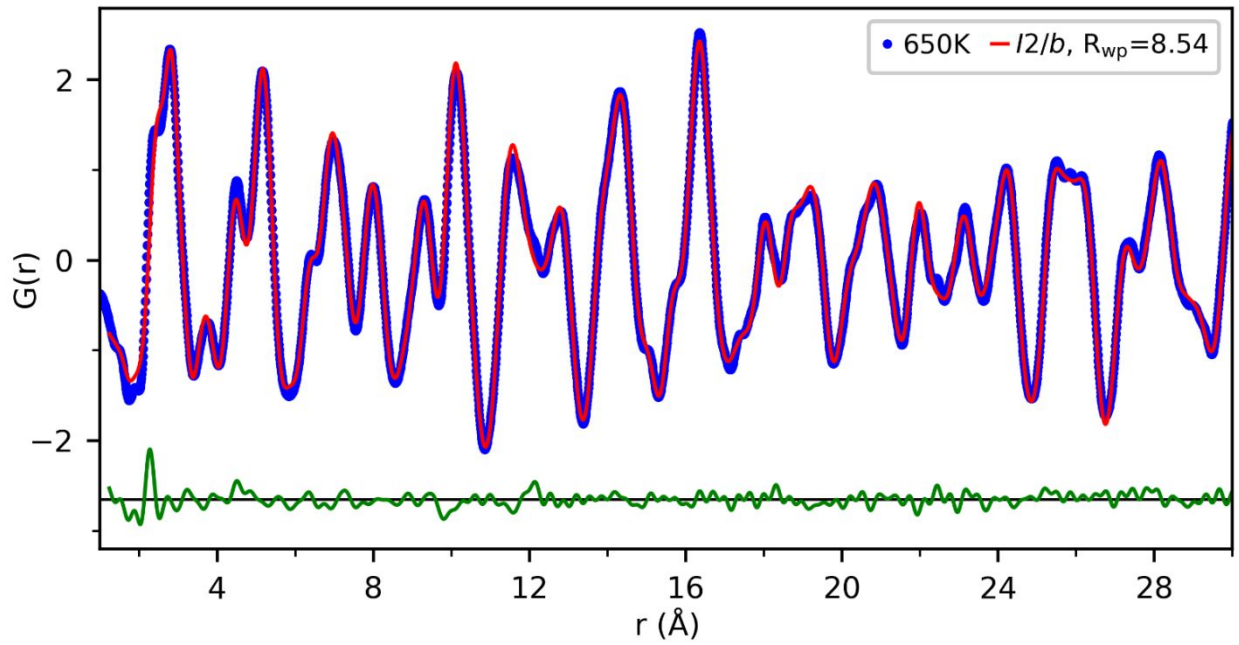

Figure S52: Neutron pair distribution function data collected on $BiVO_4$ at 650 K fitted using a single model. The blue dots represent the data, the red line represents the small box fit to the data in the monoclinic fergusonite *I*2/*b* model, and the green line represents the difference between the two.

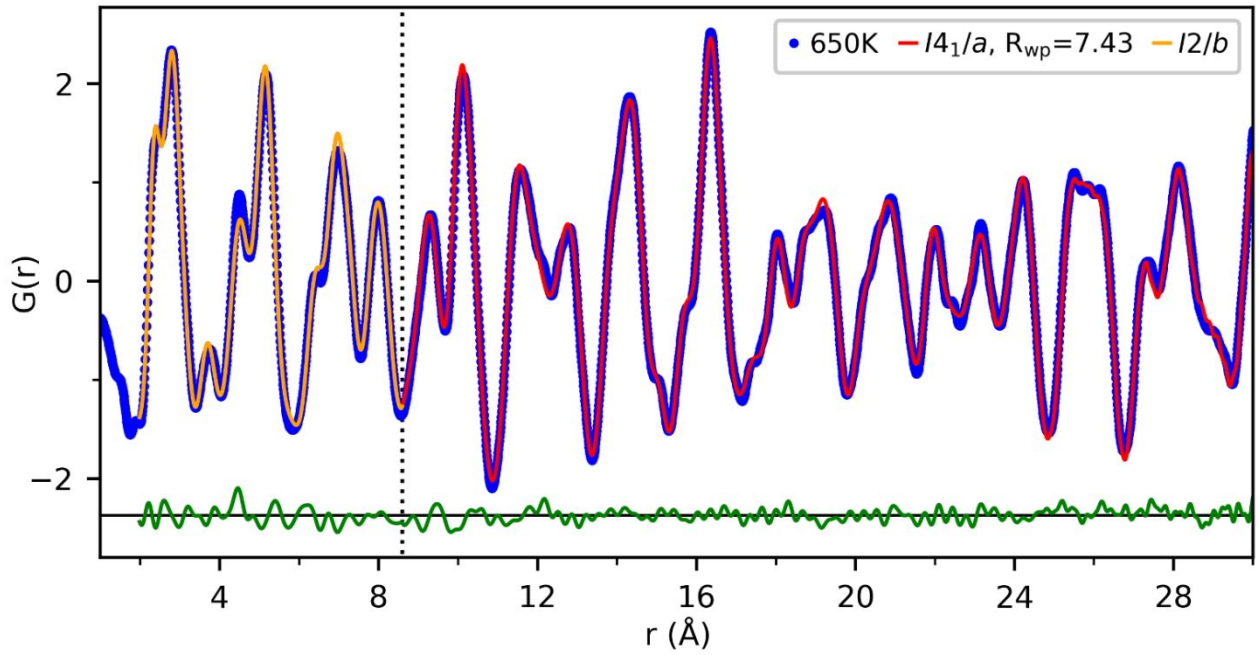

Figure S53: Neutron pair distribution function data collected on $BiVO_4$ at 650 K fitted using a two-phase model. The blue dots represent the data, the red and orange lines represent the small box fit to the data in the monoclinic fergusonite *I*2/*b* model, and the green line represents the difference between the two.

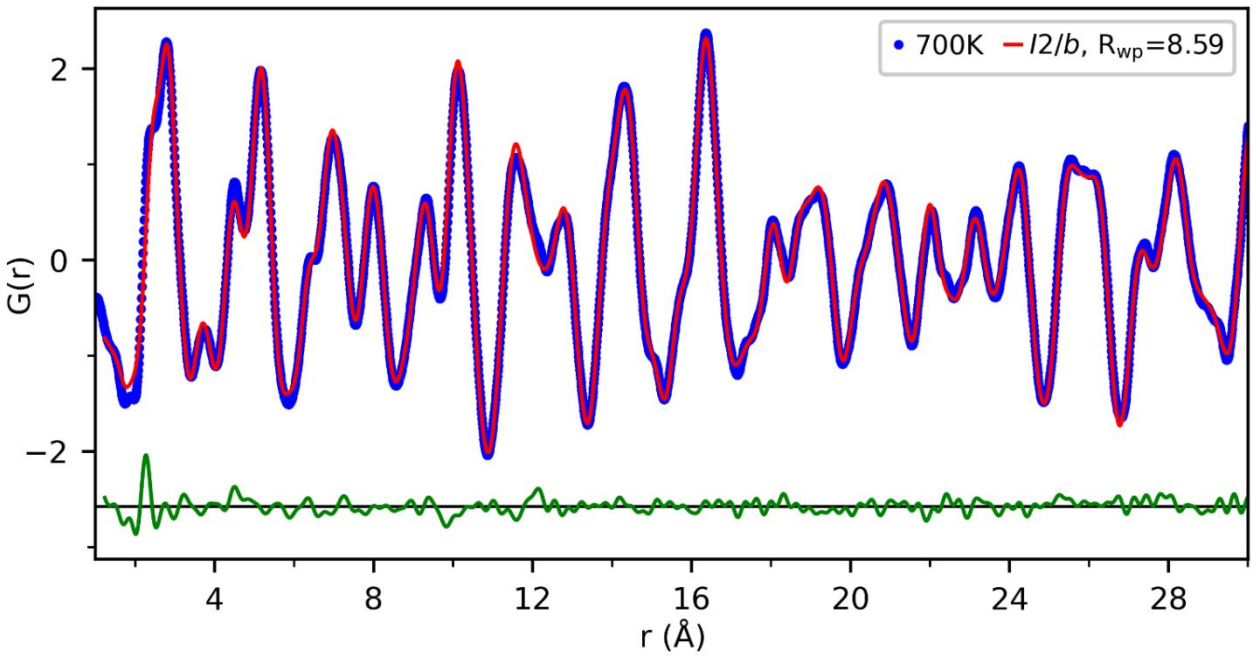

Figure S54: Neutron pair distribution function data collected on $BiVO_4$ at 700 K fitted using a single model. The blue dots represent the data, the red line represents the small box fit to the data in the monoclinic fergusonite *I*2/*b* model, and the green line represents the difference between the two.

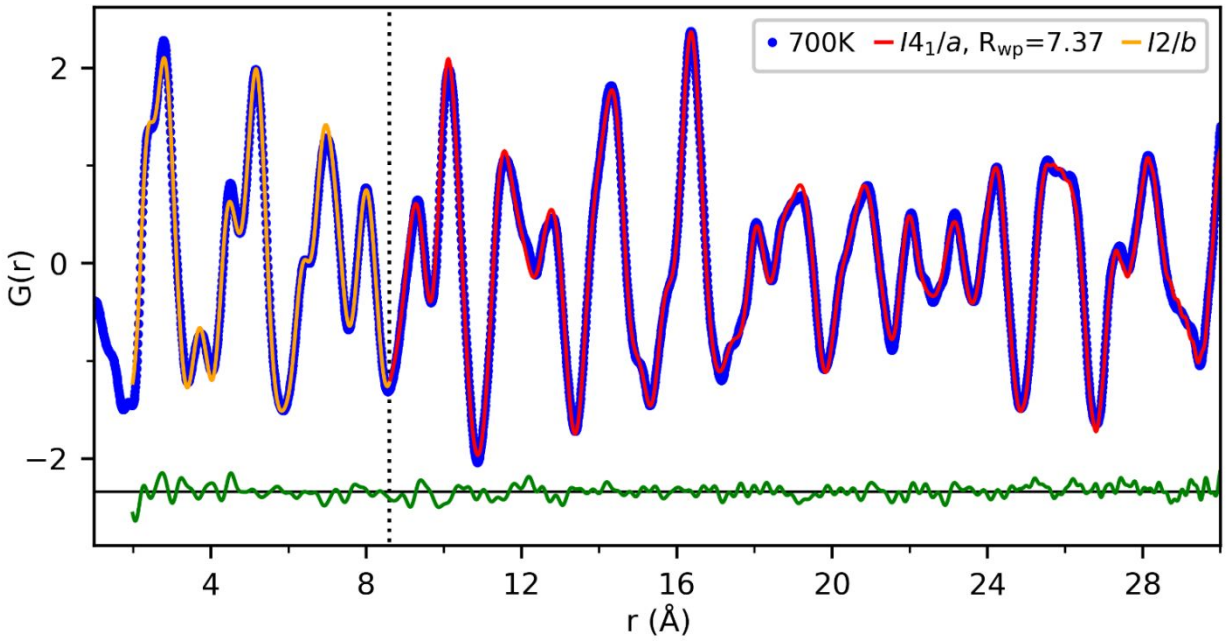

Figure S55: Neutron pair distribution function data collected on $BiVO_4$ at 700 K fitted using a two-phase model. The blue dots represent the data, the red and orange lines represent the small box fit to the data in the monoclinic fergusonite *I*2/*b* model, and the green line represents the difference between the two.

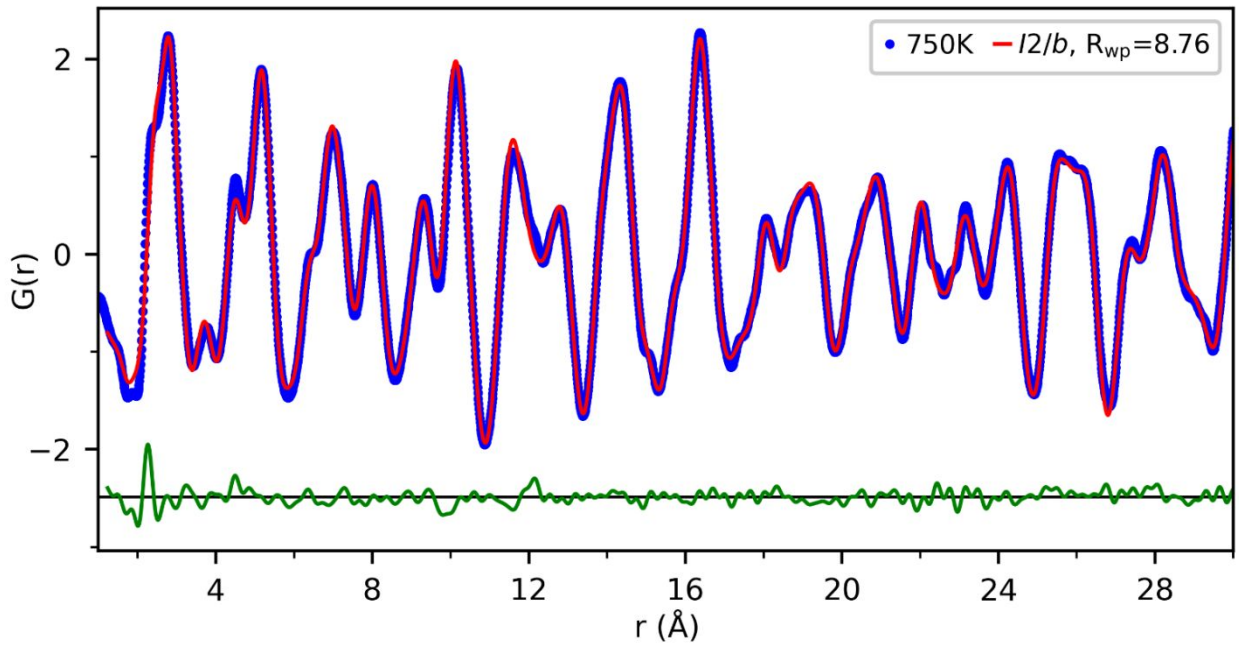

Figure S56: Neutron pair distribution function data collected on $BiVO_4$ at 750 K fitted using a single model. The blue dots represent the data, the red line represents the small box fit to the data in the monoclinic fergusonite *I*2/*b* model, and the green line represents the difference between the two.

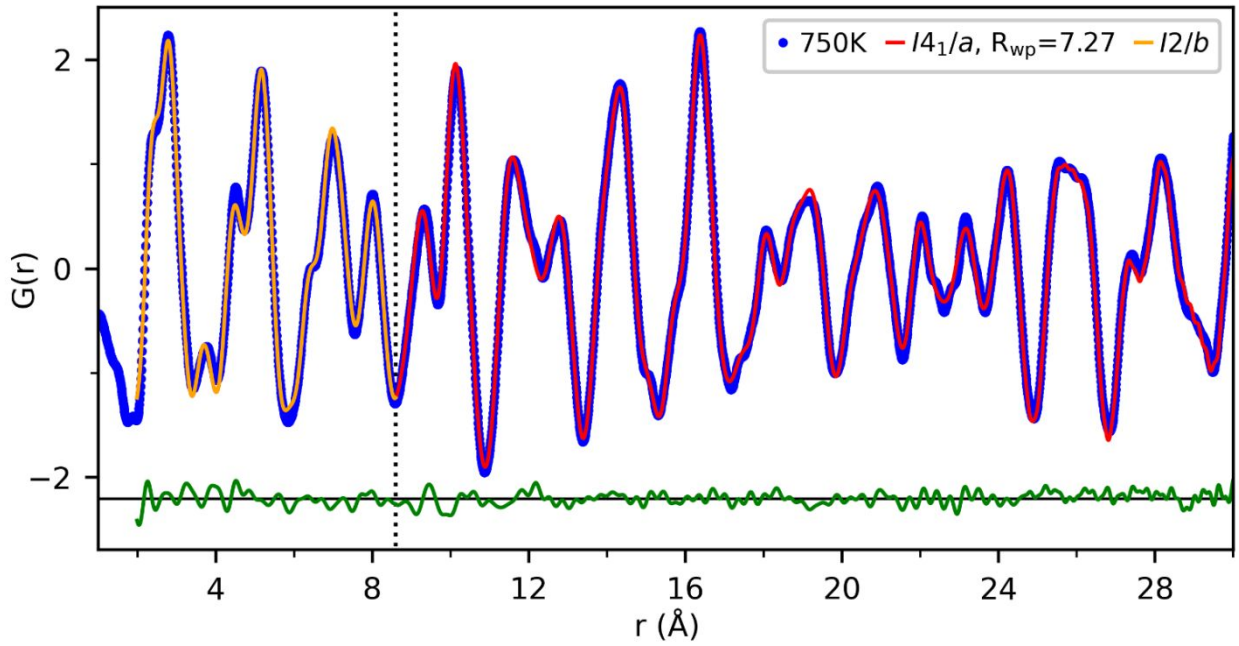

Figure S57: Neutron pair distribution function data collected on $BiVO_4$ at 750 K fitted using a two-phase model. The blue dots represent the data, the red and orange lines represent the small box fit to the data in the monoclinic fergusonite *I*2/*b* model, and the green line represents the difference between the two.

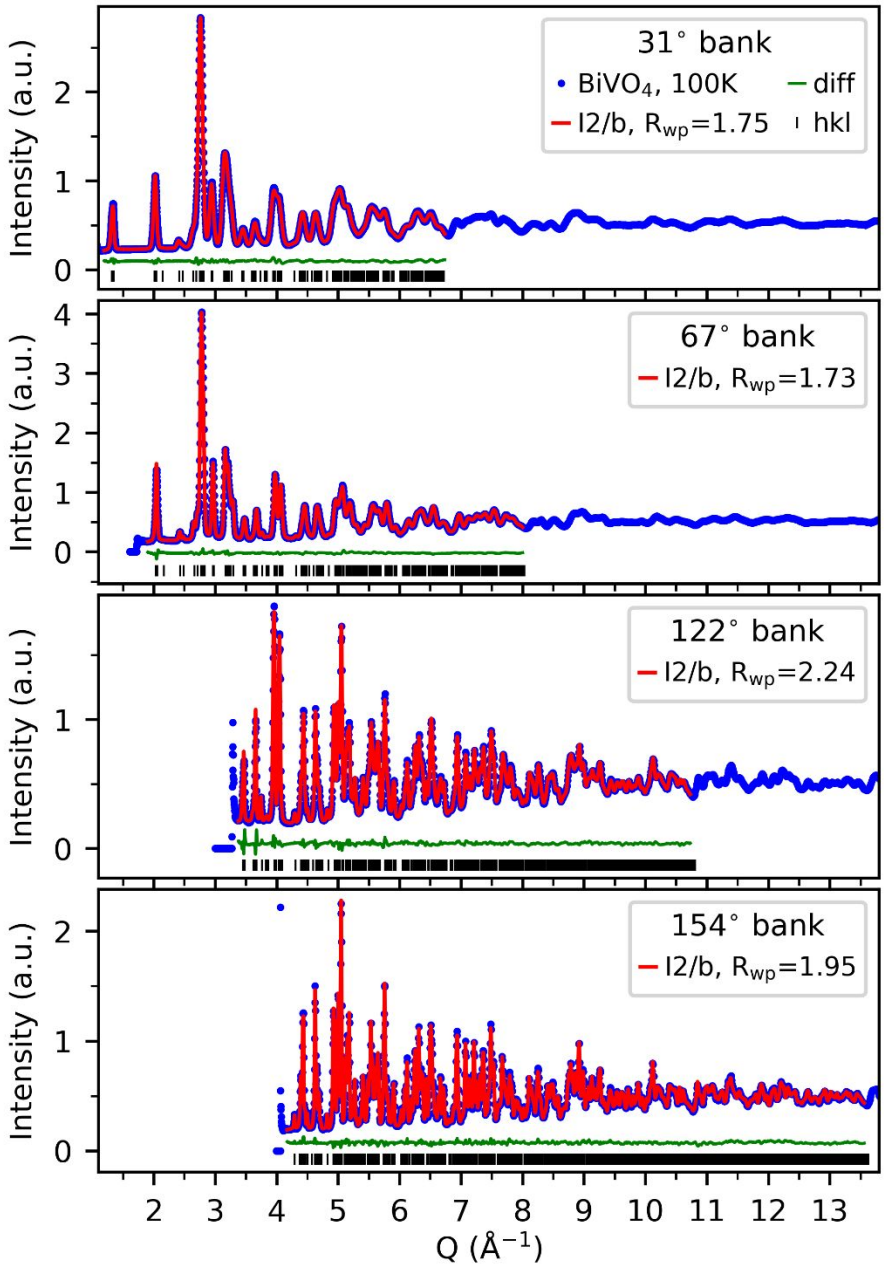

Figure S58: Neutron Bragg powder diffraction data collected on $BiVO_4$ at 100 K fitted using the monoclinic fergusonite model. The blue dots represent the data, the red line represents the Rietveld refinement to the data, the green line represents the difference between the two, and the black ticks represent the space group allowed *hkl* reflections.

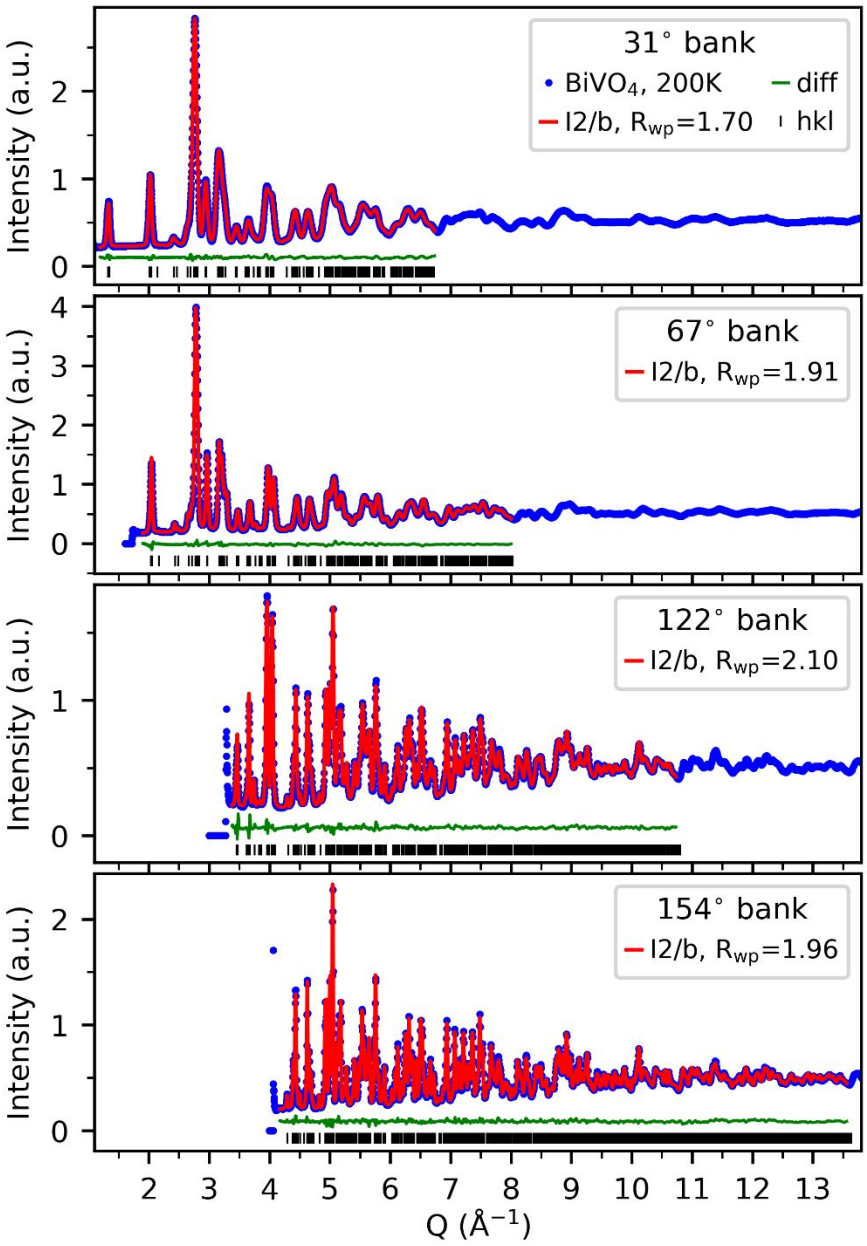

Figure S59: Neutron Bragg powder diffraction data collected on $BiVO_4$ at 200 K fitted using the monoclinic fergusonite model. The blue dots represent the data, the red line represents the Rietveld refinement to the data, the green line represents the difference between the two, and the black ticks represent the space group allowed *hkl* reflections.

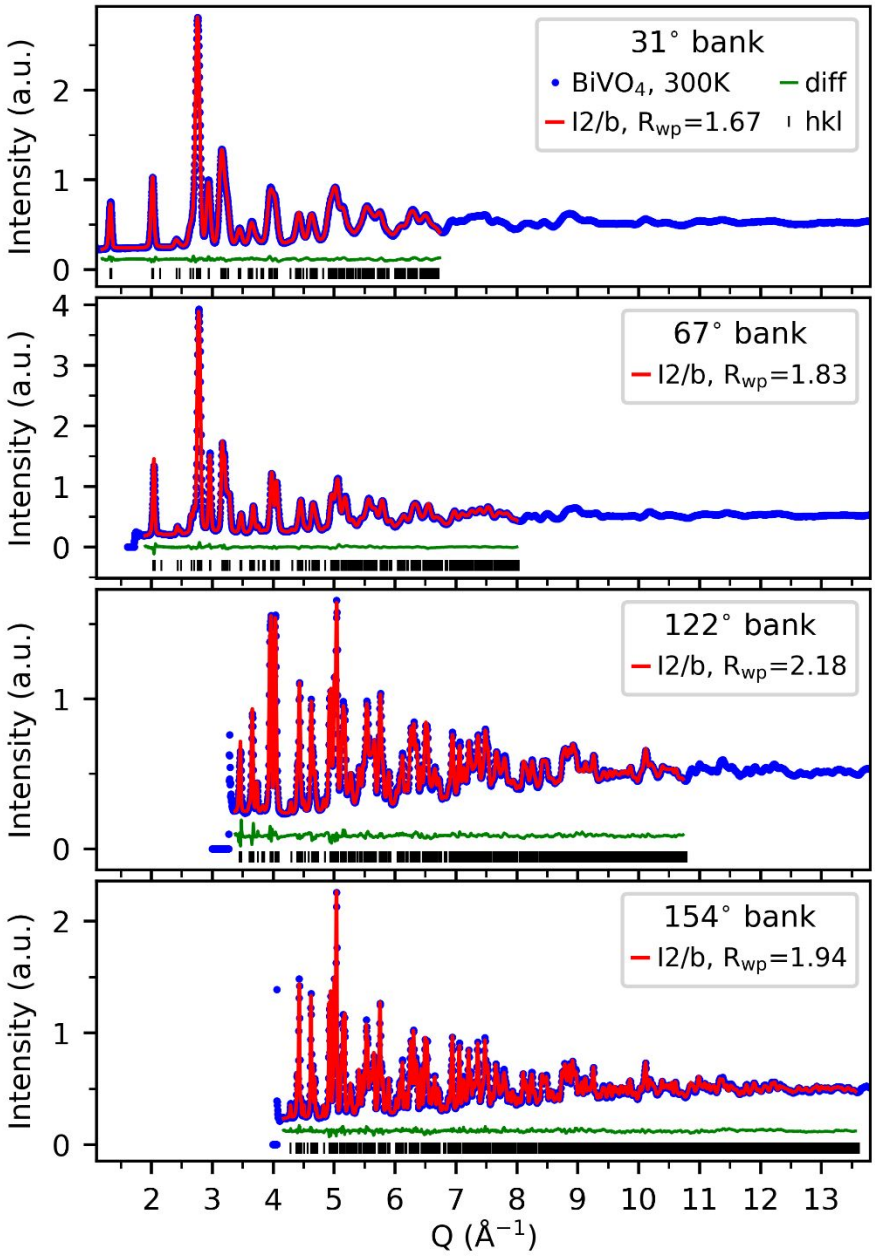

Figure S60: Neutron Bragg powder diffraction data collected on $BiVO_4$ at 300 K fitted using the monoclinic fergusonite model. The blue dots represent the data, the red line represents the Rietveld refinement to the data, the green line represents the difference between the two, and the black ticks represent the space group allowed *hkl* reflections.

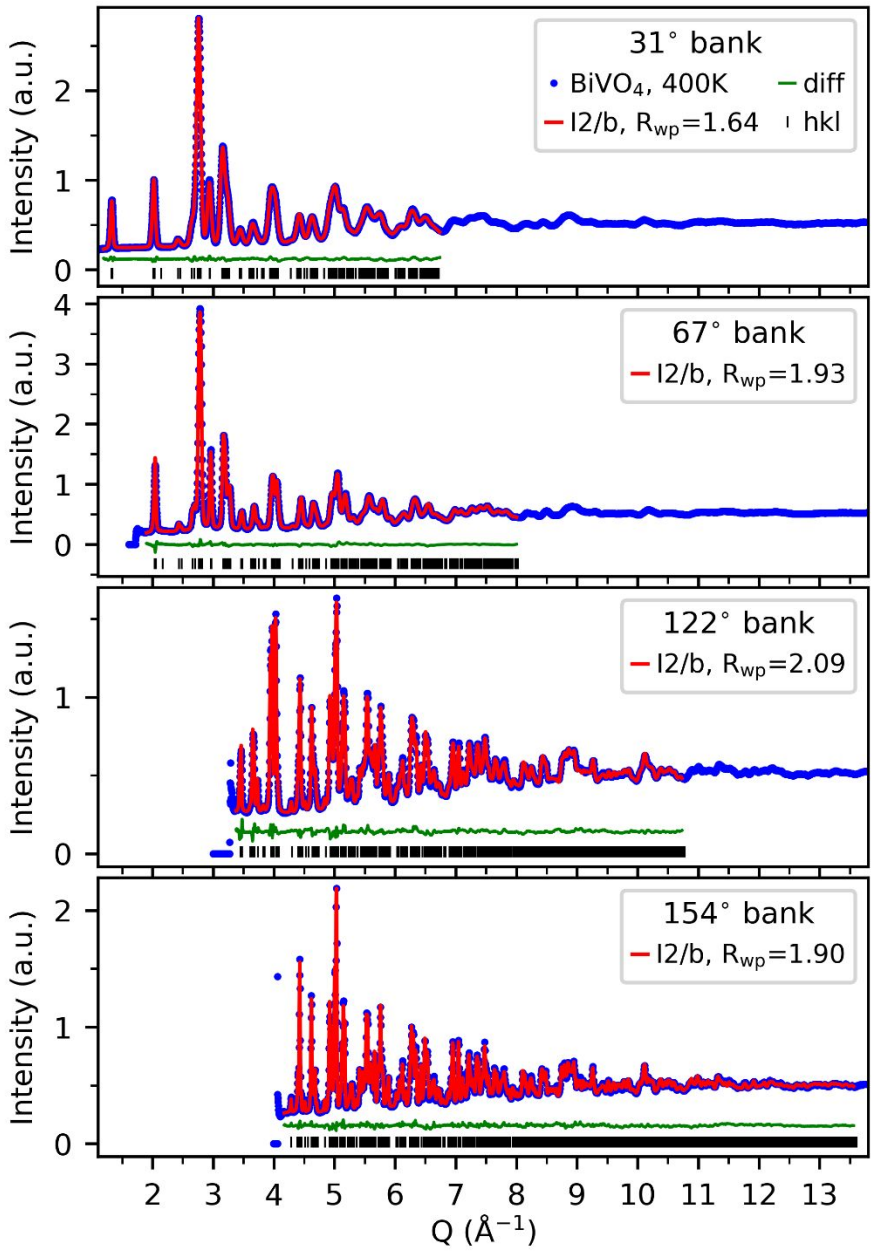

Figure S61: Neutron Bragg powder diffraction data collected on $BiVO_4$ at 400 K fitted using the monoclinic fergusonite model. The blue dots represent the data, the red line represents the Rietveld refinement to the data, the green line represents the difference between the two, and the black ticks represent the space group allowed *hkl* reflections.

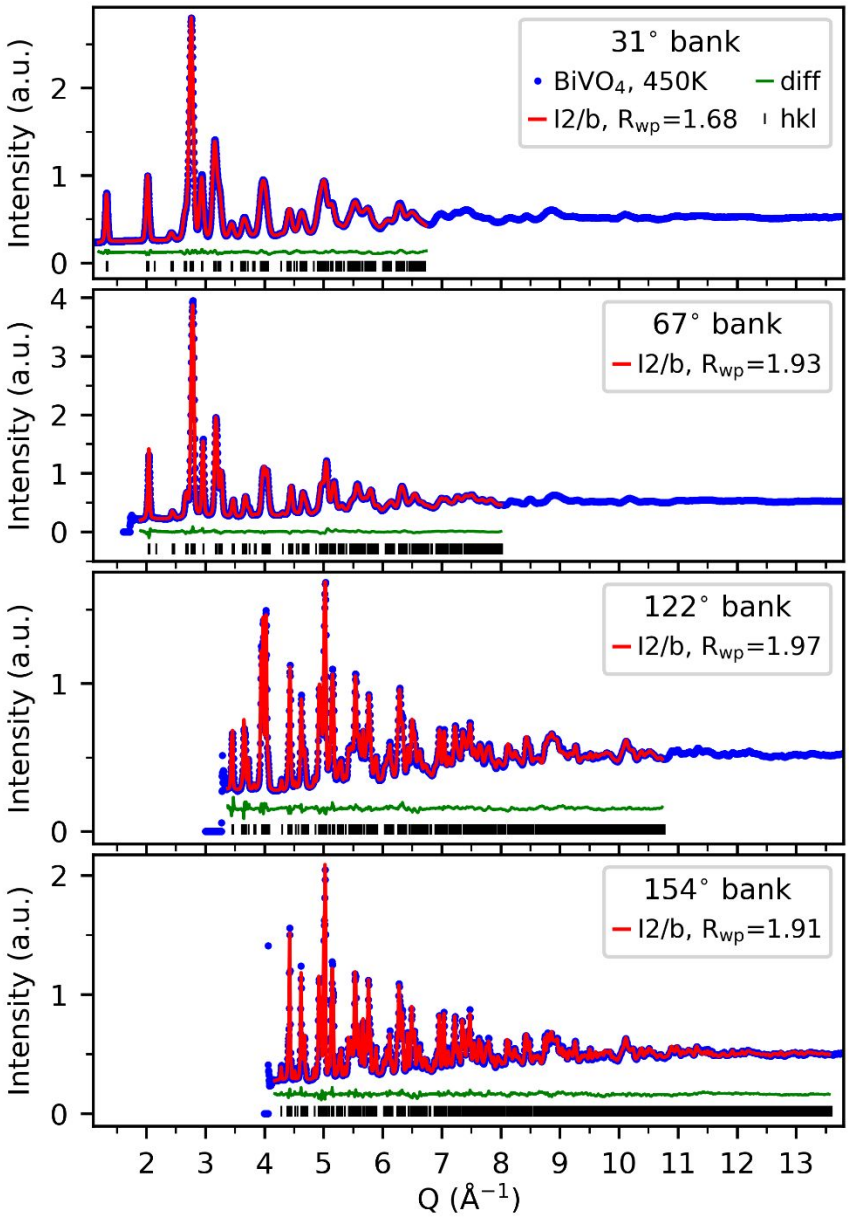

Figure S62: Neutron Bragg powder diffraction data collected on $BiVO_4$ at 450 K fitted using the monoclinic fergusonite model. The blue dots represent the data, the red line represents the Rietveld refinement to the data, the green line represents the difference between the two, and the black ticks represent the space group allowed *hkl* reflections.

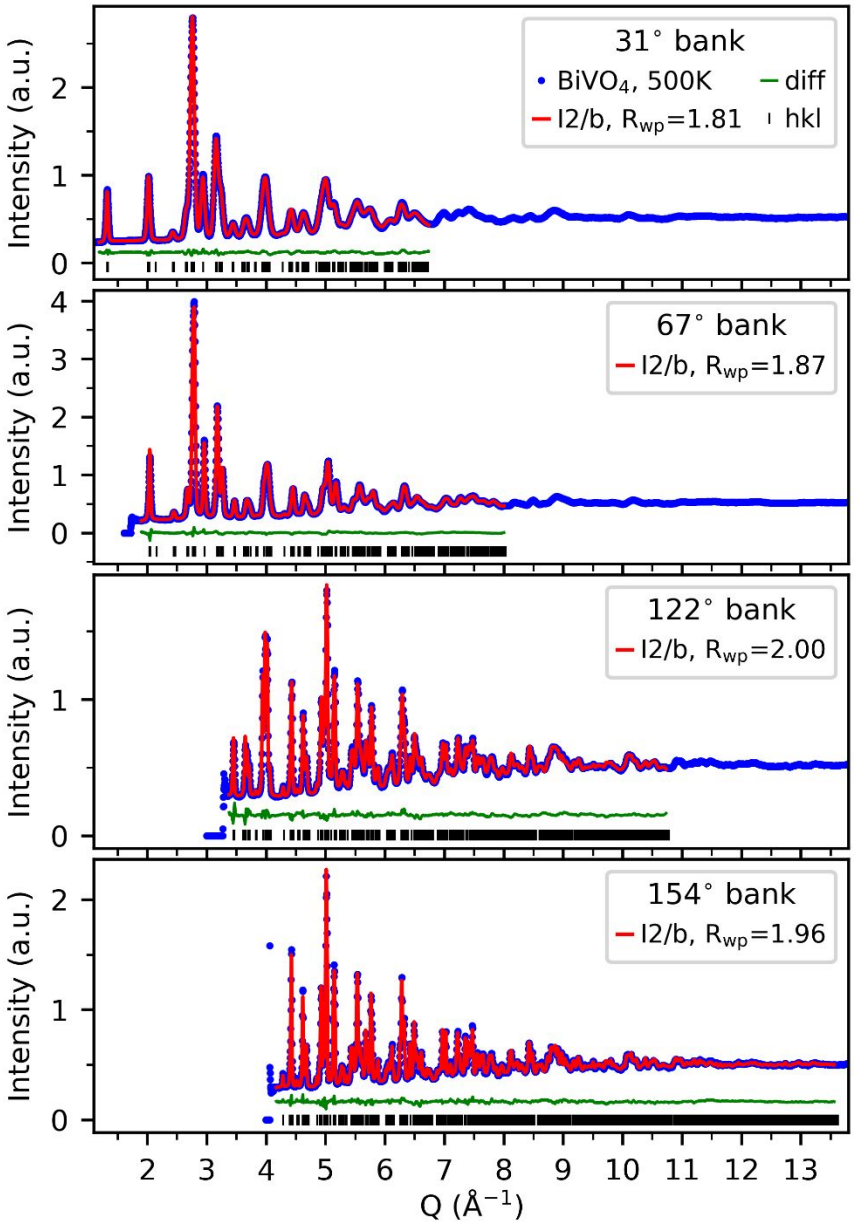

Figure S63: Neutron Bragg powder diffraction data collected on $BiVO_4$ at 500 K fitted using the monoclinic fergusonite model. The blue dots represent the data, the red line represents the Rietveld refinement to the data, the green line represents the difference between the two, and the black ticks represent the space group allowed *hkl* reflections.

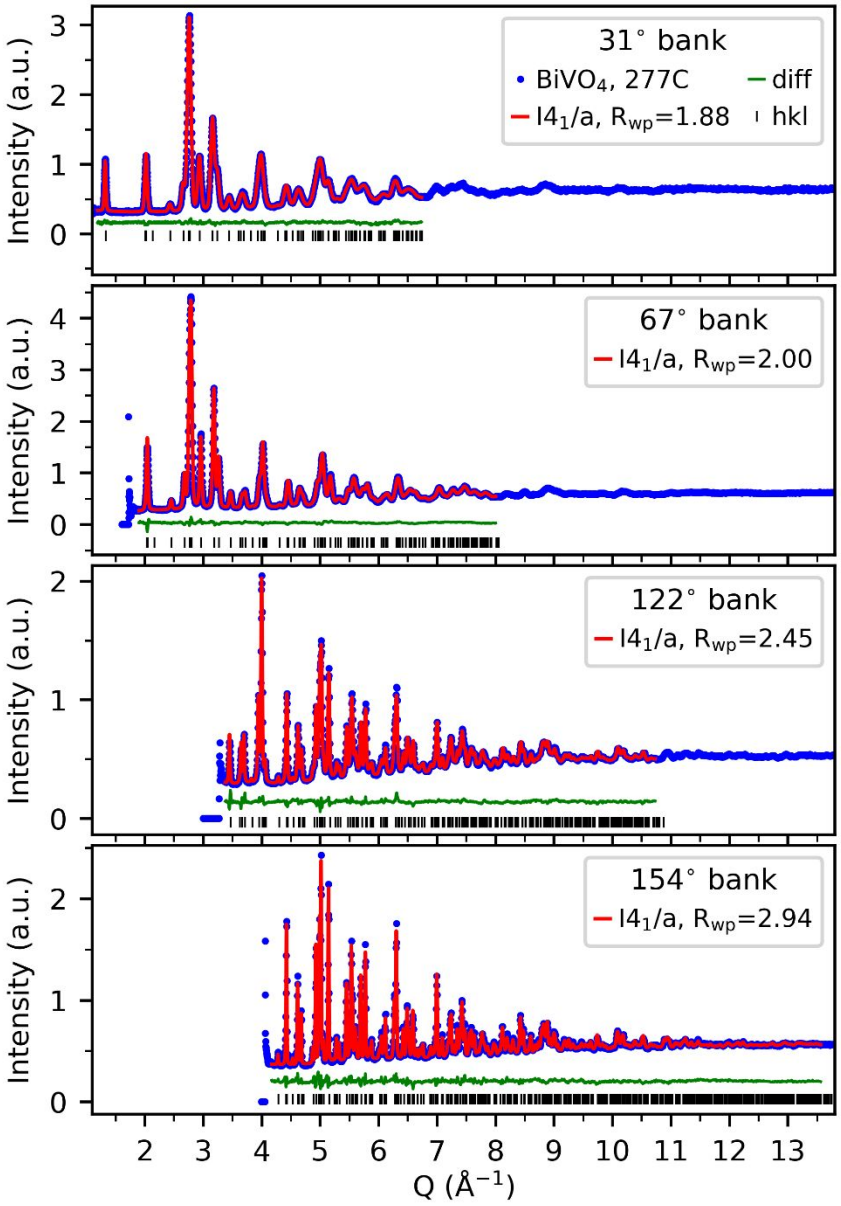

Figure S64: Neutron Bragg powder diffraction data collected on $BiVO_4$ at 550 K fitted using the tetragonal scheelite model. The blue dots represent the data, the red line represents the Rietveld refinement to the data, the green line represents the difference between the two, and the black ticks represent the space group allowed *hkl* reflections.

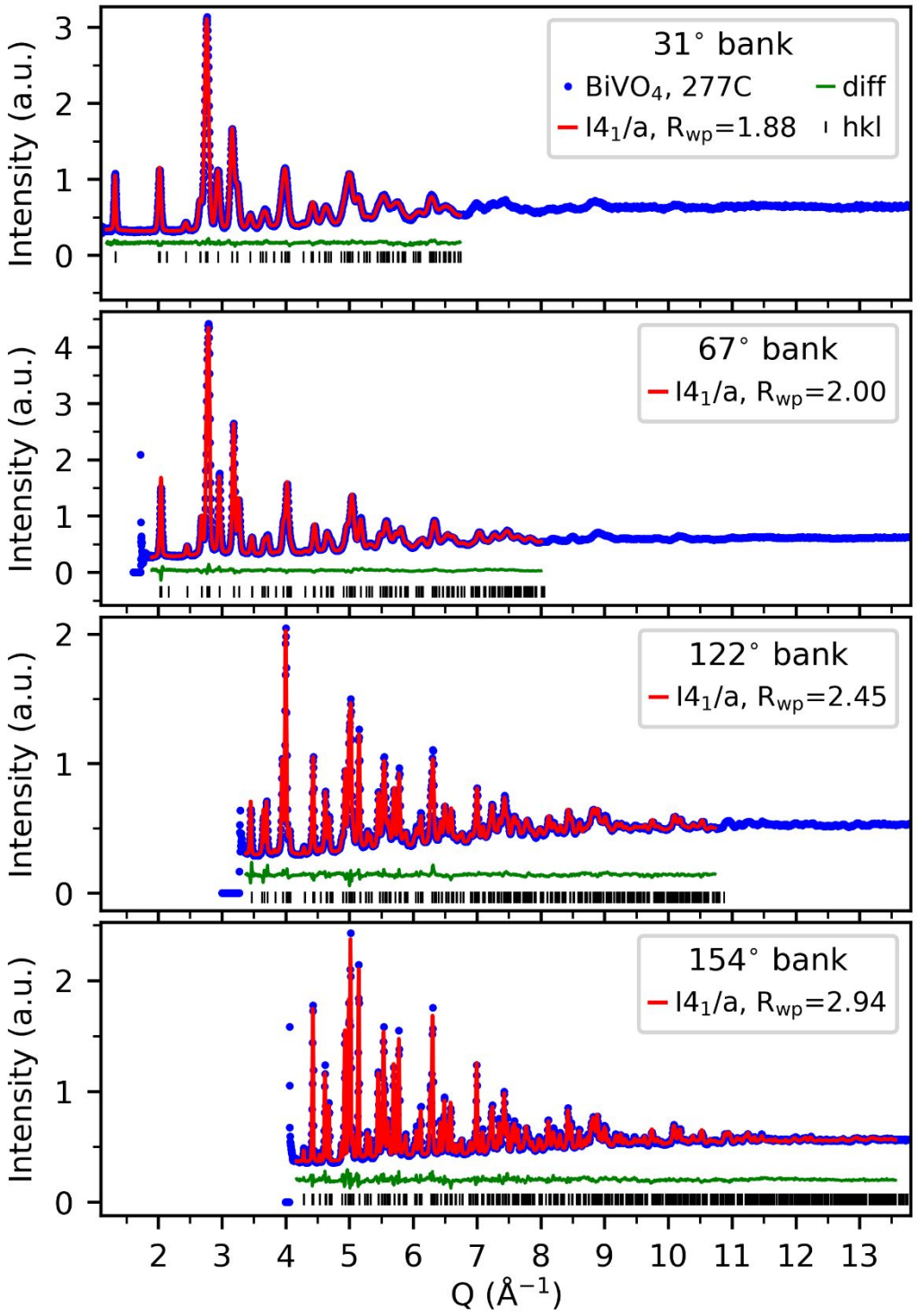

Figure S65: Neutron Bragg powder diffraction data collected on $BiVO_4$ at 600 K fitted using the tetragonal scheelite model. The blue dots represent the data, the red line represents the Rietveld refinement to the data, the green line represents the difference between the two, and the black ticks represent the space group allowed *hkl* reflections.

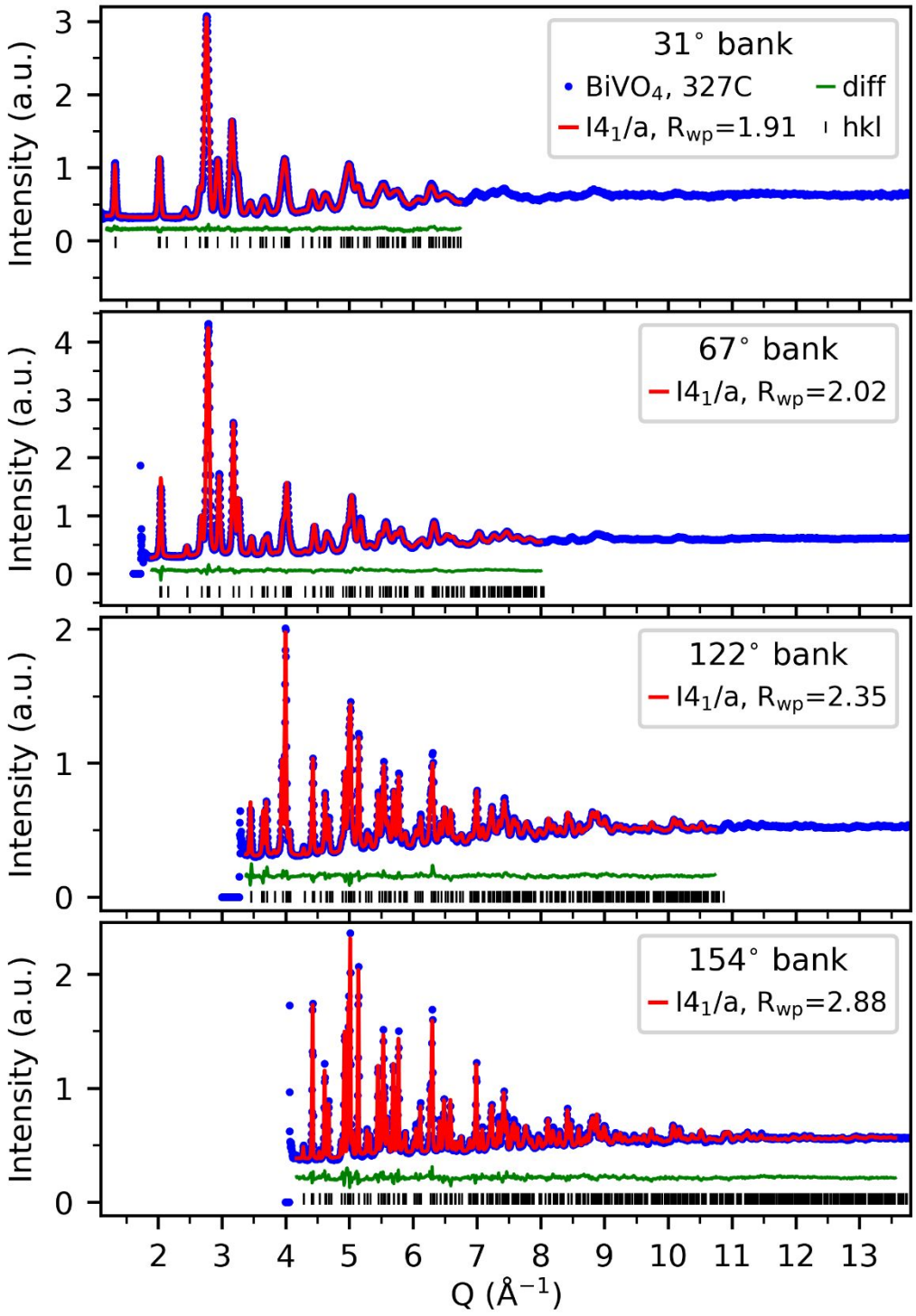

Figure S66: Neutron Bragg powder diffraction data collected on $BiVO_4$ at 650 K fitted using the tetragonal scheelite model. The blue dots represent the data, the red line represents the Rietveld refinement to the data, the green line represents the difference between the two, and the black ticks represent the space group allowed *hkl* reflections.

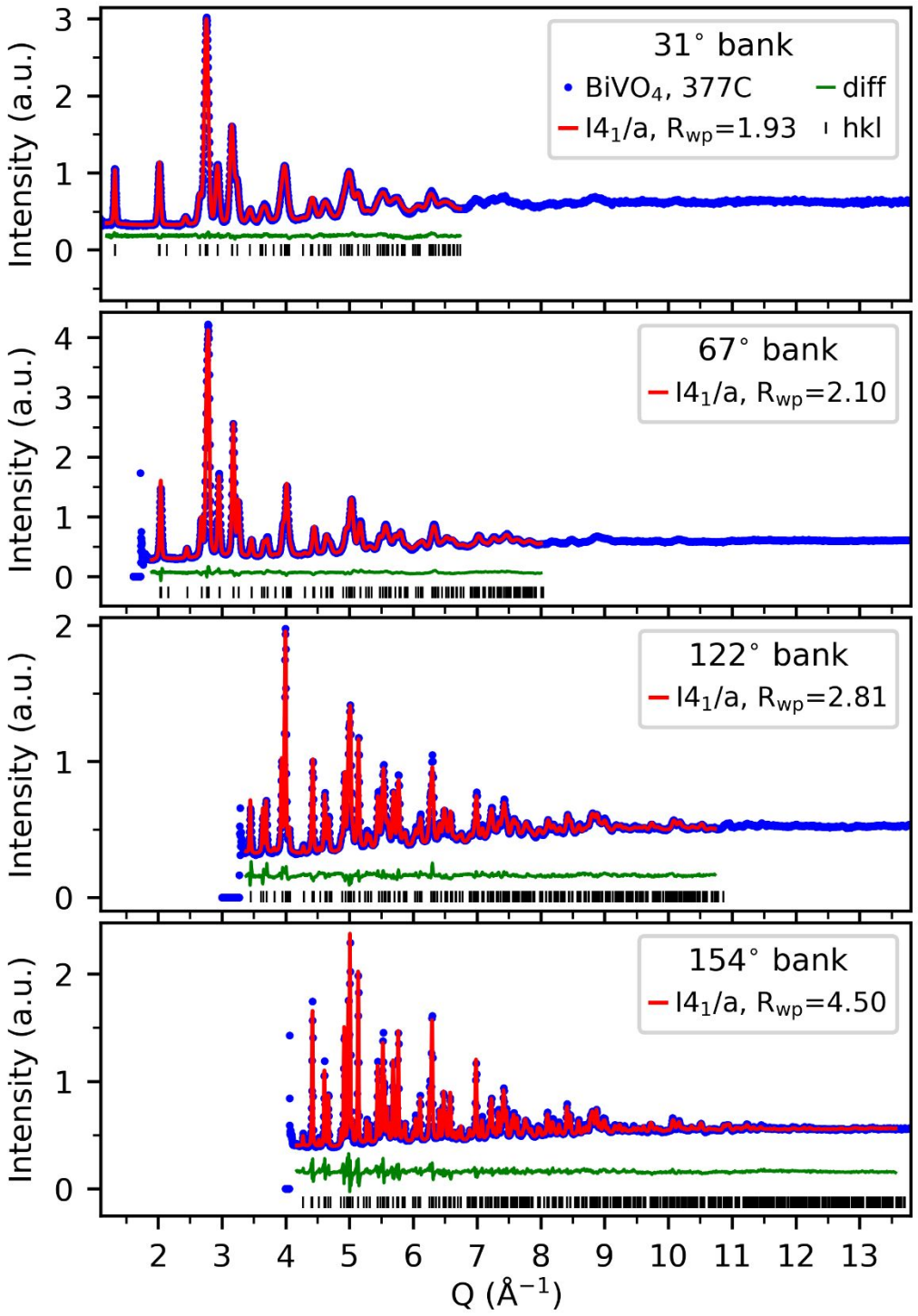

Figure S67: Neutron Bragg powder diffraction data collected on $BiVO_4$ at 700 K fitted using the tetragonal scheelite model. The blue dots represent the data, the red line represents the Rietveld refinement to the data, the green line represents the difference between the two, and the black ticks represent the space group allowed *hkl* reflections.

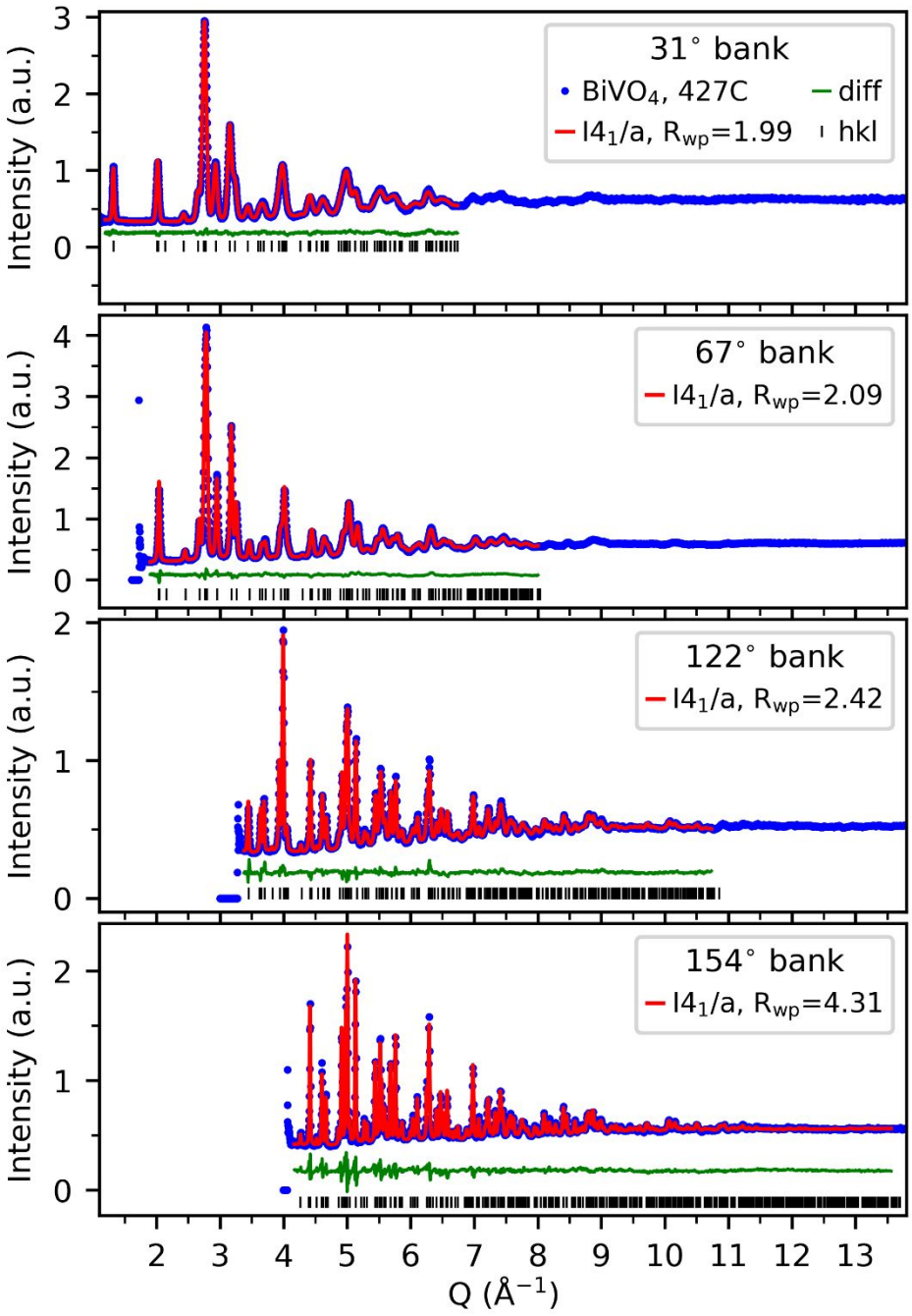

Figure S68: Neutron Bragg powder diffraction data collected on $BiVO_4$ at 750 K fitted using the tetragonal scheelite model. The blue dots represent the data, the red line represents the Rietveld refinement to the data, the green line represents the difference between the two, and the black ticks represent the space group allowed *hkl* reflections.

Neutron Powder Diffraction Data – POWGEN

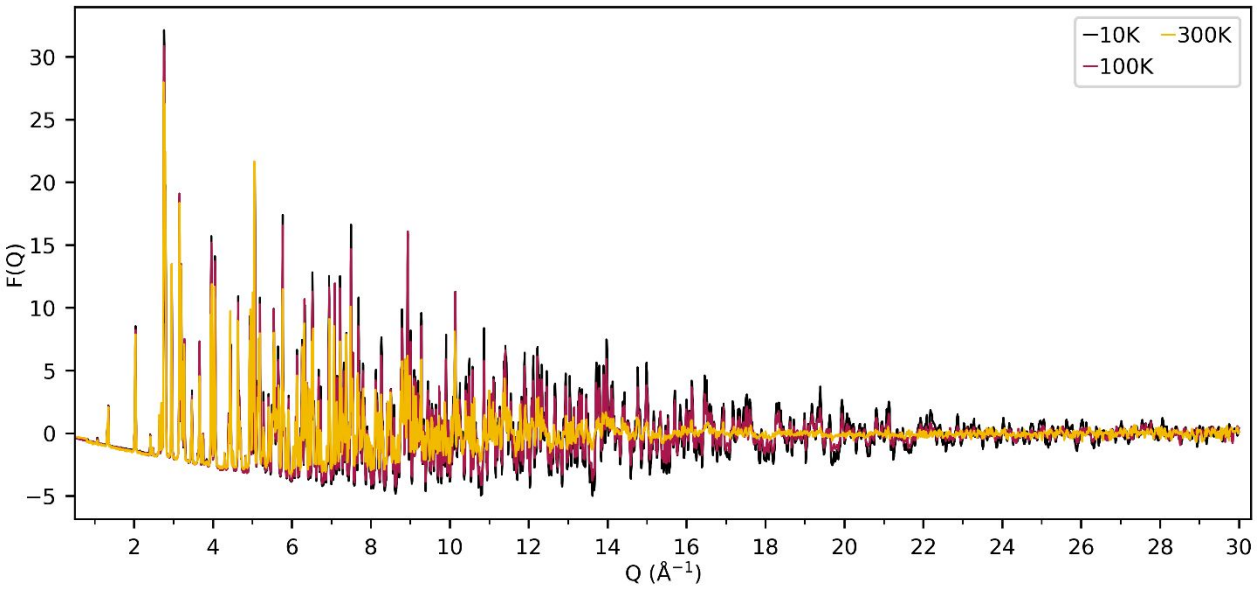

Figure S69: Variable temperature neutron total scattering data, F(Q), in the Powgen Automatic Changer environment.

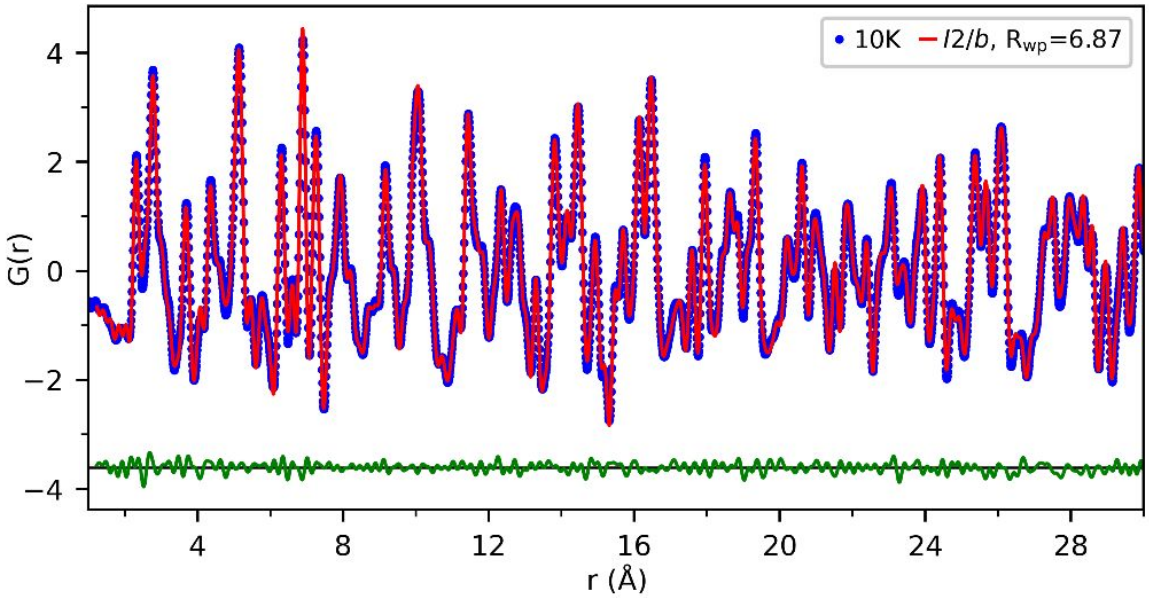

Figure S70: Neutron pair distribution function data collected on $BiVO_4$ at 10 K fitted using a single model. The blue dots represent the data, the red line represents the small box fit to the data in the monoclinic fergusonite *I*2/*b* model, and the green line represents the difference between the two.

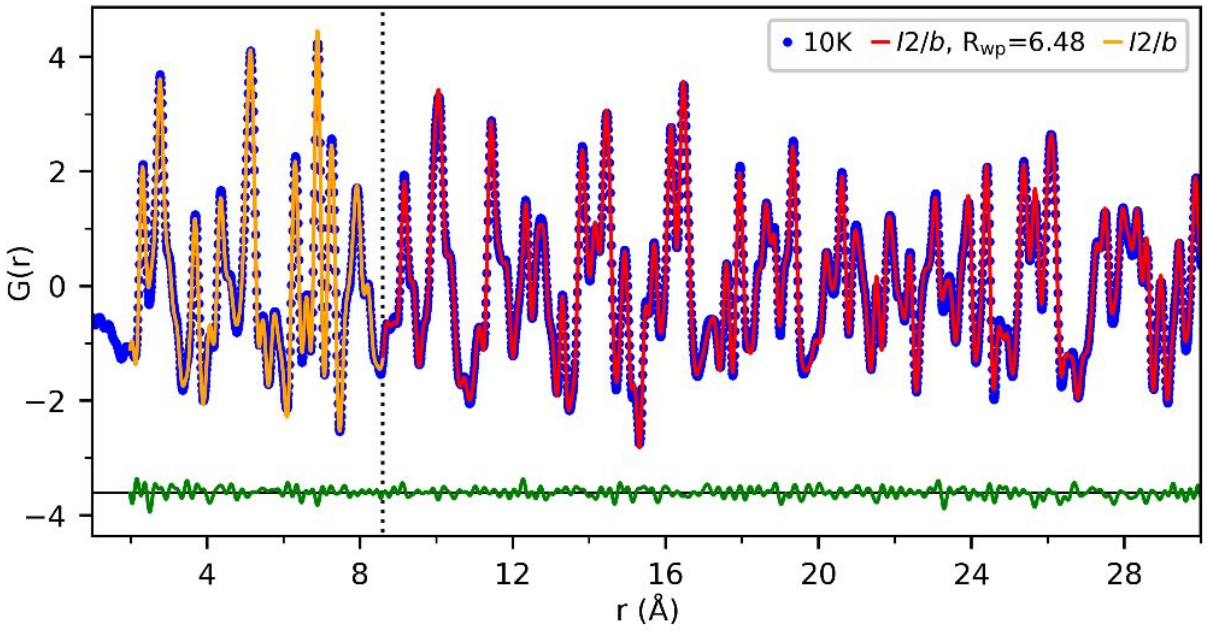

Figure S71: Neutron pair distribution function data collected on $BiVO_4$ at 10 K fitted using a two-phase model. The blue dots represent the data, the red and orange lines represent the small box fit to the data in the monoclinic fergusonite *I*2/*b* model, and the green line represents the difference between the two.

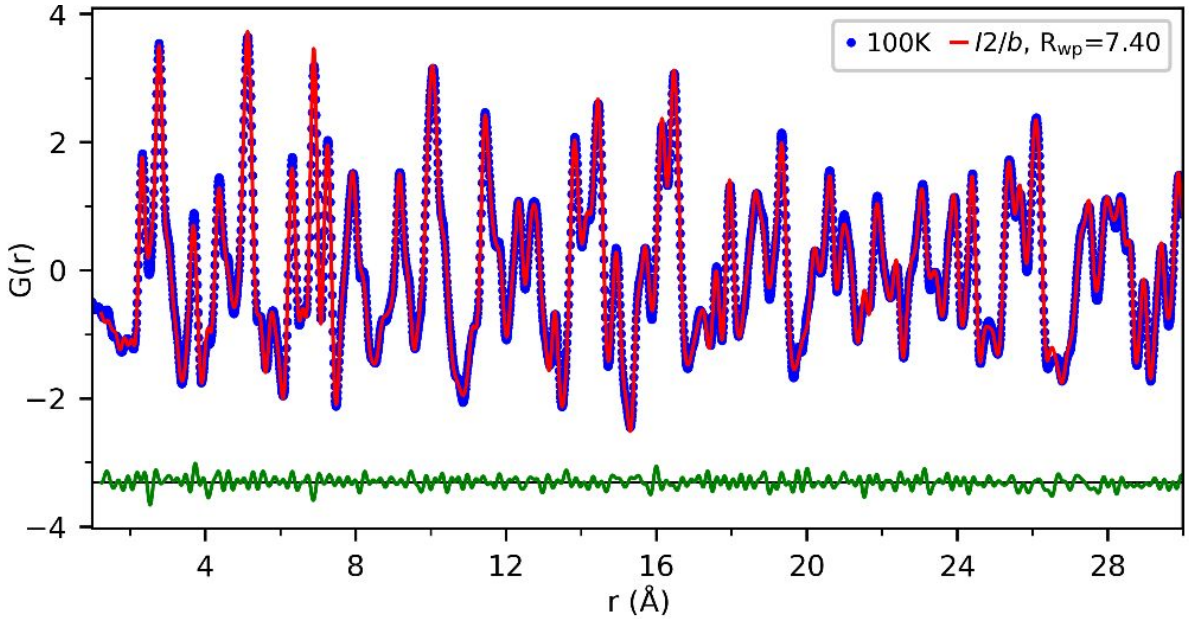

Figure S72: Neutron pair distribution function data collected on $BiVO_4$ at 100 K fitted using a single model. The blue dots represent the data, the red line represents the small box fit to the data in the monoclinic fergusonite *I*2/*b* model, and the green line represents the difference between the two.

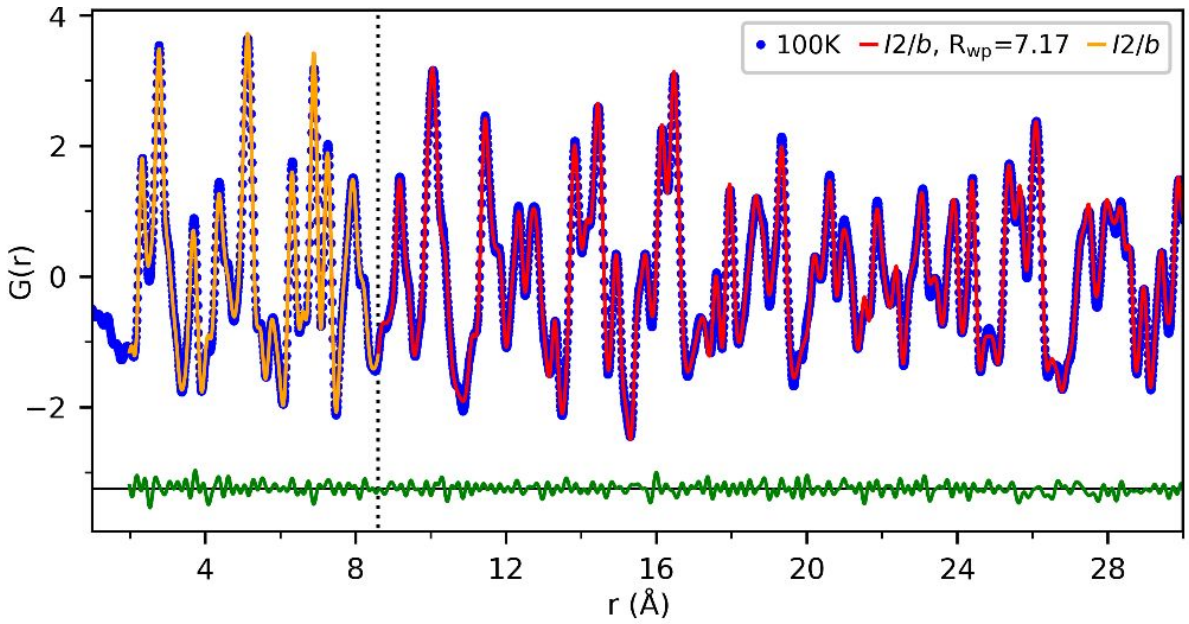

Figure S73: Neutron pair distribution function data collected on $BiVO_4$ at 100 K fitted using a two-phase model. The blue dots represent the data, the red and orange lines represent the small box fit to the data in the monoclinic fergusonite *I*2/*b* model, and the green line represents the difference between the two.

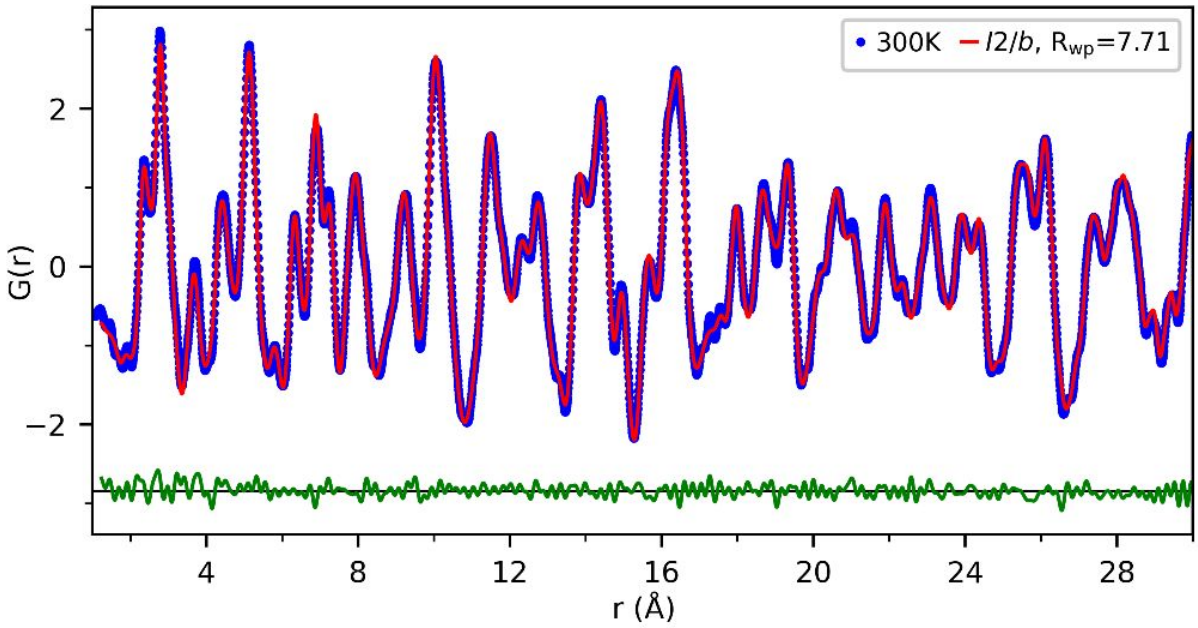

Figure S74: Neutron pair distribution function data collected on $BiVO_4$ at 300 K fitted using a single model. The blue dots represent the data, the red line represents the small box fit to the data in the monoclinic fergusonite *I*2/*b* model, and the green line represents the difference between the two.

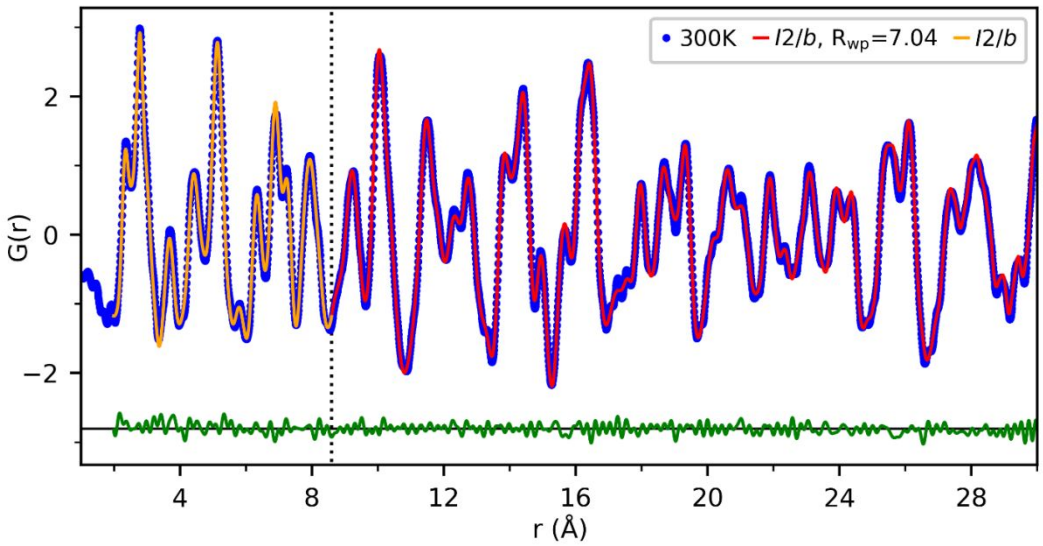

Figure S75: Neutron pair distribution function data collected on $BiVO_4$ at 100 K fitted using a two-phase model. The blue dots represent the data, the red and orange lines represent the small box fit to the data in the monoclinic fergusonite *I*2/*b* model, and the green line represents the difference between the two.

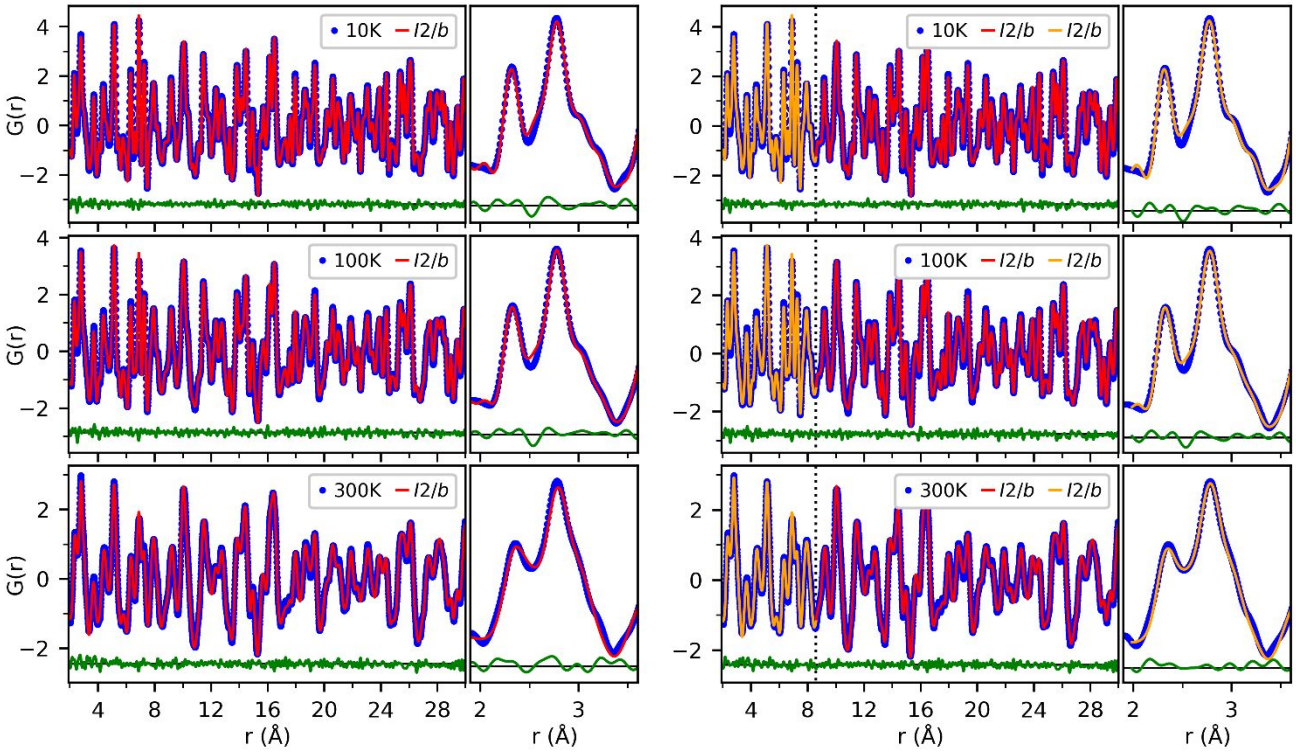

Figure S76: Neutron pair distribution function data collected on $BiVO_4$ at the POWGEN instrument at Oak Ridge National Laboratory. The blue dots represent the data, the red and orange lines represent the small box fit to the data in the monoclinic fergusonite *I*2/*b* model, and the green line represents the difference between the two.

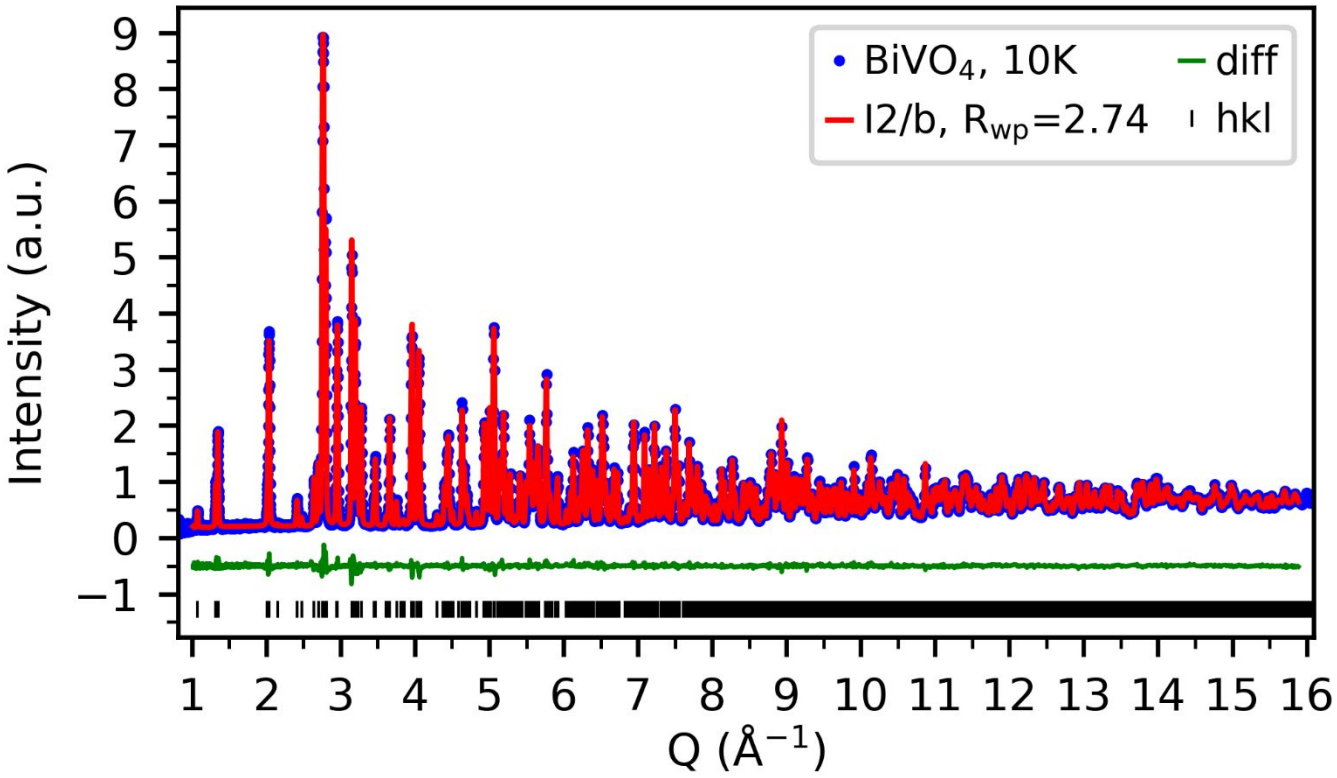

Figure S77: Neutron time of flight data collected on $BiVO_4$ at 10 K fitted to the monoclinic fergusonite model at the POWGEN instrument at Oak Ridge National Laboratory. The blue dots represent the data, the red line represents the Rietveld refinement to the data, the green line represents the difference between the two, and the black tick marks represent the space group-allowed *hkl* reflections.

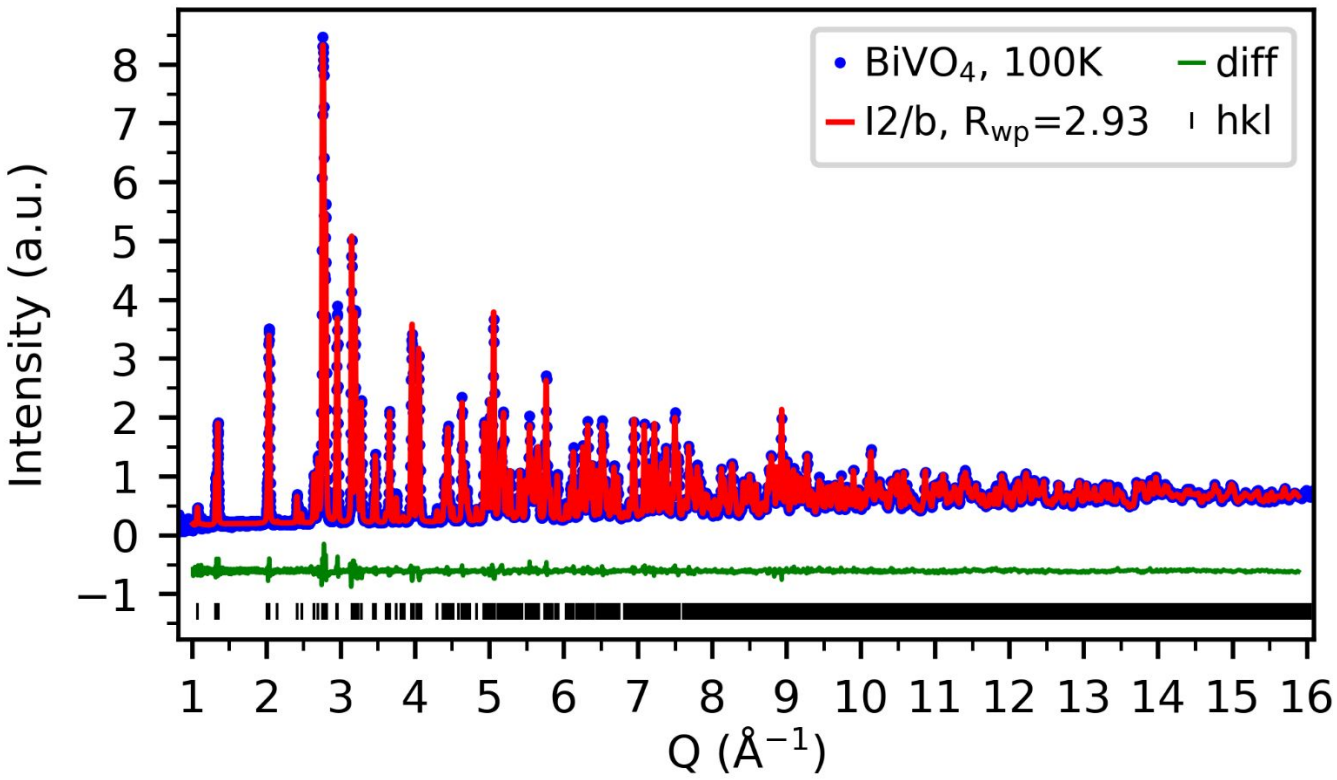

Figure S78: Neutron time of flight data collected on $BiVO_4$ at 100 K fitted to the monoclinic fergusonite model at the POWGEN instrument at Oak Ridge National Laboratory. The blue dots represent the data, the red line represents the Rietveld refinement to the data, the green line represents the difference between the two, and the black tick marks represent the space group-allowed *hkl* reflections.

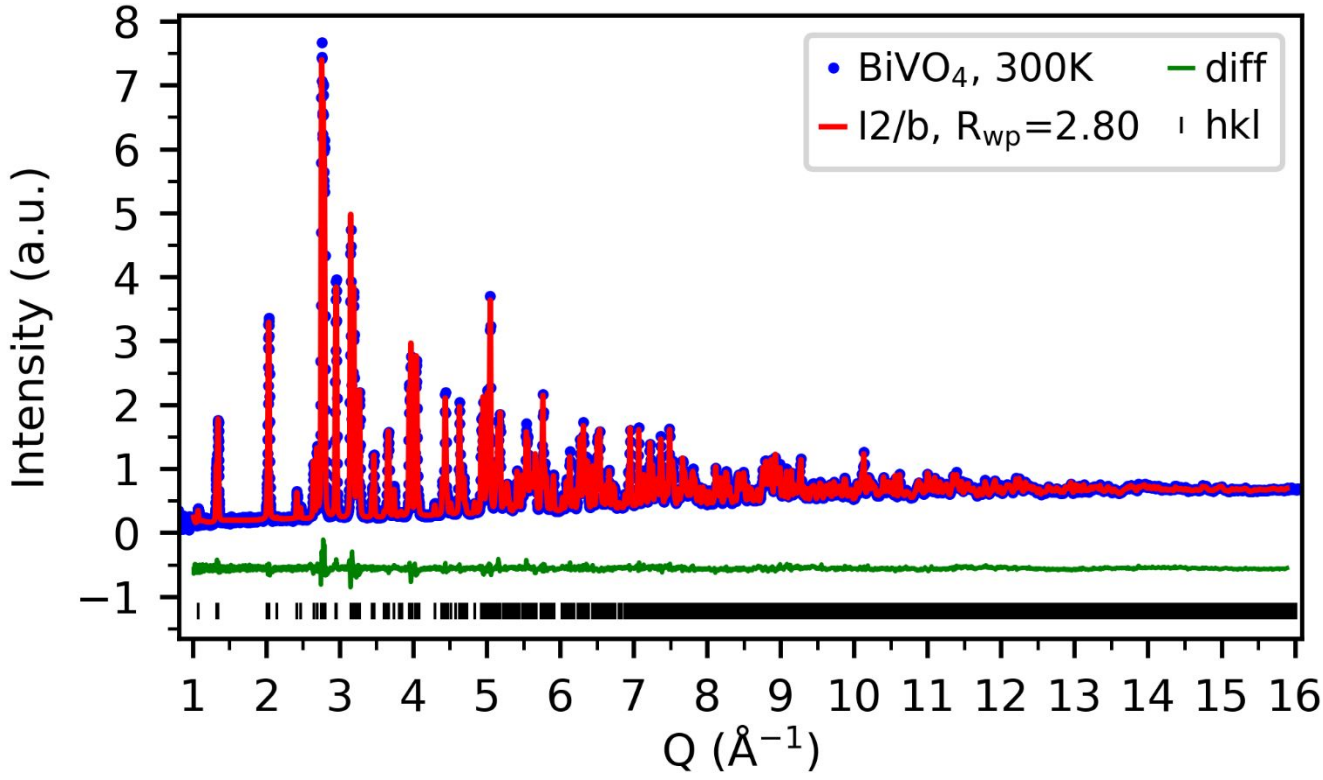

Figure S79: Neutron time of flight data collected on $BiVO_4$ at 300 K fitted to the monoclinic fergusonite model at the POWGEN instrument at Oak Ridge National Laboratory. The blue dots represent the data, the red line represents the Rietveld refinement to the data, the green line represents the difference between the two, and the black tick marks represent the space group-allowed *hkl* reflections.

References:

(1) Chupas, P. J.; Chapman, K. W.; Kurtz, C.; Hanson, J. C.; Lee, P. L.; Grey, C. P. A versatile sample-environment cell for non-ambient X-ray scattering experiments. *Journal of Applied Crystallography* **2008**, *41* (4), 822-824.
(2) Toby, B. H.; Von Dreele, R. B. GSAS-II: the genesis of a modern open-source all purpose crystallography software package. *Journal of Applied Crystallography* **2013**, *46* (2), 544-549.
(3) Juhás, P.; Davis, T.; Farrow, C. L.; Billinge, S. J. PDFgetX3: A rapid and highly automatable program for processing powder diffraction data into total scattering pair distribution functions. *Journal of Applied Crystallography* **2013**, *46* (2), 560-566.
(4) Yang, X.; Juhas, P.; Farrow, C. L.; Billinge, S. J. xPDFsuite: an end-to-end software solution for high throughput pair distribution function transformation, visualization and analysis. *arXiv preprint arXiv:1402.3163* **2014**.